

**Migration of tumor cells and leukocytes in extracellular matrix:
proteolytic and nonproteolytic strategies
for overcoming tissue barriers**

Dissertation zur Erlangung des
naturwissenschaftlichen Doktorgrades
der Bayrischen Julius-Maximilians-Universität Würzburg

vorgelegt von

Katarina Wolf

Würzburg, 2002

Eingereicht am: 4. Oktober 2002

Mitglieder der Promotionskommission:

Vorsitzender: Herr Professor Dr. R. Hedrich

Gutachter: Frau Professor Dr. E.-B. Bröcker

Gutachter: Herr Professor Dr. G. Krohne

Tag des Promotionskolloquiums: 9. April 2003

Doktorurkunde ausgehändigt am:

TABLE OF CONTENTS

ABBREVIATIONS

1. INTRODUCTION

1.1. Molecular mechanisms of cell-matrix interaction	1
1.1.1. Cell adhesion molecules	1
1.1.2. Matrix proteases - structure and functions	3
1.1.2.1. MMPs	3
1.1.2.2. ADAMs	7
1.1.2.3. Proteases of the plasminogen activator/ plasmin system	8
1.1.2.4. Cathepsins	9
1.1.3. Matrix proteases - regulation of expression and proteolytic function	10
1.1.3.1. MMPs and TIMPs	10
a) Transcriptional and post-transcriptional regulation	10
b) MMP activation	11
c) Inhibition of MMP activity	12
1.1.3.2. ADAMs	13
1.1.3.3. Proteases of the plasminogen activator/ plasmin system	13
1.1.3.4. Cathepsins	14
1.2. Cell migration in tumor invasion and metastasis	15
1.2.1. Basic mechanisms of cell migration	15
1.2.1.1. Two-dimensional cell migration	15
1.2.1.2. Three-dimensional cell migration	16
1.2.2. Cancer	16
1.2.2.1. Cancer cascade – overlook	16
1.2.2.2. Multistep cascade of tumor invasion	17
1.2.3. Contribution of MMPs and additional proteases to tumor invasion and motility	18
1.2.3.1. Pericellular localization of proteolytic activity in vitro	18
1.2.3.2. Proteases in experimental and in vivo studies of invasion	18
a) Protease-dependent invasion	18
b) Residual migration after inhibition of proteases	19
1.3. Molecular mechanisms of cell migration in T Lymphocytes	19
1.4. Diversity of cell migration mechanisms in different cell types	20
1.5. Purpose of the study	21

2. RESULTS

2.1. Expression and function of β 1 integrins and matrix proteases in MV3 melanoma and HT-1080 fibrosarcoma cells	23
2.1.1. Expression of β 1 integrins, MMPs and other proteases and endogenous protease inhibitors	23
2.1.1.1. Cell surface expression of β 1 integrins, MMPs and uPA	23
2.1.1.2. Detection of MMP protein levels by Western blot	24
2.1.1.3. Detection of MMP function and activation by native collagen zymography	25
2.1.1.4. Detection of mRNA expression by RT-PCR	26
2.1.2. Visualization of β 1 integrin-dependent and proteolytic cell migration in 3D collagen matrices	27
2.1.2.1. β 1 integrin-dependent cell contact to the collagen matrix: fiber pulling and reorganization	27
2.1.2.2. Subcellular distribution of MMPs, β 1 integrins and organization of the actin cytoskeleton; association of MMPs with collagen	29
2.1.3. Structural degradation of collagen by HT-1080 and MV3 cells	30
2.1.3.1. Collagen structure in acryl amide gel (zymography) and fibrillar 3D collagen matrix	30
2.1.3.2. Degradation of 3D collagen matrix	31
a) Structural breakdown of matrix scaffold	31
b) Quantitative detection of structural matrix breakdown	32
2.1.3.3. Distribution of proteolytic activity in situ: cleavage of collagen fibers	32
2.1.4. Proteolytic movement of HT-1080 cells: a mesenchymal migration type	33
2.2. Proteases in collagenolysis and migration of MV3 and HT-1080 cells: function-blocking studies using pharmacological protease inhibitors	34
2.2.1. Biological effects of broad-spectrum MMP inhibitor BB-2516 (marimastat)	34
2.2.1.1. Inhibition of cell-released MMP-2 and -9, and recombinant MT1-MMP in native collagen zymography	34
2.2.1.2. Inhibition of fibrillar collagen degradation by cell derived MMPs	35
2.2.1.3. Minor effects on inhibition of cell migration by BB-2516	36
2.2.2. Biological effects of broad-spectrum protease inhibitors	37
2.2.2.1. Establishment of a non-toxic broad-spectrum inhibitor cocktail	37
2.2.2.2. Inhibition of migration-associated cell-mediated collagenolysis by inhibitor cocktail	38

2.2.2.3. Lack of inhibition of cell migration by protease inhibitor cocktail	38
2.3. Mechanisms of non-proteolytic HT-1080 and MV3 tumor cell migration in the presence of protease inhibitor cocktail	40
2.3.1. Transition from mesenchymal to amoeboid morphodynamics	40
2.3.2. Altered cellular morphodynamics: squeezing through the fiber network in the absence of structural matrix breakdown	42
2.3.3. Altered distribution of $\beta 1$ integrins, MT1-MMP and F-actin in induced amoeboid HT-1080 cell migration	42
2.4. Mesenchymal to amoeboid transition in vivo	43
2.5. Protease function in T cell migration	44
2.5.1. Expression of proteases by activated primary CD4+ T cells and SupT1 lymphoma cells	45
2.5.1.1. Detection of mRNA expression	45
2.5.1.2. Detection of MMP cell surface expression	46
2.5.2. Contribution of proteases to collagenolysis and migration in T cells: function blocking experiments with protease inhibitors	47
2.5.2.1. Lack of in situ collagenolysis	47
2.5.2.2. Persistent migration in the presence of protease inhibitor cocktail	48
2.5.3. Biophysics of non-proteolytic amoeboid T-cell-migration	50
3. DISCUSSION	
3.1. Contribution of proteases to tumor cell migration	51
3.1.1. Constitutive proteolytic mesenchymal migration of tumor cells	51
3.1.2. Constitutive non-proteolytic amoeboid migration	52
3.1.3. Mesenchymal-amoeboid transition: induced amoeboid migration	52
3.1.4. MAT- molecular implications	55
3.1.5. MAT-comparison to other morphodynamic processes	55
3.2. Contribution of proteases to T cell migration	56
3.2.1. Expression of proteases in activated T cells	57
3.2.2. T cell migration in 3D collagen independent of proteolytic matrix degradation	57
3.2.2.1. Lack of in situ collagenolysis	57
3.2.2.2. Lack of inhibitory effects of protease inhibitors on T cell migration	58
3.2.3. Non-proteolytic, biophysical mechanisms supporting T cell migration through matrix barriers	59

3.3.	Diversity and plasticity of protease functions in the migration of differen	
	cell types	61
3.3.1.	Diversity	61
3.3.2.	Plasticity	62
3.4.	Implications and outlook	62
4.	MATERIALS AND METHODS	
4.1.	Antibodies	64
4.2.	Human cell lines and culture	64
4.3.	Isolation and culture of human T lymphocytes	65
4.4.	Protease inhibitors	65
4.5.	Construction of migration chambers	66
4.6.	Preparation of 3D collagen lattices	66
4.7.	Time-lapse videomicroscopy	67
4.8.	Analysis of cell viability	67
4.9.	Computer-assisted cell tracking	67
4.10.	Statistical analysis	67
4.11.	Flow cytometry	68
4.12.	Gel electrophoresis and Western blotting	68
4.13.	Zymography	69
4.14.	RT-PCR	69
4.15.	Collagenolysis assays	70
4.15.1.	Qualitative collagenolysis assay using a native non-labelled collagen matrix	70
4.15.2.	Quantitative Collagen-FITC-release-assay	70
4.16.	Confocal laser-scanning microscopy	71
4.17.	Quantitative visual analysis of cellular polarity and morphodynamics	71
4.18.	Intravital multi-photon microscopy	72
5.	SUMMARY	74
6.	ZUSAMMENFASSUNG	75
7.	REFERENCES	76

8.	LIST OF FIGURES	94
9.	LIST OF TABLES	95
10.	APPENDIX	
	Acknowledgements	97
	List of publications and abstracts	98
	Curriculum Vitae	100
	Lebenslauf	101
	Declaration	102
	Movie legends	103

ABBREVIATIONS

Ab	Antibody
ADAM	A Disintegrin And Metalloproteinase
BM	Basal membrane
BSA	Bovine serum albumin
ConA	Concanavalin A
DDR	Discoidin domain receptor
ECM	Extracellular matrix
EDTA	Ethylendiamintetraacetyl acid
EGF	Epithelial growth factor
F(ab)' / F(ab)' ₂	Antigen-binding fragments
FACS	Fluorescence Activated Cell Sorting
FAK	Focal adhesion kinase
FCS	Fetal calf serum
FGF	Fibroblast growth factor
FITC	Fluoresceine isothiocyanate
FN	Fibronectin
GPI	Glycophosphatidyl-inositol-anchoring domain
HGF	Heparin growth factor
HLE	Human leukocyte elastase
hr	Hour
HT-MT1	HT-1080 fibrosarcoma cells overtransfected with MT1-MMP
HT-neo	HT-1080 fibrosarcoma cells transfected with neo-vector
IFN- γ	Interferon- γ
Ig	Immune globulin
IL	Interleukin
LN	Laminin
mAb	Monoclonal antibody
MAT	Mesenchymal-amoeboid transition
min	Minute
MMP	Matrix metalloproteinase
MT-MMP	Membrane-type matrix metalloproteinase
PA	Plasminogen activator
PAI	Plasminogen activator inhibitor
PBMC	Peripheral blood mononuclear cell
PBS	Phosphate-buffered saline
PCR	Polymerase chain reaction
PE	Phycoerythrine
PG	Proteoglycans
RNA	Ribonucleine acid
RT	Reverse Transkriptase
SD	Standard deviation
sec	Seconds
TBS-T	Tris-buffered saline-Tween
TGF- β	Tumor growth factor- β
TIMP	Tissue inhibitor of metalloproteinases
TNF- α	Tumor necrosis factor- α
VN	Vitronectin
2D	Two-dimensional
3D	Three-dimensional

1. INTRODUCTION

Invasion of cells within surrounding tissue is of importance in numerous physiologic and pathologic processes, such as embryonic development, angiogenesis, wound repair, immune response and inflammatory diseases as well as tumor invasion and metastasis. To control the body for foreign antigens, recirculation of T-lymphocytes from blood vessels in the surrounding extracellular tissue and lymphatic organs back to the blood stream represents a lifelong, continuous physiologic process. Similarly, the invasive and metastatic potential of tumors results from the migration of single tumor cells or cell clusters detached from the primary tumor. Until now, it is not known to what extent such different migration/ invasion events equally require the function of proteolytic enzymes for removal of tissue barriers and remodeling of surrounding tissue. Therefore, studies on the role of matrix proteases for the migration of different cell types are necessary for a deeper understanding of (1) the underlying molecular mechanisms and (2) the physiologic context in which cell migration occurs, to eventually modulate pathologic processes such as uncontrolled immune reactions or tumor invasion and metastasis.

1.1. Molecular mechanisms of cell-matrix interaction

1.1.1. Cell adhesion molecules

The interaction of cells with extracellular matrix requires adhesion mediated by different cell adhesion molecules, in particular by integrin receptors. Integrins are transmembrane glycoproteins consisting of a large extracellular domain with a globular head region, single transmembrane domain and a short cytoplasmic tail, that form functional heterodimers composed of an α and β chain. The β -subunit divides the integrins into subfamilies (Aota, 1997). Each $\alpha\beta$ integrin combination has its own binding specificity, recognizing several ligands. Integrins of the $\beta 1$ - and $\beta 3$ -subfamily are known to mediate cell-extracellular matrix (ECM) contacts. Individual ECM proteins such as collagen, fibronectin (FN) or laminin (LN) are bound by several $\beta 1$ integrins (Table 1). $\alpha 1\beta 1$, $\alpha 2\beta 1$, $\alpha 10\beta 1$ or $\alpha 11\beta 1$ integrins bind to fibrillar type I or III collagens with their I domains (Kirchhofer et al., 1990; Klein et al., 1991; Tulla et al., 2001; Kagami et al., 2001; Gullberg et al., 2002) and $\alpha v\beta 3$ integrins bind to denaturated collagen through their RGD

Table 1. Cell surface receptor binding to ECM ligands associated with migration.

adhesion receptor	ligands	receptor-ligand interaction / involvement in migration
$\alpha 1\beta 1$	fibrillar type I collagen, LN	Kagami et al., 2001 Desban and Duband, 1997
$\alpha 2\beta 1$	fibrillar type I collagen, LN	Schon et al., 1996 Etoh et al., 1992
$\alpha 3\beta 1$	LN, FN	Klominek et al., 1997
$\alpha 4\beta 1$	FN	Wu et al., 1995
$\alpha 5\beta 1$	FN	Kim et al., 1992
$\alpha 6\beta 1$	LN	Hangan et al., 1997
$\alpha 10\beta 1$	fibrillar type I collagen	Tulla et al., 2001
$\alpha 11\beta 1$	fibrillar type I collagen, VN	Gullberg et al., 2002 Velling et al., 1999
$\alpha v\beta 1$	VN	Friedlander et al., 1996
$\alpha v\beta 3$	denaturated collagen, VN	Aznavoorian et al., 1996
DDR1, DDR2	fibrillar type I collagen	Kamohara et al., 2001 Shrivastava et al., 1997

sites (Davis, 1992). The discoidin domain receptors 1 and 2 (DDR1 and 2) are newly characterized alternative cell surface receptors that bind to fibrillar type I collagen (Shrivastava et al., 1997; Vogel et al., 2001).

Integrins signal through the cell membrane in both directions: intracellular signals dictate integrin binding activity to the ECM (inside-out-signaling), while binding to ECM creates signals which integrins transmit into the cell (outside-in-signaling) (Hynes et al., 1992). Binding of integrin heterodimers to the ECM occurs reversibly due to ligand pocket forming head regions in a calcium-dependent manner. This results in rapid induction of conformational changes and clustering of integrins. Since the short cytoplasmic tails are devoid of intrinsic kinase activity, integrins associate with and assemble in an organized manner with adapter molecules, such as talin, paxillin, α -actinin or focal adhesion kinase (FAK). These molecules connect integrins to signaling molecules and to the actin cytoskeleton (Miyamoto et al, 1995 and 1996; Yamada and Geiger, 1997). The accumulation of integrins, signaling and cytoskeletal proteins lead to formation of focal

adhesion sites termed focal complexes or contacts, which are more transient, or to the formation of more stable mature focal adhesions of higher adhesivity. In firmly adhering cells, stress fibers are formed consisting of polymerized actin filaments (F-Actin). At outward edges, more dynamic thin extensions (filopodia) and sheet-like structures (lamellipodia) are found, enabling the cell to extend and spread. The process of F-Actin formation is controlled by several small GTPases of the Rho-family: whereas Rho induces focal adhesions and stress fibers resulting in increased adhesion (Amano et al., 1997), Cdc42 induces filopodia, and Rac induces lamellipodia formation, both of which favor cell migration (Nobes and Hall et al., 1995; Keely et al., 1997). In contrast to focal adhesions characterized on 2D substrates, cellular focal adhesions in 3D matrix differ in their molecular compositions and structure including the content of certain integrins, and display enhanced cell biological activities, e.g. by more effective mediation of cell adhesions or faster acquisition of a spindle-shaped morphology (Cukierman et al., 2001; Geiger, 2001).

Increased levels of integrin synthesis and activation have been found to be associated with progression of some tumors, i.e., $\alpha2\beta1$ or $\alpha6\beta1$ integrins in melanoma (Danen et al., 1993), whereas in other tumors, such as breast carcinoma, a more invasive phenotype appears to be reflected by reduced levels of $\alpha2\beta1$ integrins (Zutter et al., 1995).

1.1.2. Matrix proteases - structure and functions

A variety of proteases, such as metallo-, serine, cysteine and aspartic proteases are involved in cellular interactions with the extracellular matrix during physiologic and pathologic events in cell migration and tissue remodeling. In particular, the family of matrix metalloproteinases (MMPs) is thought to comprise several key proteases involved in ECM degradation and matrix remodeling for tumor cell migration resulting in invasion and metastasis.

1.1.2.1. MMPs

MMPs are endopeptidases belonging to the multigenic superfamily of metzincins. The catalytic site of metzincins is defined by a highly conserved motif of three histidins that chelate zinc, and a proximal conserved methionin turn beneath the catalytic zinc (Stöcker and Bode, 1995). The subclass of MMPs consists of 25 members presently known in vertebrates (Table 2). The single MMPs are termed by both, a historic descriptive name

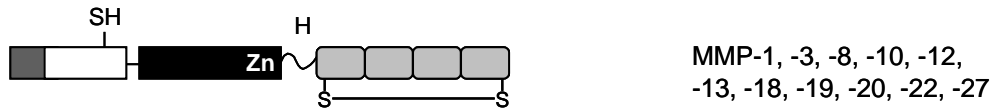
Table 2. The MMP family. Selected substrates and cell surface docking mechanisms. Adapted from Sternlicht & Werb, 2001 and Stamenkovic et al., 2000.

descriptive name	EC name	major substrates	cell surface	docking mechanisms
Collagenases				
Collagenase-1	MMP-1	collagen I, II, III, VII, X, FN, LN, VN	yes	EMMPRIN, α 2-integrins
Collagenase-2	MMP-8	collagen I, II, III, LN	yes	MT1-MMP
Collagenase-3	MMP-13	collagen I, II, III, X, FN		
Collagenase-4	MMP-18 (not human)	collagen I		
Stromelysins				
Stromelysin-1	MMP-3	PN, PG, pro-MMP-13, collagen III, IV, V; FN, LN, E-Cadherin		
Stromelysin-2	MMP-10	PG, gelatin, FN, LN, collagen III, IV, V		
Stromelysin-4	MMP-19	collagen I, IV, FN		
Gelatinases				
Gelatinase-A (72 kD type IV collagenase)	MMP-2	collagen I, III, IV, V, X, gelatin, PN, LN, FN, VN, pro-TGF- β , pro-TNF- α , PN	yes	MT1-MMP/TIMP-2 α v β 3 integrin
Gelatinase-B (92 kD type IV collagenase)	MMP-9	gelatin, collagen IV, V, X, LN, VN, pro-TGF- β , pro-TNF- α , IL-1 β	yes	CD44 collagen IV
Membrane-type MMPs				
MT1-MMP	MMP-14	collagen I, II, III, gelatin, FN, VN, MMP-2, MMP-13, pro-TNF- α	yes	TM
MT2-MMP	MMP-15	FN, LN, tenascin	yes	TM
MT3-MMP	MMP-16	collagen I, III, FN, pro-MMP-2	yes	TM
MT4-MMP	MMP-17	pro-MMP-2	yes	GPI anchor
MT5-MMP	MMP-24	pro-MMP-2	yes	TM
MT6-MMP	MMP-25		yes	GPI anchor
Others				
Matrilysin	MMP-7	gelatin, FN, LN, collagen I, IV Fas-L, proteoglycans	yes	HS-PG CD44v3
Stromelysin-3	MMP-11			
Metalloelastase	MMP-12	elastase, collagen I, IV, FN, LN, VN, PN		
Enamelysin	MMP-20			
XMMP	MMP-21 (not human)	amelogenin		
CMMP	MMP-22 (not human)			
Matrilysin-2	MMP-23			
Epilysin	MMP-26	collagen IV, fibrinogen		
	MMP-27			
	MMP-28			

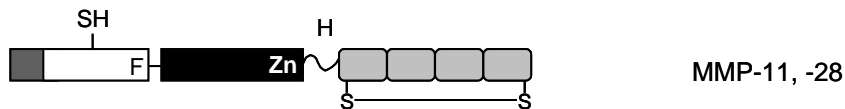
Abbreviations: PG, proteoglycans; FN, fibronectin; VN, vitronectin; LN, laminin; PN, plasminogen; TM, transmembrane domain; HS-PG, heparan sulfate proteoglycans; EMMPRIN, extracellular matrix metalloproteinase inducer.

mostly related to substrate preference, and a more recently established numbering system (Table 2). All MMPs share conserved sequence homologies and domains including prodomain, prodomain, catalytic site, and most MMPs further contain a hinge region and hemopexin domain (Figure 1). Some MMPs additionally comprise furin-recognition sites, type II fibronectin type repeats and membrane anchors (Figure 1).

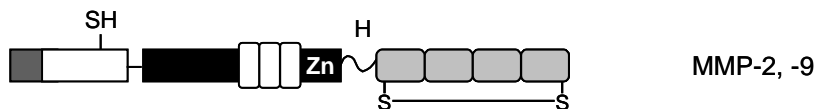
a) secreted MMPs



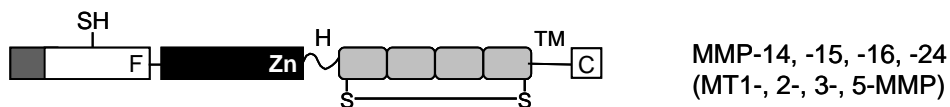
b) secreted MMPs, furin-activated



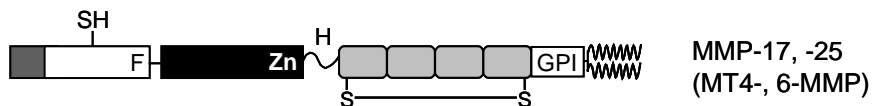
c) gelatin-binding MMPs



d) transmembrane MMPs



e) GPI-linked MMPs



f) minimal domain MMPs

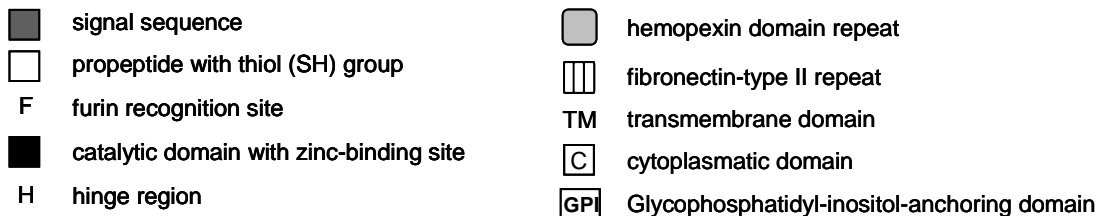


Figure 1. Schematic domain structure of vertebrate MMPs (except MMP-21 and -23). Human MMPs do not include MMP-18, -21 and -22. Modified from Sternlicht & Werb 2001.

The predomain consists of a signal peptide that targets MMP localization for secretion or membrane insertion. The prodomain includes a conserved cysteine containing motif (PRCGVPPD) and maintains the enzyme in an inactive ("latent") conformation. The catalytic domain contains a conserved zinc binding motif (HEXGHXXGXXHSX) (Woessner, 1991) that is required for hydrolysis of the peptide bond. This site is followed by a hinge or linker region, which determines the tertiary structure of the enzyme and contributes to substrate specificity (Knauper et al., 1997). The adjacent hemopexin domain indicates homology to the collagen-binding domain of vitronectin and consists of four repeats, which are linked by a disulfide bond between the first and fourth repeat, thereby forming a central Ca^{2+} -containing pore. The hemopexin domain, which is present in almost all MMPs, in proximity to the catalytic domain essentially contributes to substrate binding. Additionally, MMP-2 and MMP-9 express a fibronectin-type II gelatin-binding domain inserted within the catalytic domain, which further contains a binding site for certain substrates, such as native and denatured collagen or elastin (Murphy et al., 1994; Shipley et al., 1996). A transmembrane spanning and a short cytoplasmatic domain are present in some MMPs (membrane type (MT) –MMPs 1, 2, 3, 5), which is thought to be required for correct localization to substrate binding cell compartments, such as the leading edge of a cell (Lethi et al., 2000). In other MMPs (MT4-, MT6-MMP), membrane-anchoring is provided by a glycosylphosphatidylinositol (GPI) anchor, allowing cell surface expression.

All MMPs display overlapping substrate specificities (redundancy) and together can cleave most, if not all known ECM proteins (Table 2). However, each individual MMP displays proteolytic activity for a highly selective spectrum of substrates. Specific substrate recognition, binding and cleavage are determined by the cooperative action of catalytic site and exosites. Exosites represent secondary substrate binding regions in proximity to the catalytic site, which are provided by the hemopexin domain and by the three FN-type II modules. First, the tethering substrate is specifically bound by exosites, and is then recognized by and located in the active site cleft. An adjacent specificity subsite pocket, termed "S₁", then binds the side chain of the amino acid residue immediately after the proteolytic target, the "scissile" bond of the peptide (Welch et al., 1996). Hence, the size and chemical characteristics of the S₁' pocket have great impact in determining substrate specificity (Overall, 2001). After substrate binding, these exosites are thought to mediate (1) initial binding and orientation of a collagen fibril, and (2) local unwinding of its triple-helical structure ("triple helicase activity"), as shown for MMP-1 (Clark et al., 1989, Windsor et al., 1991). The catalytic site then mediates (3) sequential cleavage of

each single α -chain (Overall, 2001). This unwinding step is important for delivering a single peptide strand to the catalytic site, since the active site cleft is too narrow to accommodate the entire triple helix. Hence, by positioning substrate and local unwinding, a triple helical fibrillar substrate is prepared for proteolytic cleavage. The actual cleavage step is mediated by a zinc molecule located in the center of the active site. Zinc becomes accessible for a water molecule, which mediates the nucleophilic attack on the carbonyl of the substrate peptide bonds eventually causing cleavage of the peptide (Nagase, 1997).

Based on the differences in structure, substrate specificity and cellular localization, MMPs are classified in five functional subgroups: collagenases, stromelysins, gelatinases, membrane-type MMPs (MT-MMPs) and others (Table 2). Collagenases are neutral proteases that are able to cleave native fibrillar collagens into characteristic 1/4 and 3/4 fragments. Further, proteolytic cleavage of cleared collagen fragments (then termed "gelatin") is mediated by gelatinases (MMP-2 and -9). Native type I collagen-degrading ability has been described for MMP-1, -8, -13, MT1 - and MT3-MMP (Montcourrier et al., 1990; Aimes and Quigley, 1995; Ohuchi et al., 1997; Holmbeck et al., 1999), and to some lesser extent, also for MMP-2 (Overall and Sodek, 1987; Aimes and Quigley, 1995; Patterson et al., 2001). Whereas all other collagenases display characteristic 1/4 and 3/4 collagenolytic fragmentation, MT3-MMP attacks collagens by cleaving the N-terminal collagen telopeptides (Shimada et al., 1999).

Besides ECM components, MMPs cleave a number of additional substrates, such as cell surface receptors (i.e. Fas ligand, E-Cadherin), or secreted factors (i.e. IL-1, TNF α , TGF β , HB-EGF) (Imai et al., 1997; Powell et al., 1999; McCawley and Matrisian 2000; Noe et al., 2001; Mitsiades et al., 2001). Adhesion receptors or associated proteins cleaved by MMPs include $\alpha v \beta 3$ integrins (Brooks et al., 1996, Deryugina et al., 2000; Deryugina et al., 2001), transglutaminase (Belkin, 2001) or E-Cadherin (Lochter 1997). A newly discovered group of MMP substrates includes chemokines, i.e. MCP-3, which acts as functional antagonist towards its chemokine receptor (McQuibban et al., 2000). Because of multiple substrate specificities, the function of MMPs is thought to be greatly determined not only by the activation state, but also by localization and redistribution mechanisms under given pathological situations (see below).

1.1.2.2. ADAMs

The adamalysins, ADAMs (a disintegrin and metalloproteinase) comprise 29 known further members of the metzincin family. ADAMs are transmembrane cell surface

proteins (Black 1998) that consist of multiple functional domains, such as pro-, metalloprotease-, disintegrin, EGF repeat, cysteine-rich, transmembrane and cytoplasmatic domain. ADAMs share structural and functional homologies to snake venom enzymes with several functions, including adhesion and potent ECM degrading activity (Primakov and Miles 2000).

Based on homology searches, 17 ADAMs (including ADAM 9, 10, 12, 15 and 17) are predicted to be active metalloproteinases, thereby contributing to proteolysis of ECM (e.g. collagen IV) (Millichip et al., 1998; Yamamoto et al., 1999) and other targets, such as cell surface receptors (e.g. cell membrane-bound TNF α , HB-EGF, IL-6R, Fas ligand) (Muellberg et al., 1995; Black et al., 1998; Yamamoto et al., 1999; Primakov and Miles, 2000). Some ADAMs (including ADAM 1, 2, 3, 9 and 15) have been shown to mediate adhesion, most probably to integrins, by their disintegrin domain (Primakov and Miles 2000). ADAM 15 contains a conserved RGD motif within its disintegrin domain participating in adhesion to integrins such as $\alpha v\beta 3$ on adjacent cells or $\alpha_{IIb}\beta_3$ on platelets (Bauvois, 2001, Yamamoto et al., 1999).

The expression of some ADAMs, (e.g. ADAM 10 and 12), is upregulated in several tumors, e.g. of neuronal, gastric, colon, or breast origin (Yavari et al., 1998, Iba et al., 1999). Therefore ADAMs could contribute to tumor progression via mediating cell adhesion (Iba et al., 1999), or deadhesion (by competitive binding to integrins) as well as matrix degradation (Black and White, 1998).

1.1.2.3. Proteases of the plasminogen activator/ plasmin system

The plasminogen activator (PA)/ plasmin system is organized as an enzymatic cascade consisting of several enzymes, which catalyze downstream enzyme activation or inhibition. The end product of the cascade is plasmin, which is generated from its proenzyme plasminogen via limited proteolysis and by „plasminogen activators“. Plasminogen and its activators from urokinase-type (uPA) and tissue-type (tPA) are all serine proteases. UPA and tPA proforms become localized to the cell surface by binding to membrane-tethered uPA-receptor (uPA-R). Plasmin as well as uPA consist of two polypeptide chains connected by disulfide bonds and contain a serine protease domain, mediating activity in the catalytic center by a "catalytic triad" composed of serine, histidine and asparagin. The structure of plasmin consists of five „kringle“ domains, while uPA contains only one kringle and an EGF domain, which mediates binding to uPA-receptor (uPA-R). The uPA-R consists of three homologous domains and is anchored to

the cell membrane by a GPI anchor. It provides a binding site for uPA and tPA, and localizes their pro-forms at the cell surface (Andreasen et al., 1997).

Active plasmin generation results in fibrinolysis of fibrin clots in blood vessels, but also in mediation of cellular processes, such as cell migration and matrix degradation (Andreasen et al., 1997). Substrates of plasmin comprise several pro-MMPs, such as MMP-1, -3, -9, -12, -13 (Baramova et al., 1997) and MT1-MMP (Okumura et al., 1997), leading to their activation, and ECM molecules such as fibrin, vitronectin and fibronectin (Andreasen et al., 1997). UPA processes proteoglycans, FN, HGF and plasminogen (Chapman, 1997; Werb, 1997). In accordance with cell surface binding via uPAR, uPA staining at focal adhesion sites in different cell lines was detected (Hebert and Baker 1988; Andreasen et al., 1997). UPA-R also forms stable complexes with $\beta 1$ and $\beta 2$ integrins and thereby favors both, integrin adhesive function and cell motility (Wei et al., 1996).

1.1.2.4. Cathepsins

Cathepsins are lysosomal enzymes with mostly endopeptidase activity that require a reducing and slightly acidic environment for activity (Turk et al., 2000). Most cathepsins (cathepsin B, C, F, H, K, L, O, S, V, W, X) belong to the family of cysteine proteases; in contrast, cathepsin D is an aspartyl protease and cathepsin G a serine protease. Cathepsins of the cysteine protease type have a two-domain structure [left (L-) domain and right (R-) domain], that form a central V-shaped active site along the two-domain interface. The active center is formed by a catalytic cysteine and an adjacent histidine site. In their premature form, cathepsins contain a N-terminal propeptide, which lies within and thereby masks the active site cleft (Turk et al., 2001). Cellular expression of some cathepsins (i.e. cathepsin B, D, L) shows an ubiquitous pattern, whereas other cathepsins are expressed in a cell type-specific manner, such as cathepsin K in osteoclasts (Drake et al., 1996). Cathepsins degrade extracellular proteins, such as LN, FN, collagen I and IV (Koblinkski et al., 2000). In particular, cathepsins B, K and L display potent collagenolytic activity (Burleigh et al., 1974; Kirschke et al., 1982; Kagegawa et al., 1993; Bossard et al., 1996). In most cell types, cathepsins appear to be mainly involved in lysosomal protein degradation. However, under certain conditions such as failed trafficking upon neoplastic transformation, cathepsins may be released to directly degrade extracellular substrate or activate other proteases, such as uPA (Sloane et al., 1994).

Both intracellular and extracellular ECM degradation by cathepsins are thought to contribute to cancer progression. In some tumors, “misrouting” of cathepsins has been found, resulting in enhanced secretion and extracellular protein degradation, e.g., cathepsin D in breast cancer cells (Mountcourrier et al., 1990). In other tumors, membrane-anchoring of secreted cathepsins such as cathepsin B appears, which thereby focalizes its proteolytic activity (Sloane et al., 1994).

1.1.3. Matrix proteases - regulation of expression and proteolytic function

1.1.3.1. MMPs and TIMPs

The expression of MMPs and their tissue inhibitors of metalloproteinase (TIMPs) is tightly regulated by transcriptional and post-transcriptional events. Proteolytic activity of MMPs is controlled at the protein level by several activators and counterbalanced by a set of endogenous MMP inhibitors. In normal cells and times of the adult organism most MMPs are expressed at very low levels or absent. De novo expression of MMPs occurs upon cellular activation at situations of tissue remodeling, such as acute or chronic inflammation, wound healing and cancer as part of a general cell activation program (Mauviel, 1993; Coussens et al., 2001; Overall and Lopez-Otin, 2002). An exception is MMP-2, which is often constitutively expressed, particularly in stromal cells. Some MMPs are preformed and stored in secretory granules to become rapidly exocytosed upon cell activation, such as MMP-7 in epithelial cells (Dunsmore et al., 1998) or MMP-8 and -9 in neutrophil and eosinophil granulocytes (Stähle-Bäckdahl and Parks, 1993).

a) Transcriptional and post-transcriptional regulation

MMP and TIMP gene expression is cell-type-specifically regulated by several cooperating families of transcription factors, essentially c-fos and c-jun, ETS, and NF- κ B, which bind to different transcription sites, such as AP-1 (Activating Protein-1), PEA-3 (Polyoma Enhancer A-binding protein-3) and NF- κ B binding site, respectively. These transcription sites are controlled by multiple signaling pathways of cytokine and growth factor receptors, phorbol esters, transforming oncogenes, and integrins (Pendas et al., 1997; Gum et al., 1997; Westermarck et al., 1999). Among others, important cytokines and growth factors that upregulate MMP gene expression are IL-1 and IL-6, TNF- α , TGF- β , EGF, FGF, KGF, PDGF, or EMMPRIN (extracellular matrix metalloproteinase inducer). Inhibition of MMP de novo synthesis is induced by IL-4, IL-10, IFN- γ and TGF- β ,

vitamine A and corticosteroids in a cell type specific fashion (Mauviel, 1993; reviewed in Sternlicht and Werb, 2001).

MMP expression can be further induced by cell-cell or cell-ECM receptor signals (Kheradmand 1998; reviewed in Sternlicht and Werb, 1999). Binding of type I collagen to $\alpha 2\beta 1$ integrins induces MMP-1 expression in keratinocytes (Pilcher et al., 1999) or human skin fibroblasts via PKC- ξ and NF- κ B mediated signaling (Langholz et al., 1995; Xu et al., 1997). MMP expression can be further controlled by post-transcriptional mechanisms, such as differential stabilization of mRNA transcripts (Delany et al., 1995), alternative mRNA splicing or alternative polyadenylation (reviewed in Sternlicht and Werb 2001). Due to variations in the organization of the promotor regions, the response of MMP-genes in different cell types to a given stimulus may vary considerably in physiological and pathological conditions.

b) MMP activation

MMPs are produced as latent enzymes, whereby the inactive state ("latency") is maintained by an unpaired cystein sulfhydryl group covalently interacting with the catalytic zinc. For activation, this "cystein switch" requires opening, which can be achieved by limited proteolysis as well as by experimental ectopic perturbation using organomercurials. MMP activation can occur at different cellular locations: (1) intracellularly in vesicles, mediated by Golgi-associated furin-like proteases on MMPs that contain an additional furin-recognition site (MT-MMPs, MMP-11, -23 and -27) (Nagase, 1997); (2) extracellularly in solution, or (3) at the outer cell membrane mediated by other proteases (Strongin et al., 1995). MMP activation outside of the cell or at the cell surface occurs in two steps. First, the so-called "bait" region in the middle of the propeptide is attacked by different proteases, such as trypsin, plasmin, kallikrein, elastase or MMPs (Koblinski et al., 2000; Overall et al., 2001). Secondly, complete loss of the aminoterminal propeptide leading to full activation is mediated by other MMPs or by autoactivation (Birkedal et al., 1995; Nagase, 1997).

In particular, MT-MMPs have been identified as cell surface receptors that function as potent physiological activators of other MMPs. MT1-MMP cleaves and activates MMP-2 and MMP-13, and MT3-MMP activates MMP-2 (Strongin et al., 1995, Knauper et al., 1996). MMP-2, the best studied example, is resistant to activation by serine proteases, yet becomes activated by MT1-MMP through a multistep mechanism involving a tri-

molucelar complex consisting of MT1-MMP*TIMP-2*MMP-2 (Strongin et al., 1995)¹. Activated cell-surface MT1-MMP, still containing its prodomain (Cao et al., 2000), acts as a receptor for TIMP-2, which then binds by its C-terminal domain to the hemopexin domain of pro-MMP-2, thereby stabilizing this pro-enzyme. Next, an adjacent unbound MT1-MMP molecule initially cleaves the propeptide of the bound MMP-2 at Asn37-Leu38. The residual propeptide fragment is then completely removed by another MMP-2 molecule bound to $\alpha v \beta 3$ integrin, yielding a fully active, mature form of MMP-2 (Deryugina et al., 2001).

c) Inhibition of MMP activity

In the tissues, MMP activity is primarily limited by TIMPs, a family of small (20-29 kD) secreted proteins, which bind to active MMPs with a 1:1 stoichiometry (Birkedal-Hansen, 1995; Gomez et al., 1997). The four currently known members TIMP-1,-2,-3 and -4 contain each 12 cysteine residues, which form six disulfide bridges yielding in a conserved six-loop structure (Gomez et al., 1997). TIMPs block MMP activity via binding to the catalytic site of active MMPs by their N-terminal domain, thereby masking the substrate binding cleft (Gomez et al., 1997). TIMPs comprise an overlapping target spectrum and together inhibit the activity of most MMPs. On the other hand, TIMPs can bind and stabilize latent MMPs, thereby forming TIMP-2 / latent MMP-2, or TIMP-1 / latent MMP-9 complexes (Itoh Y and Nagase H, 1995; Kolkenbrock et al., 1995). TIMP-2 and -3 inhibit MT1-MMP activity, whereas TIMP-1 does not (Will et al., 1996). Besides MMP-inhibiting or -stabilizing functions, further tasks of TIMPs (TIMP-1 and -2) are promotion of cell growth by exhibiting growth factor-like activity (Gomez et al., 1997), and TIMP-3 induced cell death (Bond et al., 2000).

Additional MMP inhibitors are the $\alpha 2$ -macroglobulins and certain ECM degradation products such as a non-collagenous domain of type IV collagen that displays structural and functional similarity to TIMPs (Netzer et al., 1998). $\alpha 2$ -macroglobulin is an abundant plasma protein and a major inhibitor of MMPs in tissue fluids. It binds MMPs by forming an $\alpha 2$ -macroglobulin/MMP complex. This complex becomes then cleared via receptor-mediated endocytosis by fibroblasts, hepatocytes and macrophages (Sottrup-Jensen & Birkedal-Hansen, 1989). It is thought that inhibitors of MMP activity protect tissue and plasma proteins from uncontrolled degradation. While TIMPs act preferentially in the

¹ TIMP-2 is otherwise an inhibitor of MMPs, see 1.1.3.1., c).

cellular and tissue context, α 2-macroglobulins exert their actions preferentially in the plasma or exudates (Sottrup-Jensen & Birkedal-Hansen, 1989).

In experimental systems in vitro, MMP activity is inhibited by EDTA or the Zn^{2+} -chelator phenanthroline. Pharmacological MMP-specific Zn^{2+} chelators, such as the hydroxamate-based inhibitors, i.e. marimastat, display very efficient MMP-inhibitors in the nanomolar to micromolar range (British Biotech, Oxford, UK).

1.1.3.2. ADAMs

Little is known about the regulation of ADAM expression. Transcription of ADAM 8 is upregulated by stimulation with IFN- γ or LPS via cis-regulatory regions upstream of the ADAM 8 gene (Kataoka et al., 1997).

For maintenance of latency in protease function, ADAMs, like MMPs, contain an uncovalent cystein-zinc bond. Proteolytic activity of at least some ADAMs (ADAM 9, 10, 12, 15-17) is regulated prior to appearance at the cell surface by prodomain cleavage via Golgi-associated furin-type proteases (Bauvois, 2001; Yamamoto et al., 1999). Activation of ADAM sheddase activity was found to be inducible by the PKC activator PMA (reviewed in Yamamoto et al., 1999).

At the protein level, TIMP-1 inhibits proteolytic activity of ADAM 10, while TIMP-3 inhibits ADAM 10, 12 and 17 (Amour et al., 1998). Like all Zn^{2+} -dependent metalloproteinases, proteolytic activity is inhibited by EDTA or the Zn^{2+} -chelator phenanthroline, and, to some extent, by hydroxamate inhibitors including BB-2516 (Roghani et al., 1999; reviewed in Black and White, 1998).

1.1.3.3. Proteases of the plasminogen activator/ plasmin system

Expression of the components of the uPA-system is regulated by a large spectrum of hormones, growth factors and cytokines, or can be directly induced by activation of certain cellular oncogenes or by integrin-mediated signals leading to uPA-R upregulation (Chapman, 1997).

UPA-R-bound, as well as soluble pro-uPA becomes converted to proteolytically active uPA via cleavage of a single peptide bond resulting in a two-chain-structured protein. This step is catalyzed by several proteases, such as cathepsin B or L, or by plasmin in a positive feed back mechanism (reviewed in Andreasen et al., 1997; Koblinski et al.,

2000). Similarly, plasminogen becomes activated to proteolytically active plasmin by uPA or tPA by limited proteolytic cleavage.

Inhibitors of plasminogen activation are mainly the serpins (serine proteinase inhibitor) PAI-1 and, to some extent, PAI-2 (reviewed in Andreasen et al., 2000). For inhibition, PAI-1 and -2 interact with the active site of uPA-R-bound uPA and tPA by their surface-exposed reactive center loop in an 1:1 stoichiometry, thereby inhibiting i.e. uPA mediated ECM degradation (Caot et al., 1990; Laug et al., 1993). α 2-antiplasmin, the primary plasmin inhibitor, which mediates short plasmin half-life in blood and tissues, inhibits active soluble plasmin, however, interestingly, not plasmin bound to the cell-surface. It is assumed that plasmin generation occurs in proximity to the cell surface by uPA/ uPA-R complex. Since cell-surface-association of plasmin generated by uPA-R-bound uPA is most likely required for plasmin-dependent degradation of ECM proteins, the PA/ plasmin system might contribute to the progression of human cancer (reviewed in Andreasen et al., 2000).

1.1.3.4. Cathepsins

Similar to MMPs, cathepsin expression can be upregulated by several cytokines and growth factors, such as FGF, EGF, IGF or GM-CSF (Cavaillès et al., 1989; Ward et al., 1990). Also, cathepsin expression is upregulated in breast tissue fibroblasts upon interaction with collagen (Koblinski et al., 2000).

Conversion of lysosomal pro-cathepsins to their mature form occurs by proteolytical removal of the propeptide from the active site. This activation step is initiated at acidic pH by autocatalysis and accomplished by other proteases, such as tPA (Koblinski et al., 2000) or cathepsin D (Turk et al., 2000).

Cathepsin inhibition, on the other hand, occurs at very acidic pH drops accompanied with maturation of lysosomes causing denaturation, or by endogenous protein inhibitors, the cystatins, thyroptins or α 2-macroglobulin (Turk et al., 2000).

In summary, matrix degradation is caused by matrix-degrading enzymes, which in turn become activated by other proteases. Matrix degradation hence results from complex and, to date, incompletely understood cascades consisting of activating and inhibiting enzymes from different protease classes.

1.2. Cell migration in tumor invasion and metastasis

1.2.1. Basic mechanisms of cell migration

1.2.1.1. Two-dimensional cell migration

The basic mechanisms for integrin-mediated cell attachment and spreading described in chapter 1.1.1. are prerequisite for the process of cell migration. Lauffenburger and Horwitz established a 3-step model in 1996, which describes cell migration on two-dimensional (2D) extracellular protein surfaces: (1) Formation of filopodia and pseudopodia (at the leading edge) and attachment to the underlying matrix by newly forming focal contacts. This results in (2) stretching of the actin cortex, leading to generation of tension across the cell, followed by (3) retraction of the trailing edge (rear end), including the breakage of adhesive contacts, which finally allows forward translocation of the cell body (Regen and Horwitz 1992). For successful migration, these steps must occur in a cyclic manner. Migration is controlled by optimal concentration and affinity of the adhesion mediating receptors, the substrate concentration (Palacek et al., 1997) and strength of the integrin-cytoskeleton interaction or focal contact assembly, respectively (Lo et al., 1994). The ability to migrate is thus determined by the adhesivity of a cell to the substratum. Optimal migration rates are achieved at intermediate adhesion strength to the substrate (Huttenlocher et al., 1995). Investigations of haptokinetic cell migration across planar surfaces yielded valuable perceptions on the basic underlying mechanisms for migration, determining adhesion dependency as most important and also limiting factor for cell movement.

In addition, in 2D models, tumor cells expressing MMPs and other proteases generate proteolytic substrate degradation along their migration tracks on gelatin, matrigel or fibronectin (Nakahara et al., 1997; d'Ortho et al., 1998). However, it remains unclear, if generation of a lytic migration track is prerequisite for 2D-movement or an accompanying bystander event. Therefore, the 2D model does not represent a valuable model for degradation of ECM barriers, since, as a limitation, 2D surfaces do not reflect the complex texture of three-dimensional (3D) tissues.

1.2.1.2. Three-dimensional cell migration

Density, strength and flexibility of tissue components, such as a fibrillar collagen network (collagens I, II, III, X) provide resistance towards the migrating cells and therefore force cells to adapt to their environment. For fibroblasts, i.e., different morphologies for 2D and 3D movement were described. Heath and Peachy, 1989, observed that on a 2D surface the cell body develops a flat spread morphology and many undirectioned pseudopodia, a morphology, which is more reminiscent of keratinocytes, whereas in a 3D matrix fibroblasts form an *in vivo*-like elongated spindle-shaped morphology and cylindrical pseudopodial extensions oriented in the direction of movement. Fibroblasts and fibroblast-like cells like some tumor cells, such as HT-1080 fibrosarcoma, MV3 melanoma or MDA-MB-231 breast cancer cells develop a “mesenchymal”-type migration strategy, characterized by (i) a spindle-shaped morphology mediated by cortical F-actin and occasional stress fibers (Welch et al., 1990), (ii) $\beta 1$ integrin-adhesion and force generation-dependent migration (Doane and Birk, 1991) and (iii) the cleavage and remodeling ECM components mediated by MMPs and other proteases. In chapter 1.2.2.2., further mesenchymal characteristics are summarized. For many actively migrating cell types, i.e. fibroblasts, endothelial or cancer cells in a 3D environment, it is thought that matrix-degrading enzymes, such as MMPs, play a major role in overcoming matrix resistance by limited and regulated proteolysis (Basbaum and Werb, 1996). These findings have prompted a concept of proteolytic path generation favoring tumor cell dissemination within the tissues (Murphy and Gavrilovic, 1999; Friedl and Bröcker, 2000). For studies on MMP and other protease function on cell migration, a 3D ECM *in vitro* model was developed to allow visualization of cell migration within pure or complexed fibrillar type I collagen by time-lapse videomicroscopy or confocal microscopy (Friedl et al., 1997).

1.2.2. Cancer

1.2.2.1. Cancer cascade – overlook

Carcinoma cells are defined by their uncontrolled (1) proliferation (neoplasm) and (2) tendency to invade surrounding tissue (primary tumor) (Hanahan and Weinberg, 2000). To invade the neighbouring tissue, neoplastic cells must break through the underlying

basal membrane (BM) barrier and invade underlying interstitial tissue (Liotta et al., 1986). In order to disseminate, tumor cells enter the vascular or lymphatic system to arrest at distant sites and penetrate the vessel wall to enter and seed in other organs (metastasis) (Liotta et al., 1986; Hanahan and Weinberg, 2000). Once a colonizing tumor increases its size by proliferation, new blood vessel formation for nutrition of the metastatic site are induced, termed angiogenesis. Invasion, proliferation and angiogenetic processes are increased by adjacent reactive tissue, macrophages and fibroblasts, producing matrix degrading enzymes, cytokines and growth factors (“stroma reaction”).

Tumor metastasis is the major cause of cancer death. Therefore, therapy concepts were based on inhibition of basic mechanisms of invasion and metastasis, such as angiogenesis (Folkman et al., 1989), basal membrane penetration (Stetler-Stevenson et al., 1993), integrin function (Weaver et al., 1997) or proteolytic degradation of ECM (Stetler-Stevenson et al., 1993, Birkedal-Hansen, 1995; Coussens et al., 2002).

1.2.2.2. Multistep cascade of tumor invasion

In epithelial cancer, tumor cell interaction with the basement membrane is defined as the critical event initiating the metastatic cascade (Liotta et al., 1986; Liotta et al., 1991). It is thought that neoplastic cells proteolytically break through the normally insoluble BM layer, composed of interconnected components, such as collagen IV, heparin sulfate, proteoglycan and glycoproteins, including laminin, entactin or nidogen, and enter the underlying interstitial tissue by subsequent migration. The basic three-step concept, which is repeated in cycles, describes tumor penetration through BM and was established by Liotta et al, 1986: (1) tumor cell attachment/ detachment by cell-ECM receptors such as the laminin receptor (i.e. $\alpha 6\beta 1$ integrin) to laminin which forms a bridge to type IV collagen, (2) local degradation of matrix by tumor-cell-associated proteases, such as MMP-2 and MMP-9, and (3) tumor cell migration through the opened space modified by proteolysis. For subsequent successful invasion into the stroma, it is thought that single tumor cells detach from the primary tumor by downregulation of cell-cell-adhesion molecules such as E-cadherin and upregulation of the intermediate filament vimentin (Dandachi et al., 2000). The conversion from multicellular epithelial towards single-cell migration with fibroblast-like characteristics was termed “epithelial-mesenchymal transition” (Birchmeier and Birchmeier, 1995).

1.2.3. Contribution of MMPs and additional proteases to tumor invasion and motility

1.2.3.1. Pericellular localization of proteolytic activity in vitro

For successful and efficient invasion, tumor cells degrade matrix components in a highly regulated and subtle manner. Hereby proteases and integrins become concentrated to cell surface subcompartments, such as leading pseudopods ("invadopodia") to cooperate in a focalized manner (Nakahara et al., 1997; Ellerbroek et al., 2001; Mueller et al., 1999). The mechanisms to efficiently localize proteolytic capacity involve (1) redistribution of membrane-bound MT-MMPs and integrins towards pericellular ECM molecules, resulting in local clustering and co-clustering (i.e. MT1-MMP/ β 1 integrin, Belkin et al., 2001), (2) heterophilic binding and concentration of soluble MMPs at the cell surface (see Table 2), and (3) presence of cell surface receptors for MMP activating enzymes, such as uPA, plasmin(ogen), elastase or cathepsins (reviewed in Sternlicht & Werb 2001). The advantages of these localization mechanisms are (1) concentration of proteases within the vicinity of their targets, (2) limited but highly efficient proteolysis at discrete pericellular regions, (3) enhancement of MMP activation, and (4) limited access of MMP inhibitors. Consistent with these concepts, functional studies revealed that MT1-MMP recruitment to cellular protrusions, such as invadopodia, is required for cellular invasion (Nakahara et al., 1997) and that removal of MT1-, 2- and 3-MMP transmembrane domains generating soluble MP-MMPs reduces the ability of epithelial MDCK cells to promote cellular invasion (Hotary et al., 2000).

1.2.3.2. Proteases in experimental and in vivo studies of invasion

a) Protease-dependent invasion

Upon tumor progression, multiple classes of extracellular matrix (ECM)-degrading enzymes become upregulated and activated, including MMPs, serine proteases, and cathepsins (Birkedal-Hansen, 1995). Cell-derived proteolysis provided by these enzymes is thought to contribute to the degradation of basement membrane as well as interstitial tissue barriers including fibrillar collagen, the main constituent of the connective tissue matrix, thereby favoring tumor cell invasion. Blocking of MMPs and other proteases by pharmacological compounds reduced invasive tumor cell behavior in different migration and invasion models *in vitro*, such as ECM-coated polycarbonate filters, human amniotic

membrane or 3D type I collagen lattices (Mignatti et al., 1986; Kurschat et al., 1999; Ntayi et al., 2001). Also, tumor invasion was impaired in different experimental *in vivo* studies as detected by e.g. reduced tumor growth, invasion and spontaneous metastasis formation (DeClerck and Imren, 1994; Eccles et al., 1996; Coussens and Werb, 1996; Coussens et al., 2002).

b) Residual migration after inhibition of proteases

On the other hand, accumulating evidence suggests that, despite their established proinvasive function, ECM-degrading enzymes could be dispensable for tumor cell motility and dissemination. After blocking of MMPs or serine proteases, significant residual migration of individual cells is observed in different migration models (Deryugina et al., 1997a; Hiraoka et al., 1998; Kurschat et al., 1999; Ntayi et al., 2001). *In vivo*, protease inhibitor- or gene-based targeting of MMPs and serine proteases has prompted an unexpectedly weak benefit in some animal tumor models as well as clinical trials in humans, suggesting that a principal dissemination capacity remained intact (Della et al., 1999; Kruger et al., 2001; Zucker et al., 2000; Coussens et al., 2002). These studies, however, leave the question unresolved by which mechanisms cells in the absence of ECM-degrading capacity may maintain migration and dissemination within tissues. As one possibility, proteolytic compensation could be provided by enzymes not inhibited in these studies; alternatively, cells could sustain motility via unknown protease-independent compensation strategies.

1.3. Molecular mechanisms of cell migration in T lymphocytes

During trafficking and recirculation, T cells constantly transmigrate endothelial layers of blood vessels including densely packed basal membrane. For penetration, T cell-produced MMP-2 and -9 have been shown to be prerequisite, and accordingly, inhibition of MMP activity results in abolishment of T cell penetration of basal membranes (Leppert et al., 1995). T cells subsequently rapidly migrate through underlying interstitial tissue, thereby sensing biological mediators, such as cytokines or chemokine gradients. Migration of T cells within fibrillar ECM structures, such as 3D collagen type I (Friedl et al., 1998b) highly resembles movement characteristics described for amoeba of the lower eucaryote *Dictyostelium discoideum*. Hallmarks of „amoeboid“ migration over 2D surfaces display simple polarized cell shape, dynamic pseudopod protrusion and retraction, highly flexible

shape changes resulting in oscillatory movement and low-affinity crawling (Ueda and Kobatake, 1984; reviewed in Friedl et al., 2001). These amoeboid characteristics are in principle retained for T cells crawling through 3D interstitial tissue, such as low affinity gliding along paths of least resistance, squeezing or propulsion through matrix gaps („constriction ring“ formation, Lewis, 1934) and adaption to preformed matrix structures, respectively (Friedl et al., 1998b, Friedl et al., 2001). Consistent with low-affinity crawling of amoebas, T cells, although they express $\beta 1$ integrins, migrate independently of $\beta 1$ integrin function through 3D fibrillar collagen matrices and lack focal adhesions (Friedl et al., 1998b). Similar results, such as non- $\beta 1$ integrin-dependent migration in 3D collagen and adaptation to the preexisting meshwork of collagen fibers by formation of constriction rings and increase of pore diameter were further described for dendritic cells (Gunzer et al., 1997). To this end, it remains unclear, whether proteolysis is required for T cell migration through 3D interstitial matrix.

1.4. Diversity of cell migration mechanisms in different cell types

Due to differences in cell size and additional morphological parameter, cells may use different migration strategies in 3D ECM, such as fibrillar collagen. While small (ca. 8 μm in diameter in spherical shape) immune cells, such as T cells, migrate $\beta 1$ integrin-independently in vitro and in vivo (Friedl et al., 1998b; Brakebusch et al., 2002) by flexible, fast amoeboid movement, many tumor cells, large in size (approximately 20 μm in diameter, resulting in 10-20 times bigger volumes than T cells), migrate $\beta 1$ integrin-dependent (blocked by $\beta 1$ integrin antibody) and develop an elongated spindle-shaped cell morphology resulting in slow mesenchymal movement (Figure 2, adapted from Friedl et al., 1998). These differences result in either non-or low-adhesive interactions with collagen, observed in T cells, or in strong adhesive interactions with ECM, cell elongation and a mesenchymal-type movement. Low-adhesive and short-lived interactions of T cells and other leukocytes, such as dendritic cells with fibrillar collagen, allow for high speed, flexible stop-go-pattern and directional oscillations following preexisting collagen fibers, which lack matrix remodeling and may leave matrix fibers intact. Adhesive cell types, such as MV3 melanoma or HT-1080 cells develop stronger focal contacts resulting in slow and relatively persistent movement. Based on backscatter imaging of the collagen fiber network, tumor cells create tube-like proteolytic matrix defects that represent paths of least resistance (Friedl et al., 1997), while T cells appear to not modify the matrix network (Friedl et al, 1998).

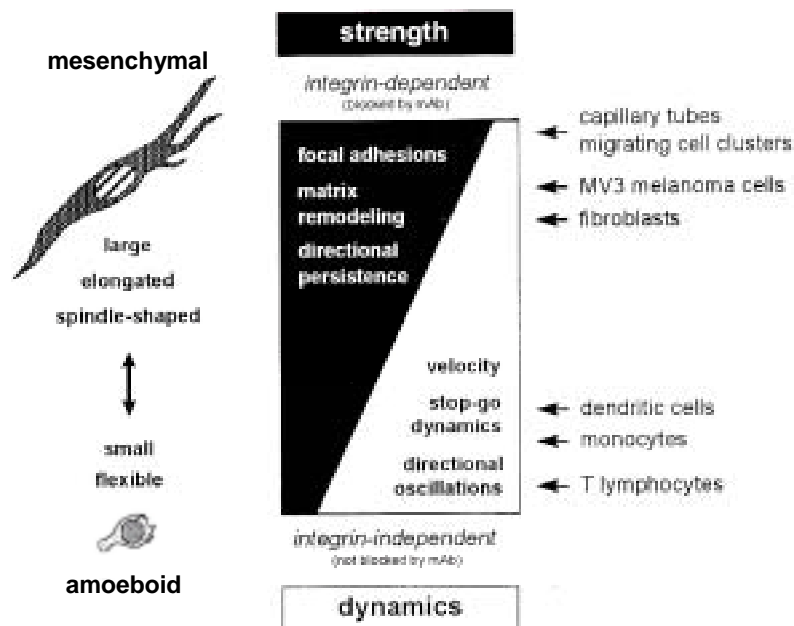


Figure 2. Model for different migration strategies on adhesive function in 3D collagen lattices. Locomotor phenotypes may constitutively vary from adhesive to non-adhesive mechanisms. Overlapping characteristics may exist. Adapted from Friedl et al., 1998a.

1.5. Purpose of the study

While most mobile cells in the body express matrix-degrading enzymes including collagenases, it remains unclear to what extent these proteases contribute to the migratory process. Therefore, based on the observations described in chapter 1.4., the purpose of this study was to investigate to what extent and how MMPs and other matrix-digesting and activating proteases contribute to the migration of highly invasive, metastatic and proteolytic tumor cells as well as leukocytes. To provide a matrix barrier that should be cleaved by proteases, a 3D type I collagen lattice was used. Some key findings were confirmed and extended by an intravital mouse dermis model.

The specific questions were:

- To what extent can proteases (collagenases) degrade the 3D type I collagen lattice?
- How do integrins and MMPs cooperate to provide adhesion and matrix degradation in the process of cell translocation?
- At what subcellular location do collagenases degrade collagen?
- To what extent does overtransfection of MT1-MMP contribute to tumor cell migration?
- Do MMP inhibitors alone reduce or inhibit proteolysis and migration of tumor cells, such as MV3 melanoma, HT-1080 fibrosarcoma and MDA-MB-231 breast carcinoma cells, or do other proteases provide compensatory proteolysis and migration?
- Do leukocytes use proteases for migration in fibrillar type I collagen in a similar manner as tumor cells?

In the course of the studies, it became apparent that blocking of proteolysis did not result in reduced migration activities for these tumor cell lines. Therefore the following questions emerged:

- Which compensation strategies exist in protease-blocked tumor cells and what might be the cellular compensation mechanism?
- How does the distribution of cell surface molecules involved in collagenolysis and migration change upon inhibition of proteases?
- Are the migration mechanisms of tumor cells in 3D collagen matrices similar to in vivo movements within interstitial tissue?

2. RESULTS

2.1. Expression and function of β 1 integrins and matrix proteases in MV3 melanoma and HT-1080 fibrosarcoma cells

2.1.1. Expression of β 1 integrins, MMPs and other proteases and endogenous protease inhibitors

Since the role of matrix-degrading proteases for integrin-dependent tumor cell migration was examined, initial experiments on expression, surface distribution and activation state of cellular proteases were performed using flow cytometry (FACS), Western blot, zymography as well as RT-PCR.

2.1.1.1. Cell surface expression of β 1 integrins, MMPs and uPA

The baseline expression of β 1 integrins and proteases on the cell surface as well as changes of expression induced by cell interaction with fibrillar collagen were studied for cells from conventional liquid culture in plastic dishes as compared to 3D collagen lattices after release by collagenase digestion (Fig.3, **color plate 1**). β 1 integrins were expressed at high levels on MV3 and HT-1080 cells in both, liquid culture and collagen culture, consistent with published data (Maaser et al., 1999; Yamada et al., 1990). In all cell types, surface expression of MT1-MMP, MMP-2, TIMP-2, uPA, uPA-R and PAI-1 was detected (Fig. 3). While MT1-MMP, uPA, uPA-R and PAI-1 were expressed at higher levels on all cells, minor expression on 10-50% of the cells was apparent for MMP-2 and TIMP-2. Culture in 3D collagen led to an increase in surface levels of MMP-2 and TIMP-2, while PAI-1 decreased and all other protein levels remained unchanged in all cell types. Compared to the neo-vector transfected control cells (HT-neo), MT1-MMP overexpressing HT-1080 (HT-MT1) cells showed strongly increased MT1-MMP cell surface staining (Deryugina et al., 1998). Consistent with increased MT1-MMP expression, HT-MT1 cells exhibited enhanced MMP-2 and TIMP-2 accumulation at the cell surface. This result is in agreement with the finding of TIMP-2 and MMP-2 accumulation by MT1-MMP (Strongin et al., 1995). Together, flow cytometric analysis showed expression of MT1-MMP, MMP-2, TIMP-2, uPA, uPA-R and PAI-1 on the cell

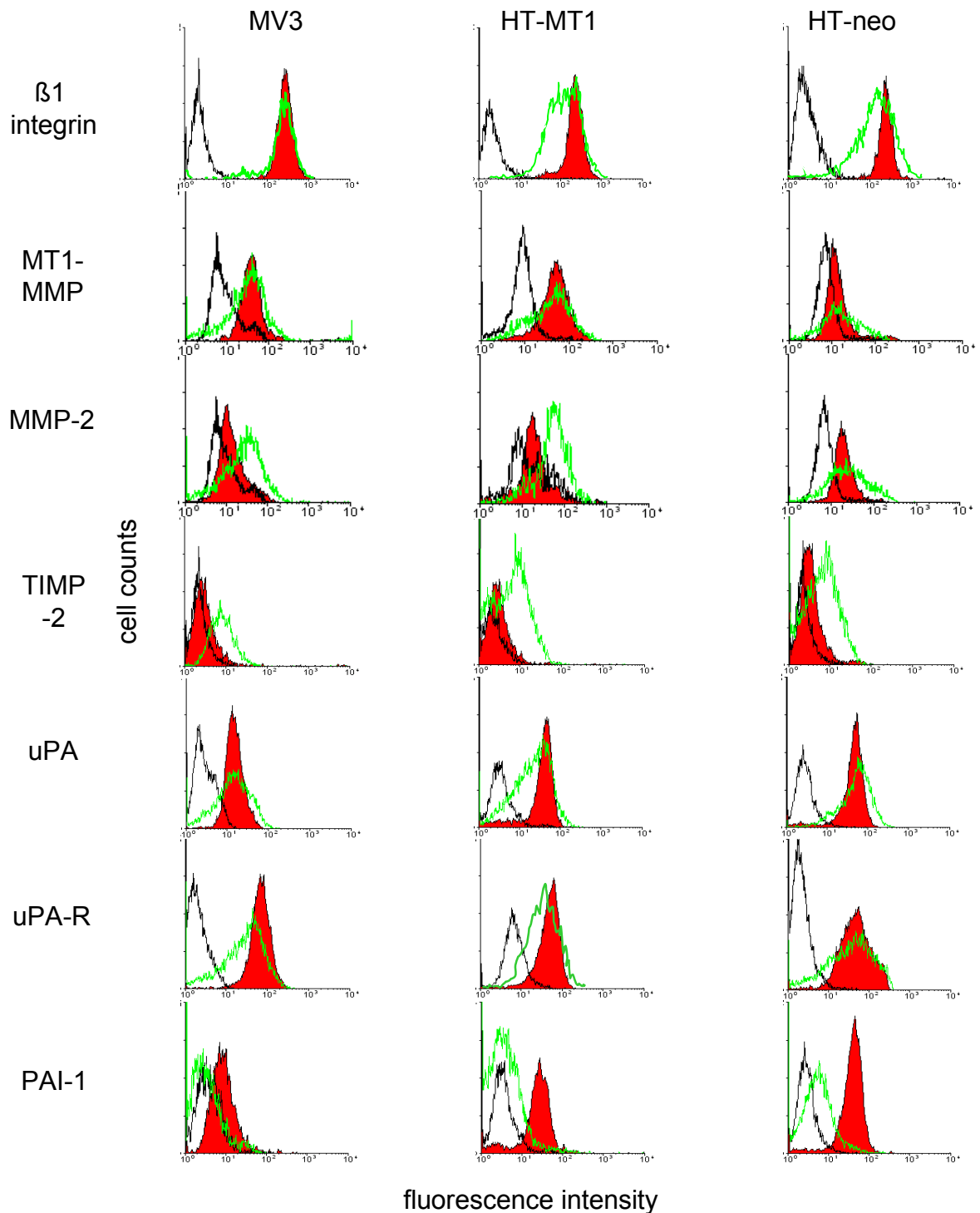


Figure 3. Cell surface expression of $\beta 1$ integrins, proteases and protease inhibitors from tumor cells migrating in liquid culture versus 3D collagen. Cells cultured on plastic or in collagen lattices for 20-24 hr were detached by EDTA or released by collagenase (type VII) digestion. Cells were labeled by primary mouse monoclonal or rabbit polyclonal Ab or IgG and secondary FITC-conjugated anti-mouse or -rabbit IgG, and monitored by flow cytometry. Staining by isotypic control antibody is shown as black line, culture on plastic as red area, and culture in collagen as green line. No cell surface expression was detected for PAI-2 and cathepsin D (not shown).

surface of MV3 and HT-1080 cells and, upon collagen culture, upregulation for MMP-2 and TIMP-2 and downregulation of PAI-1. As will be shown in chapter 2.1.2, collagen culture supported continuous and long-term migratory activity in the cells, hence representing not only a contact state to ECM, but also a mobile state. Since alterations in surface levels might be accompanied by functional changes, in e.g. motility, the activation state of selected proteases was investigated next.

2.1.1.2. Detection of MMP protein levels by Western blot

When activated, full-length (“immature”) MMP-2 and MT1-MMP become cleaved and undergo transition to defined low-molecular weight products. On cells cultured in collagen, MMP-2 was detected as the immature (68 kD), intermediate (64 kD) as well as fully activated (62 kD) form in HT-MT1 and HT-neo cells, while only minor amounts of activated MMP-2 were detected in MV3 cells (Fig. 4a).

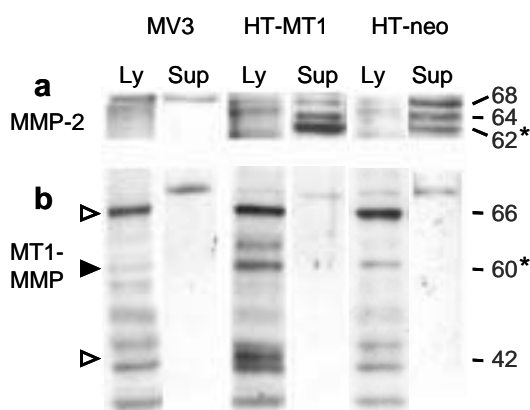


Figure 4. Protein expression of MMP-2 (a) and MT1-MMP (b) from tumor cells migrating in 3D collagen by Western blot. Total cell lysates (Ly) and supernatants (Sup) from cell culture in 3D collagen lattices were used for SDS-PAGE and Western blotting. Note the increased staining of activated (*) MMP-2 and MT1-MMP in HT-MT1 as compared to HT-neo and MV3 cells. Resulting protein bands from cell samples from collagen culture were less intensive than from conventional culture on plastic (not shown). This weaker staining is probably due to loss of cell fragments upon migration-associated shedding into the collagen matrix.

Most prominent activation products of MMP-2 were detected in HT-MT1 cells confirming the concept of MMP-2 activation by cell-surface expressed MT1-MMP (Strongin et al., 1995). MMP-2 was present mainly in supernatants of cell-containing collagen lattice, while minor amounts were detected in cell lysates. MT1-MMP (66 kD) was expressed by MV3 and HT-1080 cells (Fig. 4b); its processed active (60 kD) form was found in HT-neo and most strongly in HT-MT1 cells, which additionally showed the autocatalytic (42 kD) form. No MT1-MMP activation fragments were detected in MV3 cells. MT-1 MMP was present in cell lysates from all three cell lines, but not in the supernatants (Fig. 4b). These findings confirm active MT1-MMP as exclusive cell surface protein, while latent and activated MMP-2 is also secreted. Active proteases were detected in HT-neo and, most strongly, in HT-MT1 cells, but not in MV3 cells.

2.1.1.3. Detection of MMP function and activation by native collagen zymography

Zymography is a highly sensitive method to detect MMP function and activation state especially suitable for gelatinases MMP-2 and MMP-9 (Kleiner and Stetler-Stevenson, 1994). After 24 hr of cell culture in 3D collagen, MMP-2 and also MT1-MMP expression and activation were examined by collagen zymography (Fig. 5).

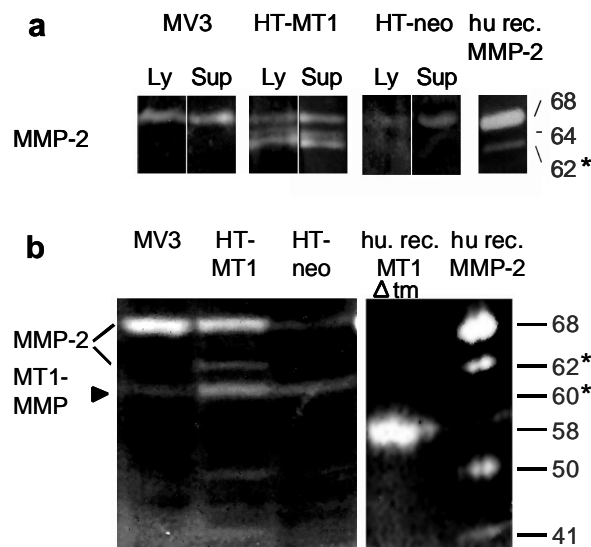


Figure 5. MMP function and activation from cells migrating in liquid culture versus 3D collagen in zymography. (a) Type I collagen zymography was performed for total cell lysates (Ly) and supernatants (Sup) of cells after culture in 3D collagen lattices for 24 hr. The collagen substrate was degraded by latent (68 kD), intermediate (64 kD) and active (*, 62 kD) forms of MMP-2; MMP-9 was detected occasionally yet not consistently (not shown). (b) Zymography was performed from cell lysates (liquid culture) for 24 hr; as positive controls, recombinant human MT1-MMP (soluble pro-form 58 kD, lacking the transmembrane domain { Δ tm}) and recombinant MMP-2 were used. Recombinant MMP-2 was fragmented further to 50 kD and 41 kD cleavage products.

Activated MMP-2 forms were detected from supernatants and cell lysates of HT-neo, and, more prominently, of HT-MT1 cells, while MV3 cells showed no activated forms (Fig. 5a). In liquid culture, besides MMP-2 an additional collagenolytic 60 kD (*) band was detected in HT-MT1 cells (Fig. 5b), corresponding to the size of active MT1-MMP (in Fig. 4b, 60 kD, *). As positive control, the collagenolytic band at 58 kD was obtained from recombinant MT1-MMP lacking the 2 kD transmembrane and cytoplasmic portion (Fig. 5b). Together, the collagen zymography data suggest that in MV3 cells cell-associated MMP-2 represent the inactivated form of MMP-2, while HT-neo and more pronounced, HT-MT1 cells contain both latent and activated MMP-2 and MT1-MMP. The data also show, that the type I collagen used as migration substrate in following studies is efficiently degraded by both, MMP-2 as well as MT1-MMP.

2.1.1.4. Detection of mRNA expression by RT-PCR

To detect a spectrum of additionally expressed proteases including enzymes that escape detection by zymography (Deryugina et al., 1997a and 1998; Ntayi et al., 2001), mRNA expression of proteases from different classes was examined, as MMPs, ADAMs, cysteine or aspartatic proteases, such as cathepsins, and serine proteases (Fig. 6).

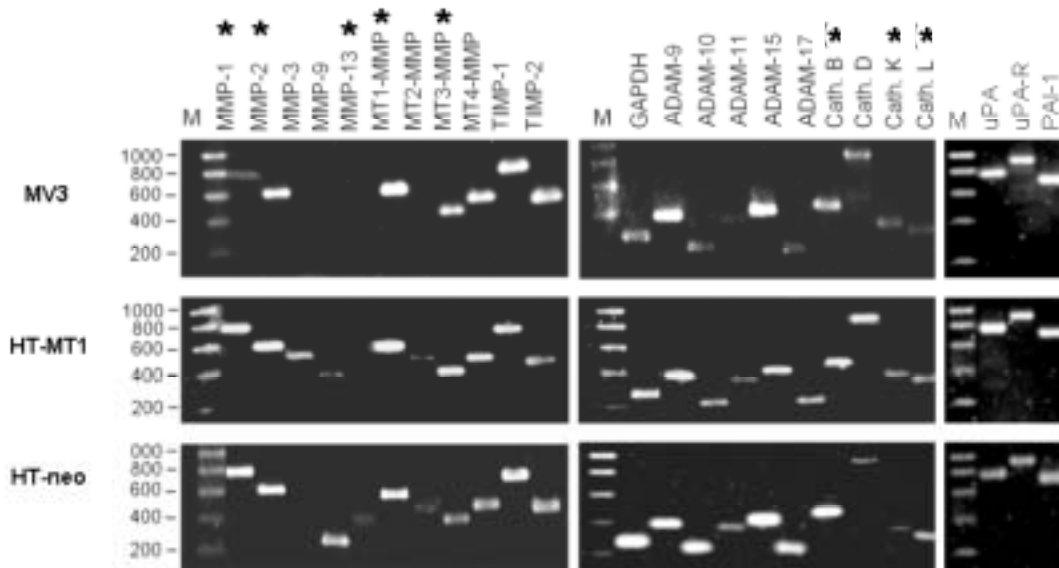


Figure 6. mRNA expression of selected tumor-associated proteases and endogenous protease inhibitors by MV3 and HT-1080 cells from liquid culture (RT-PCR). Fragment lengths conformed to the expected length using primers as summarized in Table 4 (chapter 4.14.). For HT-1080 and MV3 cells, mRNA expression was detected for ADAM-12, but not for PAI-2 and tPA (not shown). Increased fragment length of MMP-9 in MT1-MMP transfected HT-1080 cells was caused by the plasmid inserted putatively within the MMP-9 gene region (personal communication E. Deryugina). *, enzymes known to cleave fibrillar type I collagen.

All of these proteases were previously implicated in pericellular ECM degradation or activation of ECM degrading enzymes (Montcourrier et al., 1990; Aimes et al., 1995; Ohuchi et al., 1997; Holmbeck et al., 1999; Sassi et al., 2000). MV3 and HT-1080 cells all contained mRNA of most of the examined MMPs, TIMPs, ADAMs, cathepsins as well as members of the PA/ plasmin activator system. In HT-1080 cells transfected with MT1-MMP, mRNA for MMP-9 and -13 was decreased compared to neo-vector transfected HT-1080 control cells, while MMP-3 was increased. In conclusion, MV3 and HT-1080 cells expressed a spectrum of proteases from different classes including multiple enzymes with reported collagenolytic activity, most of which belong to the family of MMPs, but also cathepsins (Fig. 6, asterisks). The modulation of expression of MMP-3 and 13 could result from MT1-MMP-induced changes in intracellular signaling, direct or

indirect alterations in surface receptor expression or function if these receptors are MT1-MMP substrates. Additionally, modulation of expression might have been caused by the insertion of plasmid DNA in functional gene regions (as for MMP-9, E. Deryugina, personal communication), such as promoter regions or within exons.

2.1.2. Visualization of β 1 integrin-dependent and proteolytic cell migration in 3D collagen matrices

For examination of migration, both HT-1080 and MV3 cells represent suitable cell lines since they develop spontaneous migration in a fibrillar collagen lattice. Cell morphology and the function of β 1 integrins and proteases were visualized for migrating HT-1080 cells. The surface distribution of β 1 integrins and MT1-MMP was investigated with particular reference to their interaction with collagen fibers. Since preliminary studies with HT-MT1 cells showed best surface staining and activation of MT1-MMP, most of the following studies were performed with these tumor cells and confirmed for HT-neo and, in part, MV3 cells.

2.1.2.1. β 1 integrin-dependent cell contact to the collagen matrix: fiber pulling and reorganization

For detection of dynamic and migratory interactions of tumor cells with collagen, cells were polymerized into 3D collagen lattices and monitored by time-lapse videomicroscopy. β 1 integrin-dependent migration of HT-MT1 cells was characterized by polarized binding of the leading edge to collagen fibers generating traction and spindle-shaped elongation of the cell body (Fig. 7a, movie 1), as previously shown for MV3 cells (Friedl et al., 1997). Pseudopod protrusion was accompanied by filopodial ruffling (Fig. 7a), and followed by detachment of the trailing edge and cell translocation (Fig. 7a, movie 1). Both polarization (inset, right) and migration (black bars, left) were abrogated in the presence of adhesion-perturbing anti- β 1 integrin mAb 4B4 (Fig. 7b) resulting in non-productive membrane ruffling towards collagen and confirming β 1 integrin-mediated force generation and migration (movie 2).

With their leading front cells bundled and pulled collagen fibers (Fig. 7c,d, **color plate 2**; white arrowheads, movie 3); the detachment of the forward moving trailing edge resulted in a newly generated circumscribed matrix defect that was bordered by aligned multi-fibrillar collagen bundles (Fig. 7d, asterisks, movie 3). Cell translocation and detachment

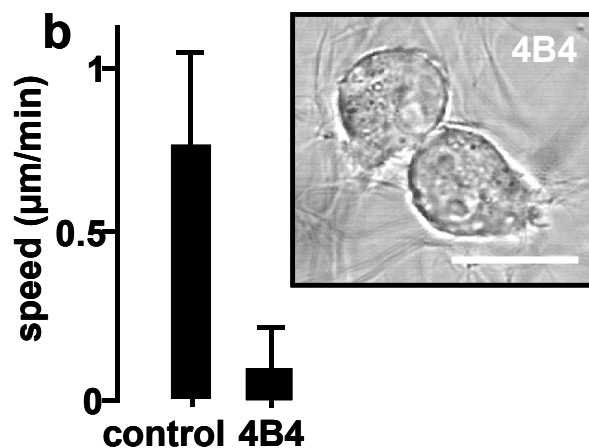


Figure 7 (c,d color plate 2). Spontaneous, $\beta 1$ integrin-dependent migration of HT-1080 cells in 3D collagen lattice. (a) Morphology of migrating HT-MT1 cell incorporated in 3D collagen lattice, as assessed by videomicroscopy (time frame: 52 min). (b) Inhibition of migration by adhesion-perturbing anti- $\beta 1$ integrin antibody 4B4. HT-1080 cells were co-polymerized into a 3D type I collagen lattice in the presence or absence of adhesion-perturbing anti- $\beta 1$ integrin antibody 4B4 and cell migration was detected by time-lapse videomicroscopy for 20 hr. Paths of 40 individual cells were obtained by computer-assisted cell tracking and migratory speed was calculated (left). Inhibition by anti- $\beta 1$ integrin antibody results in spherical morphology and immobilization as detected by confocal time-lapse microscopy (right). (c, color plate 2) 3D reconstruction of calcein-stained HT-1080 cell by time-lapse confocal microscopy and (d) reflection of a central slice in the process of migration (time frame: 60 min). Fiber traction and bundling (white arrowheads), deposition of cell fragments (black arrowhead), and newly formed matrix defect (asterisk). Bars, 20 μm . Black arrows indicate the direction of migration.

were accompanied by the shedding of surface determinants (including MMPs, see chapter 2.1.2.2.) and the release of cell fragments along the migration track (Fig 7c, black arrowhead). The localized ECM defect in the wake of the cell may indicate constitutive proteolysis upon migration, supporting the concept of focalized pericellular proteolysis (Basbaum and Werb, 1996; Murphy and Gavrilovic, 1999).

Figure 8 (color plate 2). Subcellular distribution and shedding of $\beta 1$ integrins, MMPs and organization of the actin cytoskeleton. HT-1080 cells migrating in 3D collagen lattices for 6-15 hr were fixed with either methanol (a-e) or 4% PFA (g-h) and permeabilized with 0,1% Triton-X100 (h), and stained for confocal fluorescence microscopy (a-e, g-h). MT1-MMP, MMP-2, rabbit IgG isotype control and F-actin are represented in red, while $\beta 1$ integrins are stained in green, colocalization appears in yellow. Matrix fibers and cellular structures were detected by confocal reflection mode. Black arrows, direction of migration. Bars, 20 μm . (f) Conditioned supernatants from HT-1080 cells containing soluble MMP-2 was added to plastic wells uncoated (1), coated with collagen (2), BSA (3) or both collagen and BSA (4) and incubated overnight at 4°C. The remaining supernatant containing unbound MMP-2 was analyzed by Western blot.

Figure 7

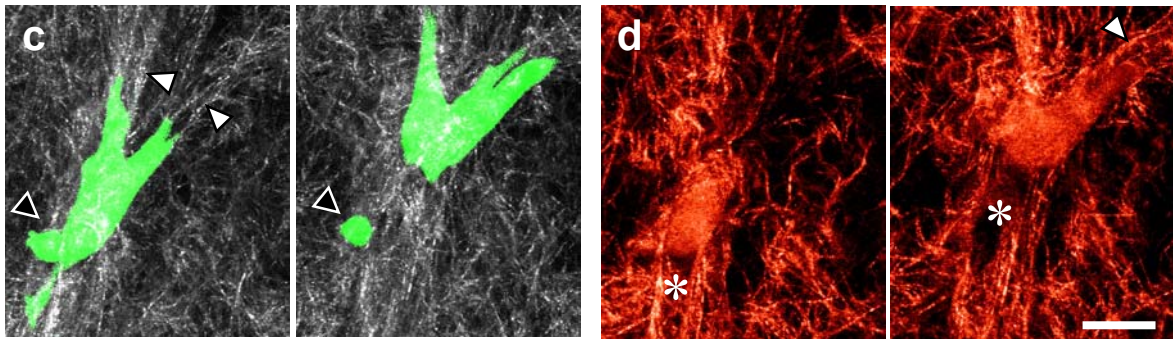
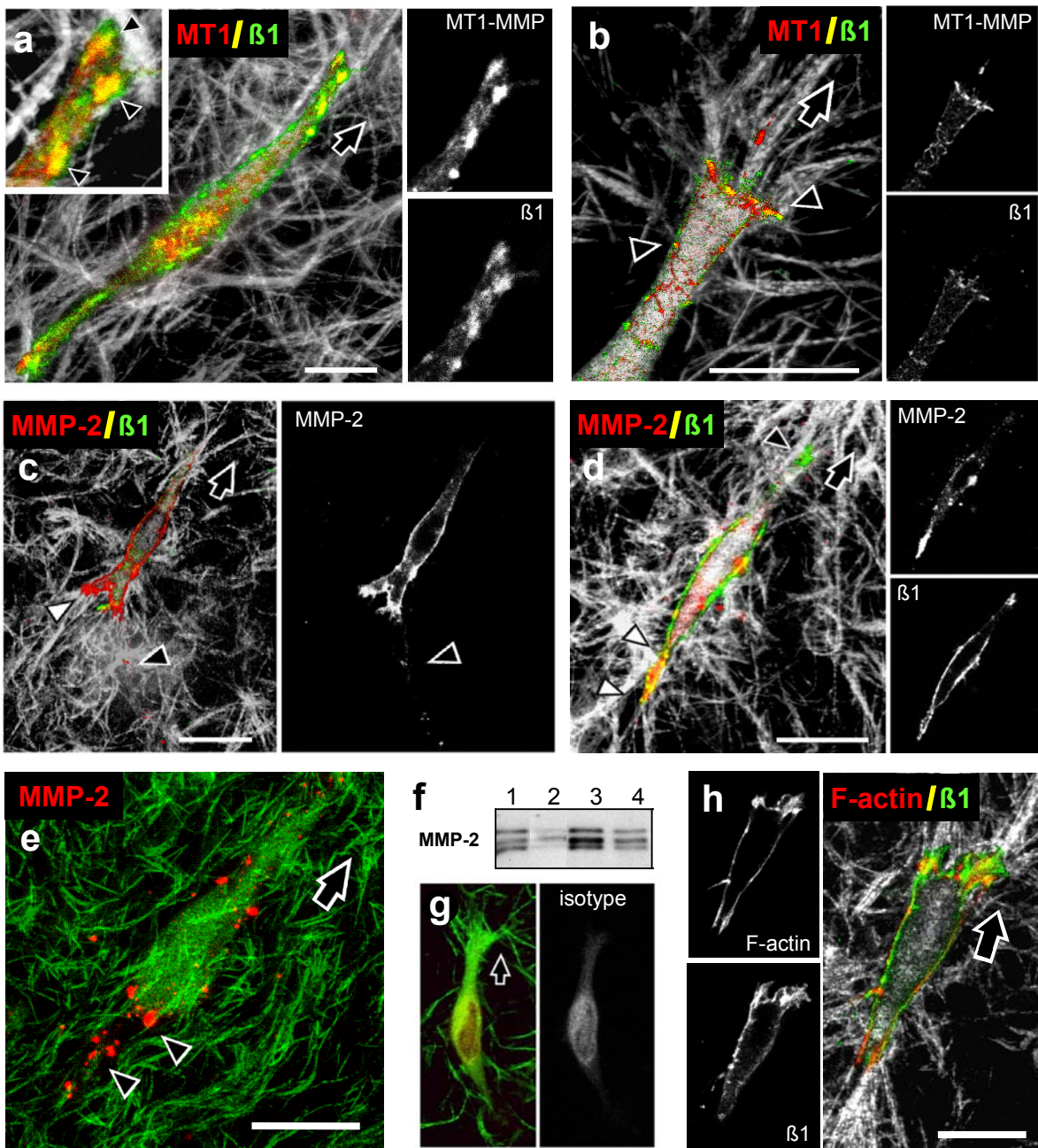


Figure 8



2.1.2.2. Subcellular distribution of MMPs, β 1 integrins and organization of the actin cytoskeleton; association of MMPs with collagen

To understand how integrins and proteases contribute to the β 1 integrin-dependent fiber pulling and localized proteolytic matrix defect generation, subcellular surface distribution of β 1 integrins and MT1-MMP and MMP-2 in interaction to collagen fibers was detected (Fig. 8, **color plate 2**). Distribution of MMPs and integrins at this resolution level was already shown for cells moving on top of a ECM coated surface (Belkin et al., 2001) but not, however, for cells migrating in a 3D environment. β 1 integrins and MT1-MMP were co-clustered at interaction sites to collagen fibers representing the location of initial fiber binding and traction towards the leading edge (Figs. 8a,b). MMP-2 only partially co-localized with β 1 integrins and was located predominantly at the trailing edge in linear as well as clustered distribution (Figs. 8,c-e). Additionally, MMP-2 deposits were detected along reorganized migration tracks (Figs. 8c,e, black arrowheads). To confirm direct biochemical association of MMP-2 with native type I collagen (as already described at Allan et al., 1995), remaining MMP-2, after it had been placed on top of a collagen matrix, was examined, showing substantial MMP-2 absorption by collagen (Fig. 8f, compare lanes 2 with 1, and 4 with 3). β 1 integrins were further co-clustered with F-actin at interactions with collagen fibers (Fig. 8h), indicating substrate-driven actin nucleation. Clustered distribution of F-actin was comparable to the actin pattern detected in fibroblasts incorporated in 3D in vitro and in vivo tissues (Welch et al., 1990; Doane and Birk, 1991). These findings confirm clustering of β 1 integrins in focal clusters at collagen fiber binding sites (Friedl et al., 1997) and indicate cooperation with collagenolytic MT1-MMP. The localization of MT1-MMP and MMP-2 with β 1 integrin at interactions to collagen fibers and the phenomena of path generation suggested the contribution of these proteases to proteolytic migration.

2.1.3. Structural degradation of collagen by HT-1080 and MV3 cells

2.1.3.1. Collagen structure in acryl amide gel (zymography) and fibrillar 3D collagen matrix

In order to find the most appropriate detection method for collagenolytic activity, it was necessary to compare the biophysical structures of collagen, incorporated in polyacrylamide gel as used for zymography (compare Fig. 5), with the collagen lattice used here as migration substrate. Confocal reflection analysis of these two substrates revealed the fibrillar structure of the 3D collagen substrate (left, upper lane: xy position) in comparison to a dot-like structure of poorly organized collagen lacking fibrils within polyacrylamide (right, xy) (Fig. 9). The xz-images represent the dot-like structure of the cross-sectioned fibrillar collagen (left) reflecting its higher degree of organization by bigger diameter as compared to the globular structure of acrylamide-complexed collagen. To provide a most appropriate substrate for the detection of collagenolysis, the fibrillar 3D collagen lattice was used to detect collagenolytic activity in addition to zymography.

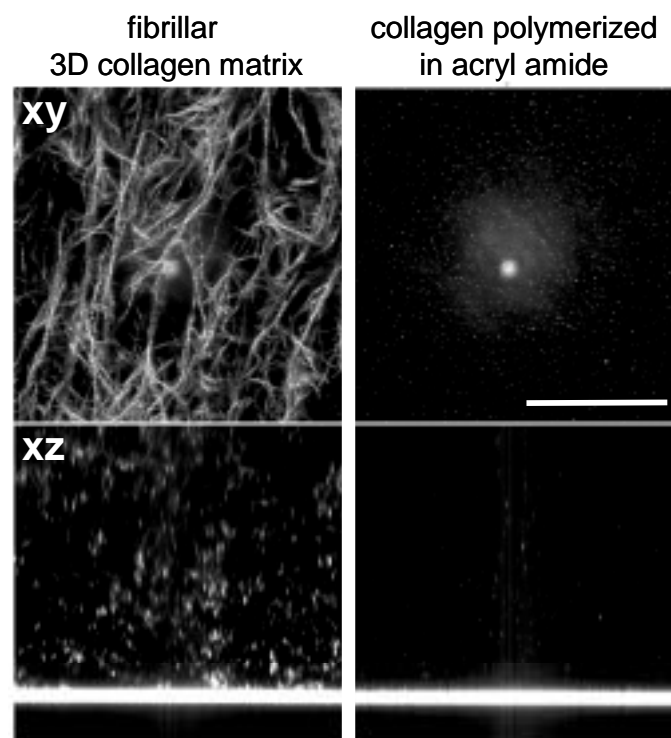


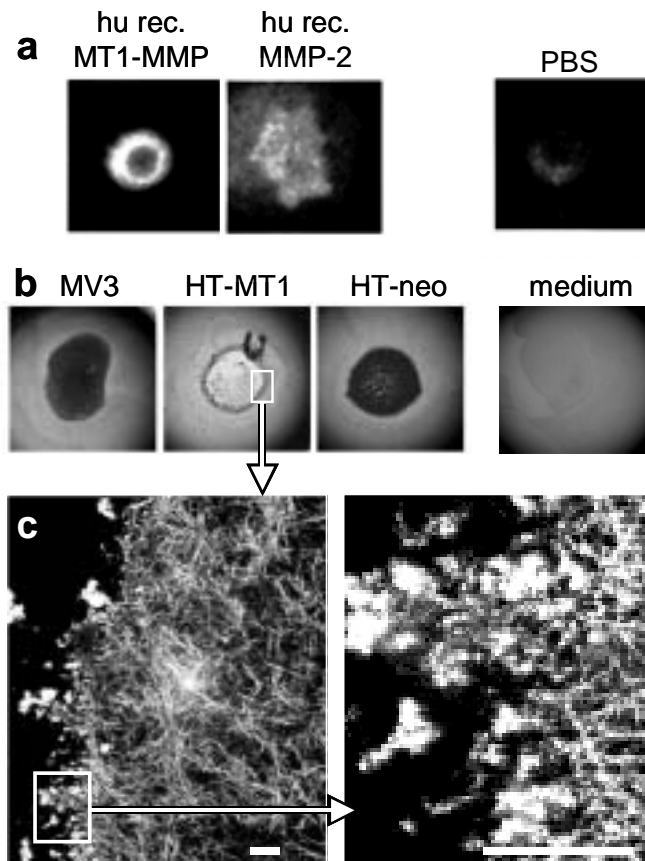
Figure 9. Biophysical organization of type I collagen: comparison of 3D fibrillar matrix to collagen in polyacrylamide gel. Samples were analyzed by confocal reflection microscopy in xy and xz position. The fibrillar structure of a native 3D collagen type I lattice (left) as compared to diffusely spot-like collagen structure within acryl amide (right) from zymography. Bar, 100 μ m.

2.1.3.2. Degradation of 3D collagen matrix

a) Structural breakdown of matrix scaffold

First, structural collagen degradation assays were established using human recombinant MT1-MMP and MMP-2 with capability for autoactivation (Prof. H.Will, InVitek, personal communication). Incubation of 3D collagen with both MT1-MMP and MMP-2 resulted in collagen degradation and reduced staining by Coomassie Blue, in comparison to PBS (Fig. 10a). Placing a drop of cells onto 3D collagen lattices followed by incubation and staining with Coomassie Blue resulted in the appearance of a dark cell protein-rich spot (MV3 and HT-neo). Depending on the collagenolytic capacity and in correspondence with the expression data shown before, partial (HT-neo) or complete (HT-MT1) lysis of the underlying collagen lattice occurred (Fig. 10b). Incubation of a medium drop indicated only minor heterogeneity in Coomassie staining intensity. Structural breakdown of the collagen matrix caused by HT-MT1 cells was examined by confocal reflection for microscopic fiber degradation (Fig. 10c). The zone of complete digestion of the matrix structure was bordered by a rim containing bundled and aggregated collagen material as well as, at 10 μm distance, non-degraded collagen fibers. In conclusion, recombinant MMPs and also living cells, according to their collagenolytic capabilities, degrade 3D fibrillar collagen matrix, which is detectable on a macroscopical and microscopical level.

Figure 10. MMP- and cell-associated degradation of 3D collagen matrices. (a) Recombinant MT1-MMP and MMP-2 or PBS alone were added on top of the center of a 100 μm thick fibrillar 3D collagen lattices, incubated for 40 hr, and then inversely detected for collagenolysis by Coomassie Blue staining. (b) Cells were placed on top of 3D collagen lattices and treated as in (a). Cell-bound lysis was detectable by partial or complete lysis of the underlying collagen lattice. The dark center within the lysis zone represents the cellular protein content. Diffuse proteolysis around the cell-associated blue staining and lysis, respectively, was detected for all cell types at similar levels. As a negative control, medium alone caused a minor reduction of Coomassie staining. (c) Microscopic analysis of degraded and reorganized collagen was performed by confocal reflexion. Bar, 20 μm .



b) Quantitative detection of structural matrix breakdown

To measure collagenolysis quantitatively, a 3D fluorometric fluorescein-(FITC)-release assay was developed, detecting the degradation of FITC-labeled collagen fibers by cells in close contact to the labeled collagen (Fig. 11a, **color plate 3**). Upon migration within FITC-collagen, MV3 and HT-1080 (HT-MT1 and HT-neo) cells released FITC to different extents into the supernatant (Fig. 11b, left). HT-MT1 cells showed most potent FITC-release (20%), consistent with the increased expression pattern of activated MMPs and the observed macroscopic and microscopic collagen fiber degradation (Figs. 10b and 7d). HT-neo released about one third FITC released by HT-MT1 cells, and MV3 cells approximately 2% of the total FITC content. Interestingly, virtually all proteolytic activity remained cell surface-associated with almost no proteolytic activity detectable in the supernatant, as shown for HT-MT1 cells (Fig 11b, right). In the absence of FCS (containing collagenases and their natural inhibitors from blood of the fetal calf), the capacity for cell-surface-associated proteolysis was reduced by 20% while the order of magnitude remained unchanged (Fig 11b, right).

2.1.3.3. Distribution of proteolytic activity in situ: cleavage of collagen fibers

Next it was investigated, if MMPs co-clustered with $\beta 1$ integrins at fiber binding sites were proteolytically active to focally degrade collagen fibers. Focal cleavage or partial degradation of collagen fibers associated with quenched FITC-molecules results in an increase of focal fluorescence at absorption of appropriate laser light. At the leading edge of migrating cells in FITC-labelled collagen, focal fluorescence was localized at lateral portions of growing pseudopods (black arrowheads) and at locations of circular fiber insertions and cell constrictions (white arrowheads) (Fig. 12, **color plate 3**). Highest intensity of focal fluorescence was detected at the growing leading edge of the cells, followed by decreasing fluorescence intensity at the middle part of the cell body and the trailing edge. This finding is in accordance with the functionality of collagenases being active at locations of matrix barriers and may provide a mechanism on how proteolytically modified matrix widenings facilitate cell gliding through through matrix barriers.

Figure 11. In situ collagenolysis by migrating cells within FITC-labeled collagen matrix.

(a) Distribution of and physical cell contact with FITC-labeled collagen fibers, as shown by confocal reflection (gray) and FITC-fluorescence (green). Cell body and all collagen fibers were detected by confocal reflection, while FITC signal was limited to collagen fibers only. Bar, 20 μ m. (b) Quantification of collagenolysis was carried out by a FITC-collagen release assay. FITC-incorporated collagen samples contained either 1×10^5 migrating cells or the conditioned concentrated media of 1×10^5 cells. The collagen degradation assays were carried out in the presence of FCS, unless indicated otherwise. FITC-release from the collagen lattice was quantified by fluorometric analysis of the supernatant. As a negative control, ConA activated migrating T cells did not release FITC above background levels (compare to Fig. 28a).

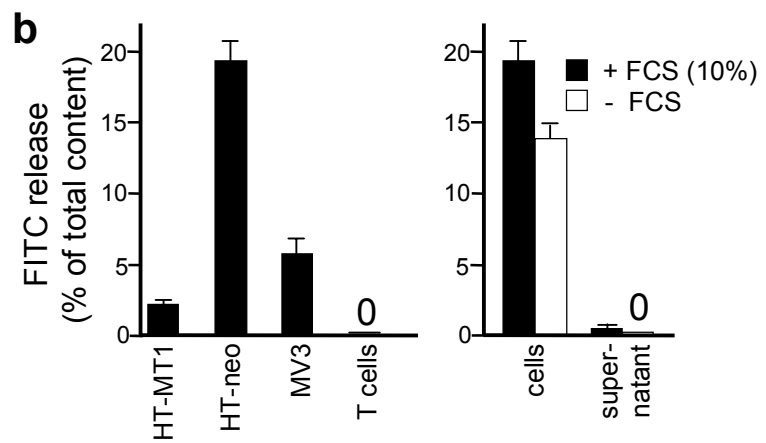
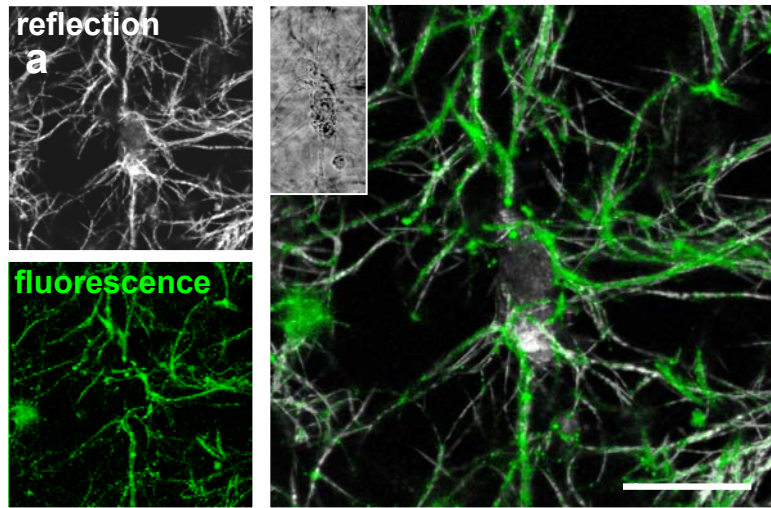
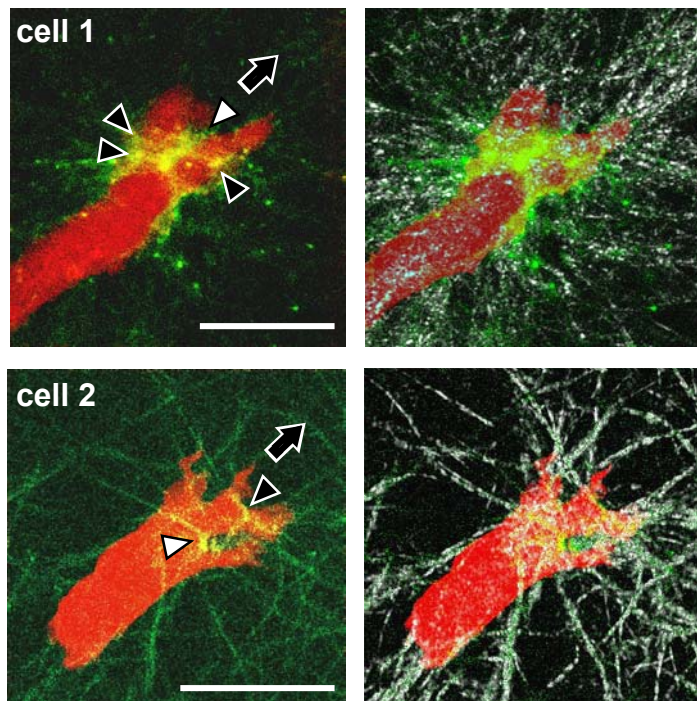


Figure 12. Detection of in situ collagenolysis by HT-MT1 cells. Cells were incorporated in a 3D collagen lattice containing 5% quenched FITC-collagen. After polymerization of the lattice, living cells were stained with Orange Cell Tracker and examined at 37°C by confocal microscopy. Images show cell body (red) and focal FITC-fluorescence (green). Right images are overlaid with the reflection signal (i.e. collagen fibers). Bars, 20 μ m. Black arrows, direction of migration.



2.1.4. Proteolytic movement of HT-1080 cells: a mesenchymal migration type

Since MT1-MMP overtransfected HT-1080 cells develop increased collagenolysis and clustering of MT1-MMP at collagen fibers, and since migration is associated with focal matrix degradation, it was tested whether MT1-MMP overexpression enhances migration of HT-1080 cells through 3D collagen. HT-MT1 cells displayed a 30% higher average migration speed compared to neo-vector transfected HT-1080 cells (Fig. 13a). To resolve individual subset behavior, both cell types were examined for single cell migratory parameters. As visualized by 3D diagrams, the total distance migrated within a 17 hr period (here vertical axis) represents the product of the mean velocity and the amount of time the cell was moving (in percent) (both diagonal axis). While both cell types displayed the same stop- and go-pattern (shown as percent time migrated), HT-MT1 cells moved in general faster (only 5% of HT-neo but 24% of HT-MT1 cells faster than 0.8 $\mu\text{m}/\text{min}$), which resulted in a longer migrated distance (product of percent time locomotion and velocity) (Fig. 13b). Hence, overexpression of MT1-MMP increases the migration velocity and thereby efficiency of HT-1080 tumor cells to penetrate 3D collagen barriers.

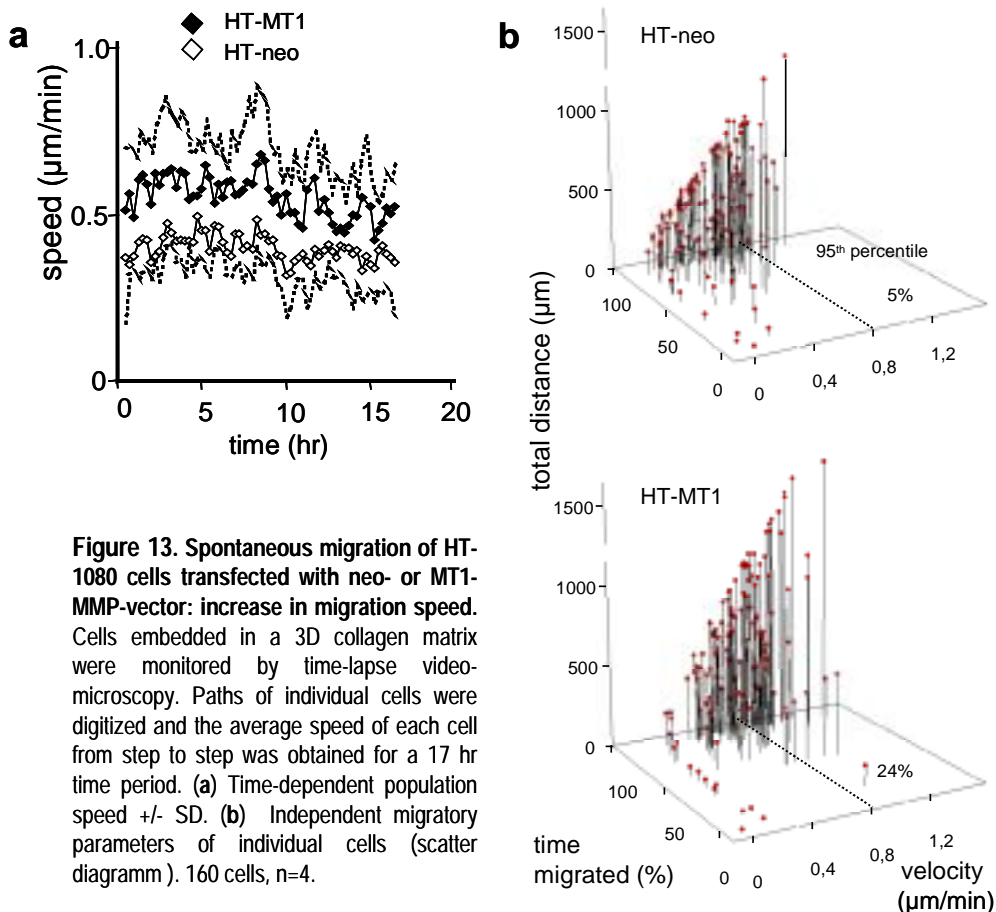


Figure 13. Spontaneous migration of HT-1080 cells transfected with neo- or MT1-MMP-vector: increase in migration speed. Cells embedded in a 3D collagen matrix were monitored by time-lapse videomicroscopy. Paths of individual cells were digitized and the average speed of each cell from step to step was obtained for a 17 hr time period. (a) Time-dependent population speed \pm SD. (b) Independent migratory parameters of individual cells (scatter diagram). 160 cells, $n=4$.

2.2. Proteases in collagenolysis and migration of MV3 and HT-1080 cells: function-blocking studies using pharmacological protease inhibitors

As shown in the last chapter, overexpression of the collagenase MT1-MMP favors tumor cell migration through a 3D fibrillar collagen lattice. To show whether this proteolytic type of movement was indeed dependent on this collagenolytic action, pharmacological inhibitors were used.

2.2.1. Biological effects of broad-spectrum MMP inhibitor BB-2516 (marimastat)

Since MMPs including MT1-MMP have been shown to display potent ECM-degrading capacity towards collagens and other proteins, initial experiments were performed using the highly efficient broad-spectrum MMP-inhibitor BB-2516 (marimastat; British Biotech, Oxford, UK). BB-2516 is inhibitory at the nM range for most MMPs (see Table 3, chapter 2.2.2.1.).

2.2.1.1. Inhibition of cell-released MMP-2 and -9, and recombinant MT1-MMP in native collagen zymography

The efficiency of BB-2516 directed against different MMPs was controlled by native collagen zymography. Native collagen instead of gelatin as substrate in zymography was chosen because of its putatively higher degree of organization and the lack of denaturation. Degradation of native collagen by MMP-2, MMP-9 and MT1-MMP was inhibited by BB-2516 (Fig. 14). Inhibition was complete at 1 μ M BB-2516 for all three MMPs, confirming efficient MMP-inhibitory activity for at least two detected collagenases MT1-MMP and MMP-2.

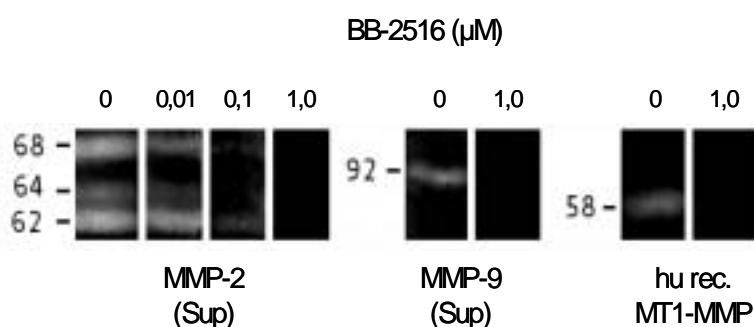


Figure 14. Collagen zymography for MMP-2, -9, and MT1-MMP: inhibition by BB-2516. MMP-2 and MMP-9 from supernatants (HT-1080 cells) and recombinant human MT1-MMP lacking the transmembrane domain were used for collagen zymography. Zymograms were developed by adding MMP-inhibitor BB-2516 at different concentrations to the enzyme buffer followed by negative staining with Coomassie Blue.

2.2.1.2. Inhibition of fibrillar collagen degradation by cell derived MMPs

Before examining the inhibitory effect of BB-2516 on cell-mediated degradation of fibrillar collagen, possible absorption or inactivation of BB-2516 by fibrillar collagen were tested. As detected by zymography, both BB-2516 preexposed to 3D collagen and non preexposed BB-2516 exhibited the same inhibition towards MMP-2 (Fig. 15). Therefore, absorption or inactivation of BB-2516 by collagen was unlikely.

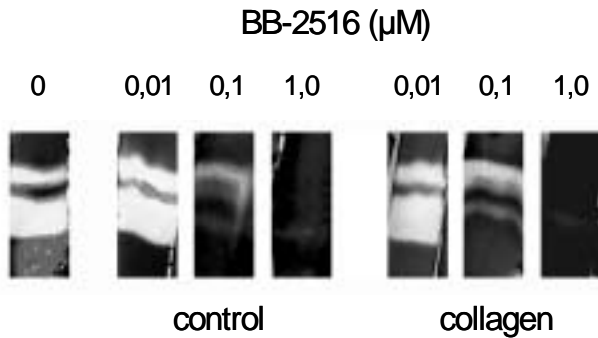


Figure 15. Lack of BB-2516 absorption by fibrillar collagen. MMP-2 from supernatants (HT-1080 cells) was used for collagen zymography. Zymograms were developed by adding BB-2516 or supernatants from 3D collagen, copolymerized with BB-2516 for 20 hr, to the enzyme buffer. Remaining collagenolytic activity of MMP-2 from HT-1080 supernatant in zymography was detected by negative staining with Coomassie Blue.

Degradation of fibrillar collagen by MV3 and HT-1080 cells was significantly inhibited by BB-2516 up to 85% as detected by the FITC-release-assay (Fig. 16a), without affecting cell viability (Fig. 16b). This finding confirms that MMPs from the examined tumor cells provide major collagenolytic activity, which can be blocked to a significant extent by MMP-inhibitor BB-2516.

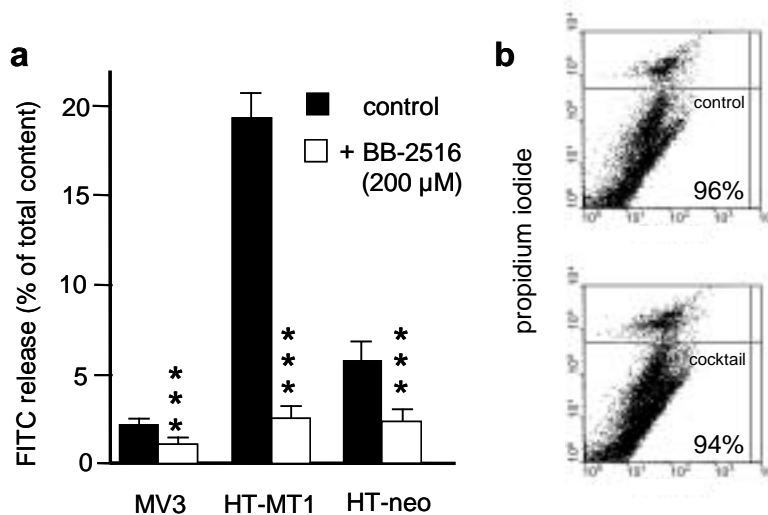


Figure 16. Reduced collagenolysis from cell-derived MMPs by BB-2516. (a) Cells were cultured in FITC-collagen for 40 hr in the absence or presence of 200 μM BB-2516, and FITC-content in the supernatant was monitored. 200 μM BB-2516 was used because it was the maximum inhibitory concentration that lacked cytotoxic effects. Concentrations of 1 or 10 μM BB-2516 already showed inhibition values nearly as 200 μM BB-2516 (not shown). Control values were simultaneously obtained and previously displayed in Fig. 11b. *** P<0,001; two-tailed t-test for independent means for difference to untreated control cells. (b) After 40 hr of incubation, cell viability was not affected by BB-2516, as examined by collagenase digestion, cell staining by propidium iodide, and flow cytometry. The percentage of propidium iodide negative cells representing non-damaged cells is indicated.

2.2.1.3. Minor effects on inhibition of cell migration by BB-2516

An extensive number of published work already showed that MMPs positively contribute to tumor cell invasion in various ECM-based models (see introduction). The ECM network is assumed to provide a complex barrier towards migrating cells, a process which can be blocked by natural and synthetic MMP inhibitors. In 3D collagen lattices, BB-2516 at 1 and 10 μM , though complete blocking of MV3 cell derived MMP activity, however, resulted in undiminished average migration speed of MV3 cells for 18 hr (Fig. 17a). Increase of BB-2516 concentration up to 500 μM resulted in a dose-dependent reduction (up to 50%) of the median cell speed from single cells averaged over 18 hr (Fig. 17a, right). For highly collagenolytic HT-MT1 cells, the median single cell speed at 200 μM BB-2516 was reduced only by 30% (Fig. 17b, left), and HT-neo cells did not show any reduction (Fig. 17b, right). Therefore, a discrepancy between blocked collagenolysis at 1 μM and undiminished migration rates exists. Because partial reduction in migratory speed was only reached at high BB-2516 doses, additional effects besides inhibition of collagenolysis might be present.

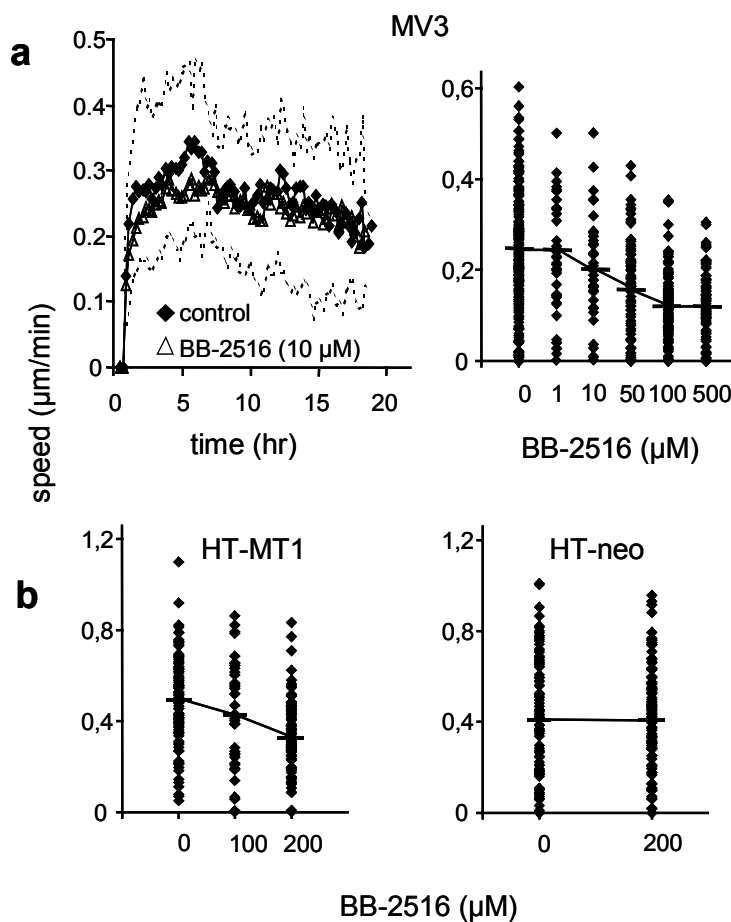


Figure 17. Persistent migration of MV3 and HT-1080 cells in the presence of BB-2516. Cells were embedded in a 3D collagen matrix in the presence or absence of BB-2516 and monitored by time-lapse videomicroscopy. Paths of individual cells were digitized and the average speed of each cell from step to step was obtained for a 18 hr time period. (a) Persistent migration of MV3 cells in the presence of 10 μM BB-2516 for total population \pm SD (left) and partial reduction in migration at increasing BB-2516 concentrations, as tested for individual cells (right, lines indicate median). (b) Dose-response of HT-1080 migration in the absence and presence of BB-2516, represented as the mean population speed from individual cells. Data represent three independent experiments, 120 cells. Unspecific dose-dependent reduction in migration was observed only for doses that were magnitudes higher than the MMP-inhibitory concentrations in collagen zymography (0,1–1 μM BB-2516; see Fig. 14). After each migration experiment, unaffected viability was assessed by propidium iodide staining (not shown).

2.2.2. Biological effects of broad-spectrum protease inhibitors

2.2.2.1. Establishment of a non-toxic broad-spectrum inhibitor cocktail

Since all examined tumor cells exhibited persistent migration upon inhibition of MMP function while 10-50% residual collagenolysis was left (see Fig. 16a), collagenolytic redundancy was anticipated. Besides MMPs, tumor cells expressed cathepsins with collagenase activity, as detected by RT-PCR, and putative yet unknown collagenases or proteases. To simultaneously target a wide spectrum of proteolytic activity, a cocktail of broad-spectrum protease inhibitors was established (Table 3). For maintainance of sufficient inhibitory activity within the matrix, the employed concentrations of protease inhibitors were orders of magnitudes higher relative to the known maximum inhibitory values (IC_{50}), unless cell viability was dose-limiting (Table 3).

Table 3. Cocktail of broad spectrum protease inhibitors for simultaneous targeting the spectrum of endoproteolytic activity.

inhibitor	target protease	IC_{50} (μ M) values	source	used concentration (μ M)
BB-2516	MMPs	0.002 - 0.2	Guidelines for the clinical use of marimastat, British Biotech Inc., UK (1998)	100
E-64	cysteine proteases, cathepsin B, H, L, K	0.001– 20	Bedi and Williams, 1994	250
pepstatin A	aspartatic proteases, incl. cathepsin D	0.0001- 5	Laurent and Salzet, 1995; Nisbet and Billingsley, 1999	100
leupeptin	cathepsin D	0.1– 10	Bedi and Williams, 1994	2 *
aprotinine	serine proteases, uPA, PA	0.15 - 3.5	Callas et al., 1994	2.2 *

*, highest non-toxic concentration

2.2.2.2. Inhibition of migration-associated cell-mediated collagenolysis by inhibitor cocktail

The effect of the protease inhibitor cocktail was monitored by the fluorometric FITC-release as already shown (see Figures 11b and 16a). The inhibitor cocktail greatly reduced cell-mediated FITC-release generated by all cell lines (up to 95%) (Fig. 18a). This strong inhibitory effect was confirmed by complete inhibition of structural fiber-breakdown caused by HT-MT1 cells (Fig. 18b). After 40 hr of cell migration culture within collagen lattices in the presence of inhibitor cocktail, viability was not affected, as measured by propidium iodide assay (Fig. 18c). In conclusion, the protease inhibitor cocktail almost completely blocked cell-mediated collagenolysis of the 3D collagen barrier in the absence of cytotoxic effects.

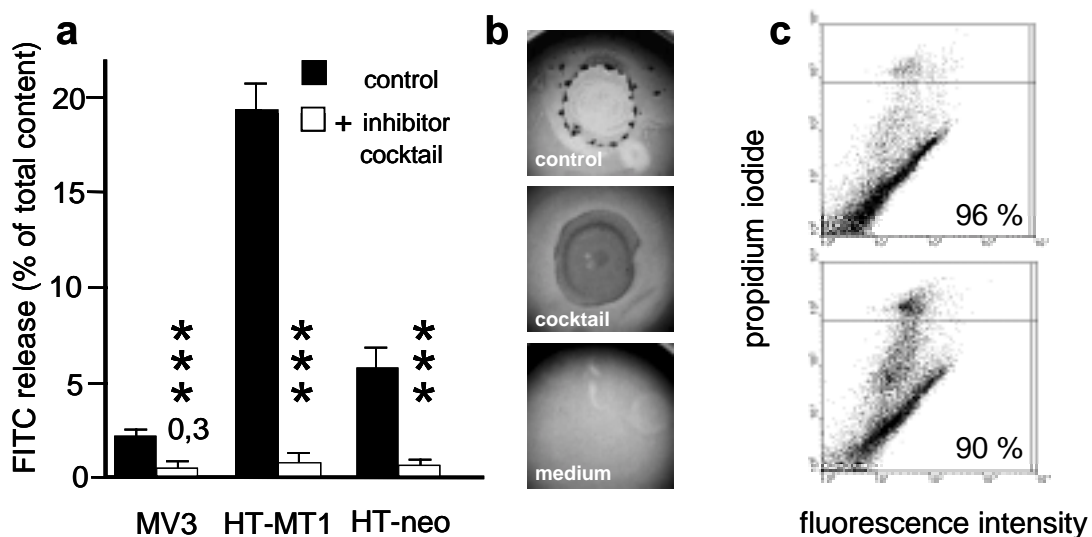


Figure 18. Subtotal inhibition of collagenolytic activity by protease inhibitor cocktail. (a) Cells were incubated in the absence or presence of protease inhibitor cocktail (see Table 3, chapter 2.2.2.1.), and FITC-content in the the supernatant was monitored. *** $P < 0,001$; two-tailed t -test for independent means for difference to untreated control cells. Control values correspond to Figs. 11 and 16. (b) Inhibition of collagenolysis by HT-MT1 cells was confirmed by qualitative collagenolysis assay, as described for Fig. 10b. (c) Unaffected cell viability after 40 hr in the absence or presence of protease inhibitor cocktail, as shown by propidium iodide staining. The percentage of propidium iodide negative cells representing non-damaged cells is indicated.

2.2.2.3. Lack of inhibition of cell migration by protease inhibitor cocktail

Unexpectedly, although inhibition of collagenolysis by protease inhibitor cocktail was near-complete, the migration efficiency of HT-MT1 cells within 3D collagen lattices was barely reduced (Fig. 19a).

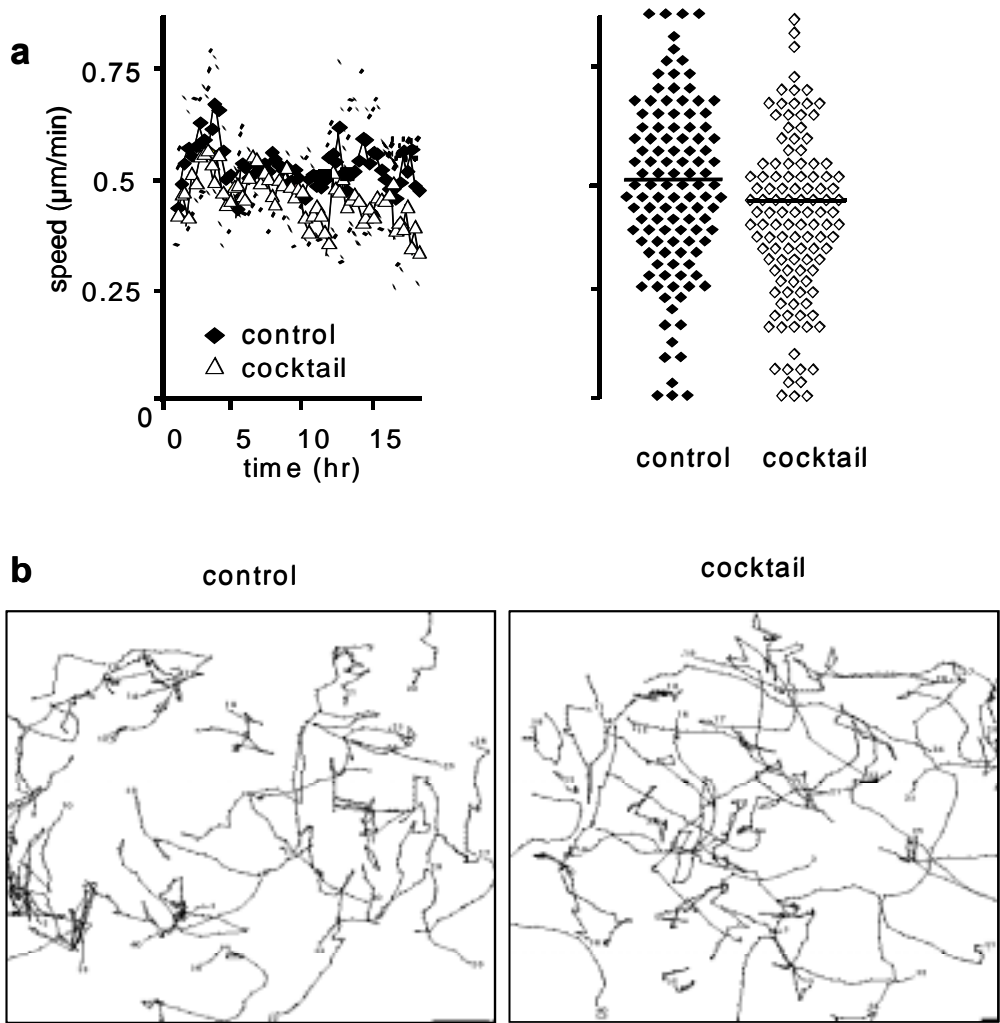


Figure 19. Persistent migration in the presence of protease inhibitor cocktail. (a) Cell migration was evaluated for total populations (left) and for individual cells (right). Data represent the means \pm SD of the population speed (left) and the mean speeds of each individual cell for the 18 hr tracking period (right). $n=3$, 120 cells. After time-lapse videomicroscopy, cell viability was not affected by inhibitor cocktail (not shown). (b) Orthotopic representation of cell paths from 40 randomly selected untreated control cells as well as from protease cocktail inhibitor-treated cells (18 hr observation period of one representative experiment).

Persistent migration was monitored by real-time analysis of time-dependent population speed (Fig. 19a, left) and the median speed derived from single cell analysis (Fig. 19a, right). Similar high migration rates were obtained from HT-neo and wild type cells in the presence of inhibitor cocktail (not shown). The tracking pattern of cell paths shown for each 40 cells reflects undiminished migration capacity of inhibitor cocktail-treated compared to non-treated HT-MT1 cells (Fig. 19b). Since the capacity to move, i.e. to generate traction and overcome physical matrix constraints appeared intact after blocking of collagenolysis, the existence of compensation strategies to counterbalance the loss of pericellular proteolysis was hypothesized.

2.3. Mechanisms of non-proteolytic HT-1080 and MV3 tumor cell migration in the presence of protease inhibitor cocktail

2.3.1. Transition from mesenchymal to amoeboid morphodynamics

As observed from the videorecordings (movie 4), the presence of protease inhibitor cocktail changed several aspects of migratory behavior in HT-MT1 cells (Fig. 20). While spontaneously moving cells maintained a spindle-shaped, elongated morphology (Fig. 20a, left), this “mesenchymal”, fibroblast-like migration type (see chapter 1.2.1.2 in introduction) was converted to less polarized, more spherical morphodynamics in the presence of protease inhibitor cocktail (Fig. 20a, right; movie 4). Spherical-shaped cells sustained migration (Fig. 20b) and exhibited a significant reduction in median length axis compared to control cells (Fig. 20c). In the presence of protease inhibitors, spherical morphodynamics included flexible shape change and forward propulsion guided by multiple anterior and outward ruffling filopodia, as detected by high resolution videomicroscopy (movie 5). Morphodynamic analysis showed a reduced number in mesenchymally moving HT-MT1 in the presence of protease inhibitor cocktail, while the percentage of the more spherical, “amoeboid” phenotype was at least tripled (Fig. 20d) or doubled by BB-2516 alone. This novel non-proteolytic phenotype was reminiscent of *Dictyostelium* amoeba migrating across 2D surfaces (Yumura et al., 1984; Killich et al., 1993;), as well as leukocytes crawling through 3D ECM substrata (Gunzer et al., 2000; Friedl et al., 2001) [for comparison see amoeba (movie 6, from <http://www.dicty.cmb.nwu.edu/dicty/dicty.html>) and T lymphocytes (movies 11, 12)]. Very similar observations were obtained for invasive MDA-MB-231 mammary carcinoma cells, expressing soluble and membrane-tethered MMPs, serine proteases, and cathepsins (Ishibashi et al., 1999; Bachmeier et al., 2001; Saad et al., 2002) (Fig. 21). A similar transition from constitutive spindle-shaped (left) to less polarized, ellipsoid (right) morphodynamics (Fig. 21a; movie 7) was induced upon inhibition of proteolysis in MDA-MB-231 cells by protease inhibitor cocktail (Fig. 21b), albeit slightly less efficiently than in the other examined tumor cells. Similar to HT-MT1 cells (Fig. 20), this transition was accompanied by a significantly shortened median length axis (Fig. 21c) and a switch from mesenchymally to amoeboid moving cells in the presence of protease inhibitor cocktail (Fig. 21d). Similar to HT-MT1, the percentage of mesenchymally moving cells decreased, while the number of amoeboid moving cells greatly increased (Fig. 21d).

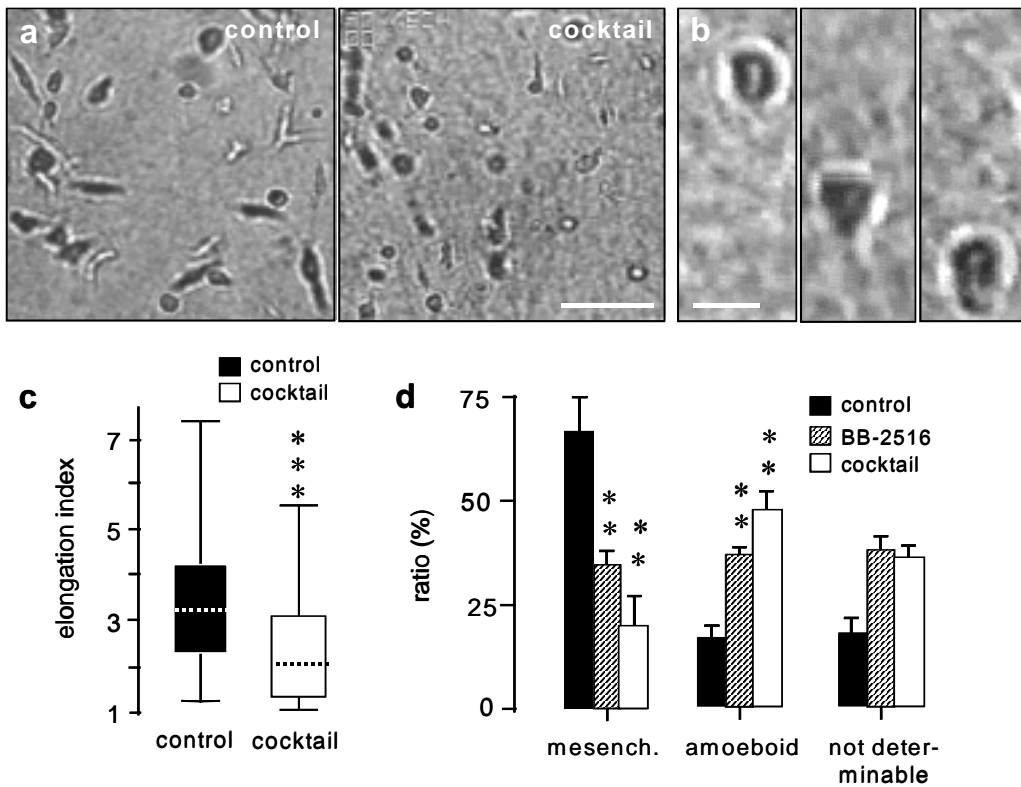


Figure 20. Protease inhibitor cocktail: Conversion of spindle-shaped (fibroblast-like, mesenchymal) to spherical (amoeboid) morphodynamics and migration in HT-MT1 cells. (a) Conversion of elongated, polarized shape (left) towards spherical morphology (right) in the presence of protease inhibitor cocktail, respectively. (b) Higher magnification of migrating cell in presence of protease inhibitors (time frame: 117 min). (c) Polarity index of cells migrating in the presence of protease inhibitor cocktail as compared to untreated control cells, 170 cells; ***, $P < 0.0001$, Mann-Whitney U -test. (d) Frequency of fibroblast-like and amoeboid cells migrating in the presence of BB-2516 and protease inhibitor cocktail as compared to untreated control cells. $n = 3$, 100 cells. **, $P < 0.01$ for difference to untreated control; two-tailed t -test for independent means. Cells of indeterminate morphology (15 - 40%) were excluded from analysis, as described in Materials and Methods. Bars, 100 μm (a) and 20 μm (b).

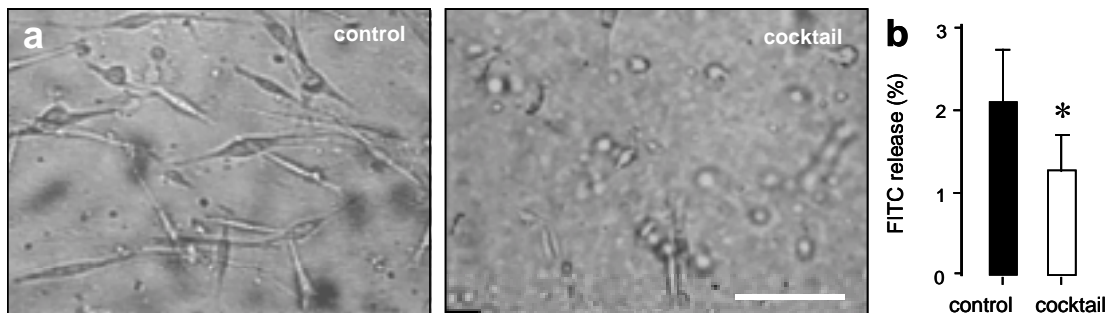


Figure 21. Protease inhibitor cocktail: Conversion of spindle-shaped (fibroblast-like, mesenchymal) to spherical (amoeboid) morphodynamics and migration in MDA-MB-231 cells. (a) Conversion from spindle shaped (left) to more spherical morphology (right) in the presence of protease inhibitor cocktail. Bar, 100 μm . (b) Inhibition of collagenolysis in MDA-MB-231 cells by protease inhibitor cocktail ($n = 3$; **, $P < 0.05$, unpaired two-tailed t -test). (c) Reduced elongation index in the presence of protease inhibitors ($n = 3$, 200 cells; ***, $P < 0.0001$, Mann-Whitney U -test). (d) Frequency of mesenchymal and amoeboid morphodynamics in migrating cells for protease inhibitor cocktail and untreated control cells.

c

Condition	Median Elongation Index	Q1	Q3	Min	Max
control	~3.2	~1.5	~4.2	~1.0	~6.5
cocktail	~1.8	~1.2	~3.0	~1.0	~5.0

d

Morphology	control (%)	cocktail (%)
mesenchymal	~55	~30
amoeboid	~5	~30
not determinable	~5	~30

2.3.2. Altered cellular morphodynamics: squeezing through the fiber network in the absence of structural matrix breakdown

Consistent with impaired collagenolysis, amoeboid moving HT-MT1 cells did not cause structural remodeling of collagen fibers (Figs. 22a and b, **color plate 4**; movie 8). Both, amoeboid movement and lack of collagen fiber degradation was reproduced for reduced protease inhibitor cocktail concentrations (see legend of Fig. 28a) (not shown). Induced protease-independent migration resulted from adaptation and alignment of the cell body along preformed fiber strands (Fig. 22a, white arrowheads) and consecutive migratory guidance along fibrillar scaffolds (Fig. 22b, black arrowheads). Upon cell detachment, no remodeling, bundling, or destruction of the collagen network were formed, leaving behind the intact reticular texture of individual fibers at their original position (Fig. 22a, black arrowheads; movie 8). To overcome regions of narrow space by changing shape, an initial pseudopod elongation through a preformed matrix gap (Fig. 22c, black arrowhead; 4 μm pore diameter from the central section; 18 μm cell diameter) was followed by propulsion of the cell body and the development of a narrow region confined by matrix fibers (“constriction ring” (Lewis, 1934); Fig. 22c, black arrowhead). Constriction rings persisted until the cell body had squeezed or pulled forward, while no matrix defect was apparent after cell detachment (Fig. 22c; movie 9). Migratory alignment and shape change along preformed fiber strands, constriction, and propulsion hence represent non-proteolytic, physical strategies employed by large tumor cells (10 – 30 fold larger volume than amoeba or leukocytes) to bypass structural ECM barriers.

2.3.3. Altered distribution of $\beta 1$ integrins, MT1-MMP and F-actin in induced amoeboid HT-1080 cell migration

Because the structure and location of adhesive cell-matrix contacts control cell shape and migration dynamics (Palecek et al., 1997; Sheetz et al., 1998), the cytoskeletal structure and integrin distribution in amoeboid HT-MT1 cells were investigated (Fig. 23, color plate 4). Induced amoeboid morphology was characterized by diffuse cortical actin rims and small actin-rich spots at interactions with collagen fibers (Fig. 23a). In amoeboid HT-MT1 cells, $\beta 1$ integrins showed non-clustered, linear surface distribution at contacts to collagen fibers (Figs. 23a and b; movie 9) deviating from clustered $\beta 1$ integrins and prominent actin nucleation zones in spindle-shaped control cells (see Figs. 8b and h). MT1-MMP was consistently dissociated from fiber binding sites but accumulated

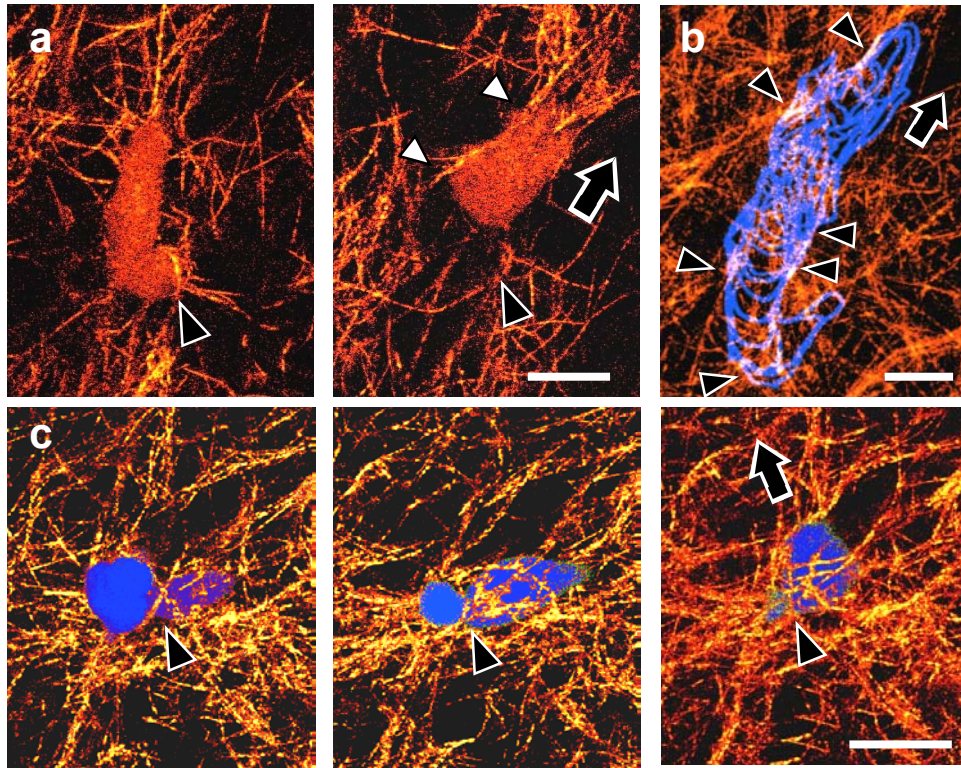


Figure 22. Squeezing through the fiber network: Induced amoeboid migration lacks fiber degradation and matrix remodeling. (a) Alignment of cell body along a preexisting fiber (white arrowheads) and intact individual collagen fiber at its original position after cell detachment (black arrowhead); time frame: 35 min. (b) Migratory alignment of the cell depicted in (a) along the preexisting fiber texture. The outline of the cell edge for each 2.5 min time interval (blue lines) was superimposed with the 3D reconstruction of the matrix structure. Bright pixels indicate colocalization of the cell boundary with fibers (arrowheads), time frame: 65 min. (c) A calcein-labeled cell transmigrating through narrow space exhibiting profound morphological adaptation (constriction, arrowhead), time frame: 20 min. Bars, 20 μ m.

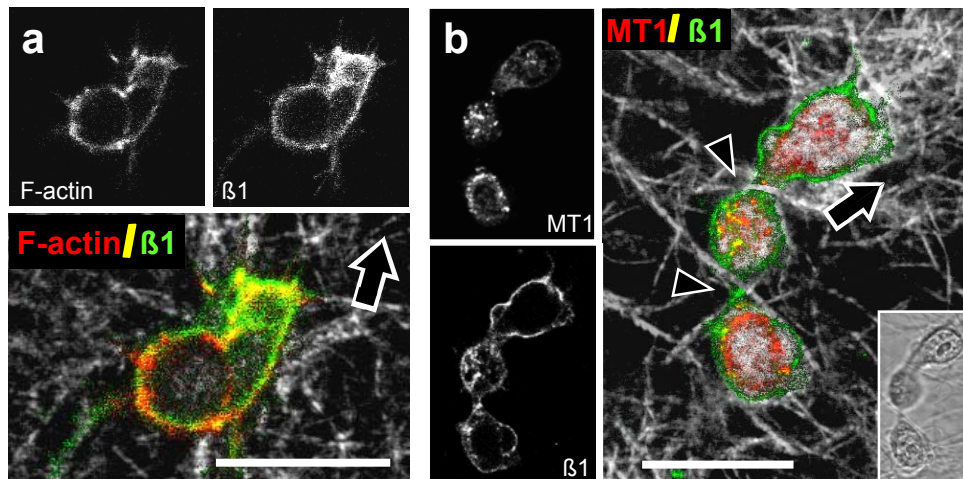


Figure 23. Changes in β 1 integrin and MT1-MMP distribution and cytoskeletal structure in induced amoeboid migration. HT-MT1 cells migrated in 3D collagen in the presence of protease inhibitor cocktail for 6-12 hr. Lattices were fixed with 4% PFA and permeabilized with 0,1% Triton-X100 (a) or methanol (b) and stained for confocal microscopy. Both cells show a non-clustered diffuse to linear surface-distributed β 1 integrin pattern (green). (a) HT-MT1 cell displays a cortical F-actin cytoskeleton (compare with control cell in Fig. 8h). (b) Loss of MT1-MMP (red) from interactions with collagen fibers (compare to untreated control cells in Fig. 8a,b), while evenly distributed β 1 integrins remain at the surface. Note the appearance of two simultaneous constriction rings bordered by perpendicular collagen fibers (black arrowheads). Black arrow, direction of migration. Bars, 20 μ m.

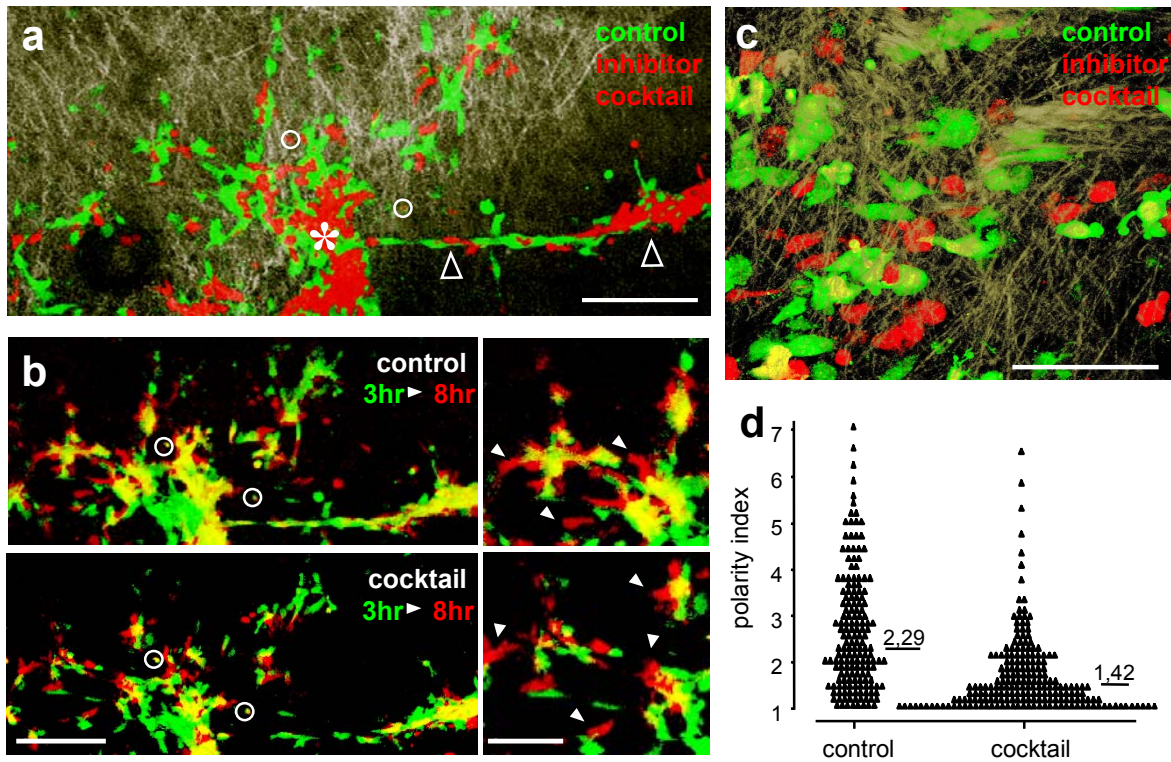


Figure 24. In vivo translocation and morphology of HT-MT1 cells in the mouse dermis. Intravital microscopy of ECM structure (light brown) and labeled cells, 3 hr (a-d) and 8 hr (b) after injection. (a) 3D reconstruction of scattered cells and matrix structure. Control cells are shown in green, cells pretreated with protease-inhibitor cocktail in red. Asterisk, center of injection site. Black arrows, multicellular cord following a putative lymph vessel. **(b)** Position change of control cells (top) and cells pretreated with protease inhibitor cocktail (bottom) from injection site depicted in (a). False-colour reconstructions were obtained for each fluorescence channel 3 hr (green) and 8 hr (red) after injection. Orthotopic superimposition was controlled by the position of co-injected fluorescent beads (circles) as well as position of the multicellular cord. Arrows indicate regions of cell translocation (right). **(c)** Morphology and **(d)** polarity index of control cells (green) and cells pretreated with protease inhibitor cocktail (red). The polarity index was calculated for each 170 cells from control and inhibitor cocktail experiments, respectively (6 independent experiments); ***, $P < 0.0001$ (Mann-Whitney U-test). Bars, 200 μm (**a**; **b left**); 100 μm (**b right**; **c**).

intracellular (Fig. 23b). The gain of spherical morphology coupled to diffuse $\beta 1$ integrin distribution suggests the transition from a focal contact-driven mode of substrate interaction (Sheetz et al., 1998; Maaser et al., 1999) to more diffuse, structurally less defined interaction points, that are, again, hallmarks of amoeboid crawling (Yumura et al., 1984; Friedl et al., 1998b; Friedl et al., 2001).

2.4. Mesenchymal to amoeboid transition in vivo

Although collagen lattices provide a complex 3D ECM scaffold and a barrier for moving cells, a putatively different spacing and molecular composition of life connective tissue may impose additional physical and molecular constraints, potentially yielding distinct migration mechanisms. Therefore, in vivo migration of HT-MT1 cells within the mouse dermis was investigated by multi-photon microscopy (Fig. 24, **color plate 5**). 3 hr after the injection of HT-MT1 cells into the loose connective tissue of the mouse dermis (Fig. 24a), both non-treated control cells (green) and cells pretreated with protease inhibitor cocktail (red) were detected at the injection site (asterisk), individually scattered within the tissue, or located within multi-cellular cords (Fig. 24a, black arrowheads). In control experiments in vitro, pre-incubation of cells with protease inhibitors resulted in stable amoeboid movement for at least 10 hr, indicating relatively slow turn-over of the target proteases after inhibition (not shown). In the mouse dermis, ortotopic 3D reconstruction of the injection site 3 and 8 hr after injection identified considerable position changes for both, control cells (Fig. 24b, top) and inhibitor-pretreated HT-MT1 cells (Fig. 24b, bottom). This position change corresponded to a translocation of 4 – 10 $\mu\text{m}/5$ hr (Fig. 24b, white arrowheads), in part approximating migration velocities present in collagen matrices in vitro (6 – 36 $\mu\text{m}/5$ hr; compare Fig. 19a, right). At high resolution reconstruction, cells pretreated with protease inhibitors developed a significantly reduced elongation reminiscent of amoeboid morphology (Fig. 24c, red cells) and a near-round median shape (Fig. 24d), while control cells retained their constitutive spindle-like elongation (Fig. 24c, green cells; movie 10). In summary, similar to 3D collagen matrices, abrogation of matrix protease function in HT-MT1 cells resulted in persistent movement and concomitant induction of amoeboid morphology in vivo, confirming migratory plasticity for dermal connective tissue.

2.5. Protease function in T cell migration

Since protease-blocked migrating tumor cells show amoeboid movement characteristics and thereby resemble migrating T cells, peripheral activated T-lymphocytes were examined for proteolytic function in migration. T cells develop when migrating spontaneously in 3D collagen lattice a highly flexible and characteristic morphology and generate an oscillatory path (Fig. 25) corresponding to an amoeboid migration type. This migratory process lacks focal contacts and $\beta 1$ -integrin dependent adhesion and traction (Friedl et al., 1998b). As already mentioned in chapter 2.3.1., the morphodynamics of T cells is highly adaptive and thus resembles protease-independent movement of tumor cells. On the other hand, activated T cells and T-lymphoma cells SupT1 were shown to use functional proteases to penetrate basal membrane or its equivalents, such as matrigel (Leppert et al., 1995; Xia et al., 1995). For T cell movement in intersitial tissue, however, it remains unclear whether proteases are involved. Therefore it was examined whether T cells and SupT1 cells express and utilize functional proteases to migrate through 3D collagen matrices. The main focus was laid on peripheral Concanavalin A (ConA) activated CD4⁺ T lymphocytes, and SupT1 lymphoma cells, which were previously examined by Xia et al., 1995, were used for confirmatory experiments.

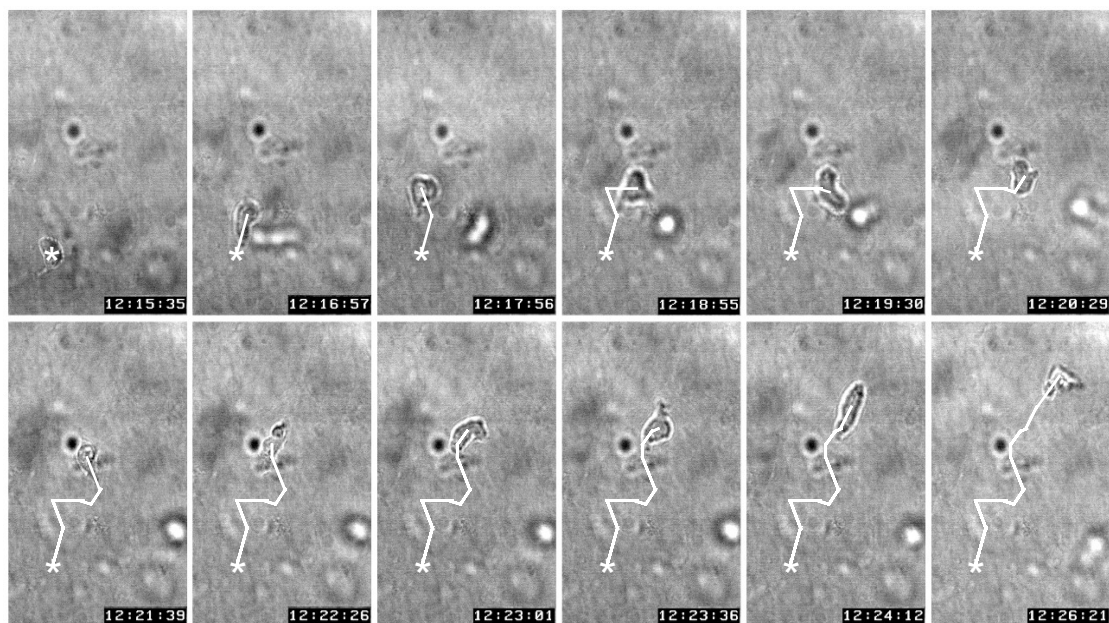


Figure 25. Spontaneous locomotion of a CD4⁺ T cell through 3D collagen lattice: Changes in morphology and oscillatory path development. CD4⁺ ConA blast migrating in a 3D collagen matrix. Time frame: 11 minutes.

2.5.1. Expression of proteases by activated primary CD4+ T cells and SupT1 lymphoma cells

2.5.1.1. Detection of protease mRNA expression

As already described for tumor cell mRNA expression, proteases from different classes were examined for T lymphocytes and SupT1 (Fig. 26). CD4+ T cells expressed MMP-9, MT1-MMP, MT4-MMP, TIMP-2, ADAM-9, -15, and 17, cathepsin L, and proteases from the PA/ plasmin system. SupT1 cells expressed MT1-MMP, TIMP-2, ADAM-9, -10, -11, -17 and uPA. As the only collagenase, MT1-MMP was expressed by both cell types. In contrast to Leppert et al., 1995a and b, MMP-2 was not detected in both, primary activated CD4+ T cells and SupT1 cells.

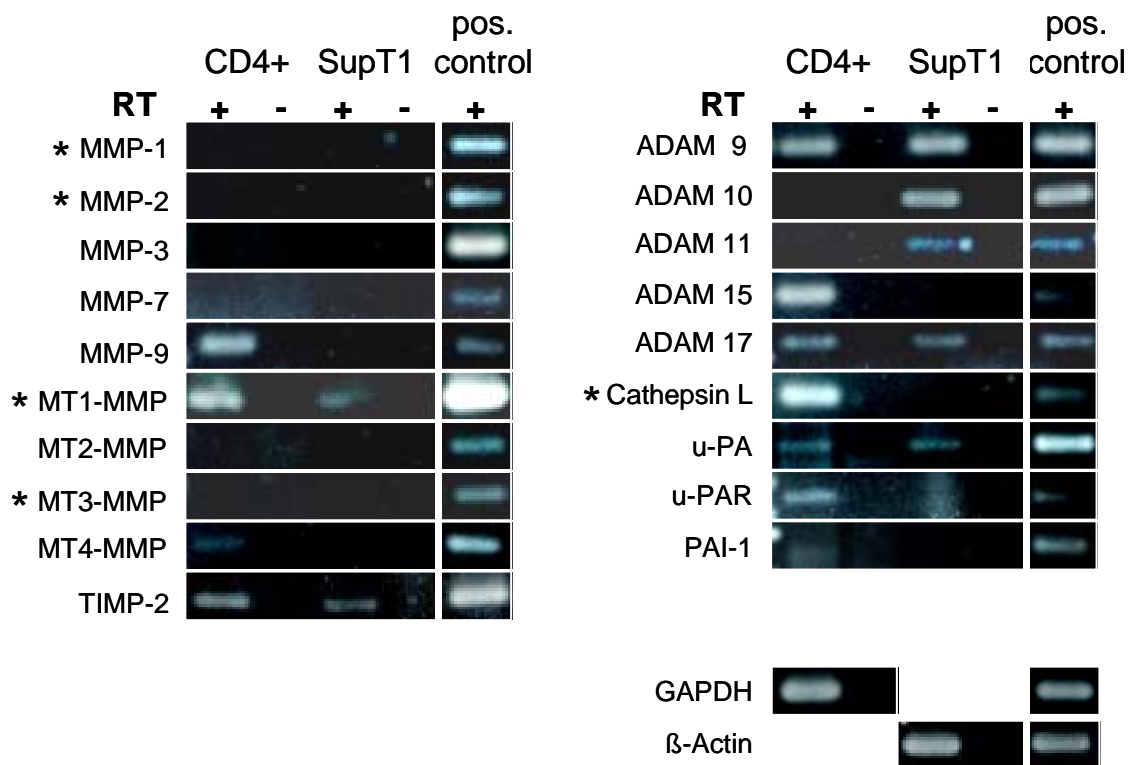


Figure 26. mRNA expression of proteases and endogenous protease inhibitors in CD4+ T cells and SupT1 cells. Total RNA from CD4+ T cells stimulated with ConA for 3 days and SupT1 cells was isolated, reversely transcribed (RT) to cDNA, multiplied by PCR reaction (30 cycles) and subjected to agarose gels. Fragment lengths conformed to the expected size using primers as shown in Table 4 (chapter 4.14.). mRNA was detected for ADAM-12, but not for MMP-8, -13, cathepsin B and K in either cell type (not shown). Positive controls were performed from cDNA of HT-MT1 and, in the case of MMP-7 and -9, by HT-neo cells. *, enzymes known to cleave native type I collagen.

2.5.1.2. Detection of MMP cell surface expression

Because MT1-MMP was the only established cell-surface collagenase expressed by T cells, the cell surface expression of MT1-MMP and others was analyzed by flow cytometry (Fig. 27). ConA stimulated CD4⁺ T cells were gated for small, not proliferating cells as well as blast formation (Fig. 27a). Both MMP-9 and MT1-MMP were barely present at the cell surface of small cells, but, however, to some limited extent on blasts (Fig. 27b). As positive controls, abundant cell surface expression of MT1-MMP was detected on HT-1080 cells (see Fig. 3). Since some collagenase expression was present at the surface of T cell blasts, possible functional collagenase activity was examined.

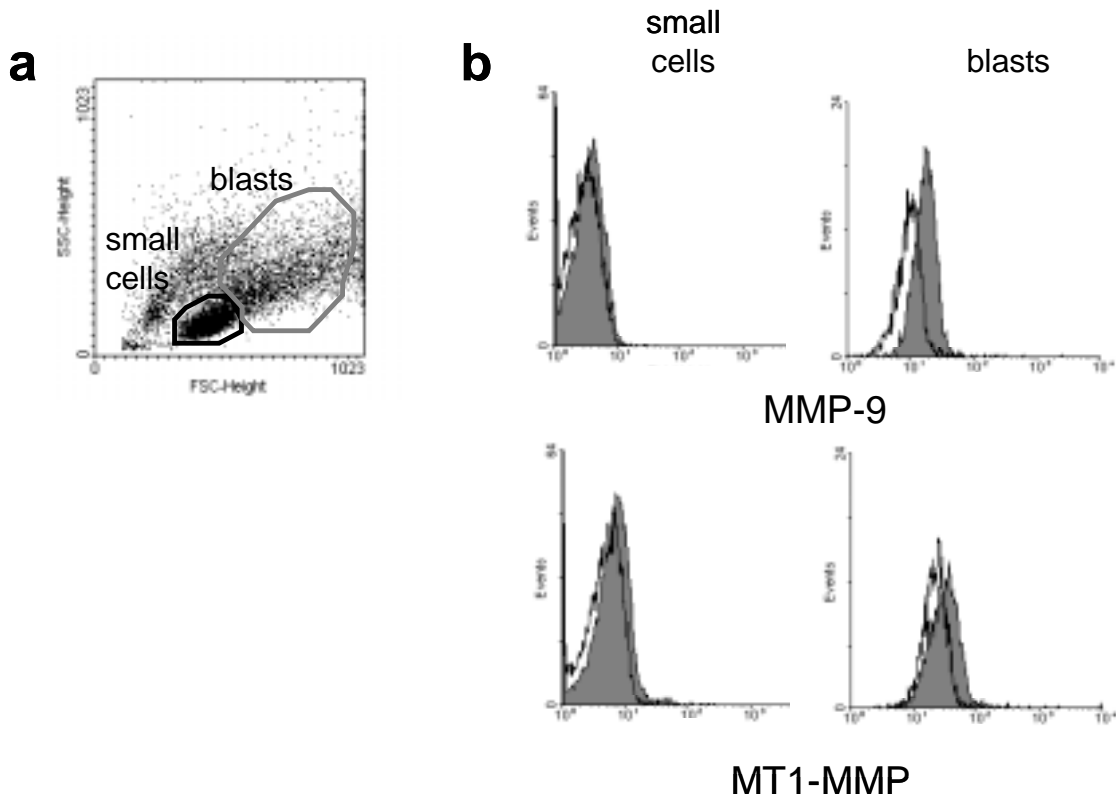


Figure 27. Upregulation of cell surface-located MMP-9 and MT1-MMP on CD4⁺ T cells upon activation. (a) Cells were stimulated with ConA for 3 days, which resulted in blast formation in approximately 30% of the cells. (b) Cells were stained for MMP-9 and MT1-MMP cell surface expression and analyzed by flow cytometry. Profiles represent gated small non-activated cells (left) and blasts (right).

2.5.2. Contribution of proteases to collagenolysis and migration in T cells: function blocking experiments with protease inhibitors

2.5.2.1. Lack of in situ collagenolysis

For examination of collagenolysis, Con A stimulated CD4⁺ T blasts and SupT1 cells migrated in FITC-containing collagen lattice, but, however, did not release soluble FITC-fluorescence above background levels, in contrast to collagenolytic HT-MT1 cells (Fig. 28a). For functional collagenase blocking experiments, the modified protease inhibitor cocktail with reduced concentrations (see legend Fig. 28) was used to maintain non-toxic conditions for T cells (Fig. 28b). The efficiency of the modified cocktail was confirmed using HT-MT1 cells as positive control (Fig. 28a). In the presence of inhibitor cocktail, CD4⁺ and SupT1 cells did not release fluorescence upon migration within FITC-collagen (Fig. 28a).

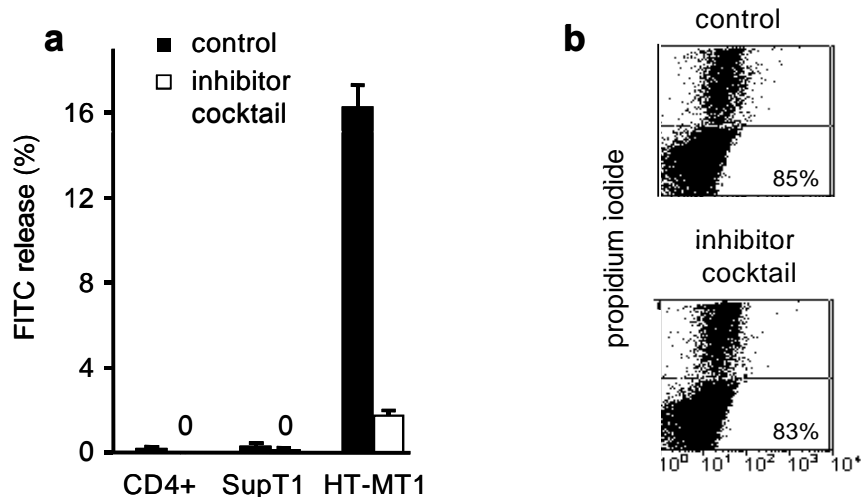


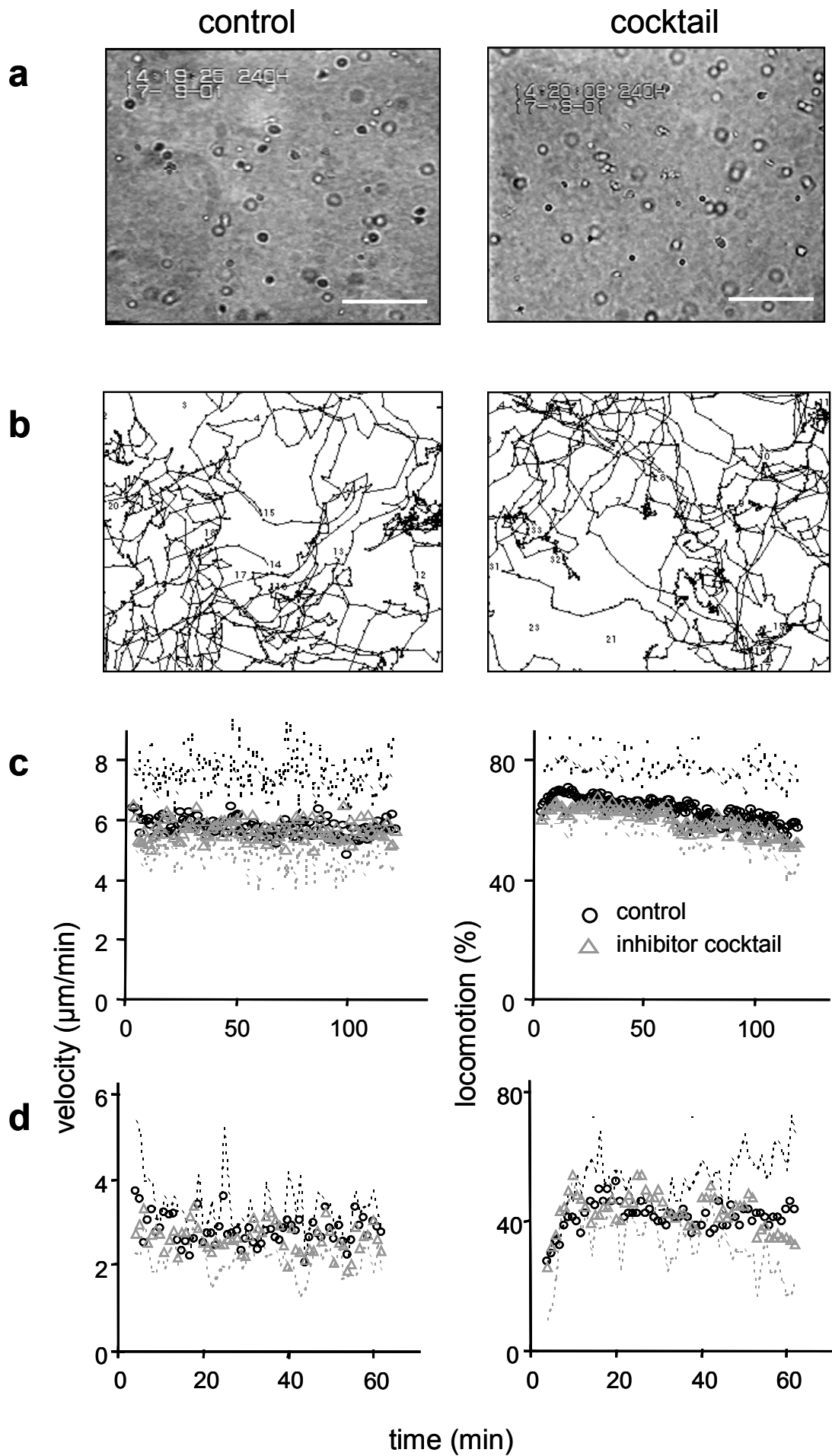
Figure 28. Lack of in situ collagen degradation by T blasts and SupT1 cells. (a) ConA stimulated CD4⁺ T cells and SupT1 were incorporated in a 3D collagen lattice containing 2% FITC-collagen in the absence or presence of modified protease inhibitor cocktail (marimastat, E-64, pepstatin A, each 20 μ M, aprotinin 0,7 μ M, leupeptin 1 μ M) for 40 hr. No FITC-fluorescence was released above background levels, in contrast to HT-MT1 cells (positive control; compare with Fig. 11b), $n=3$. (b) After 40 hr of migration in collagen in the absence or presence of inhibitor cocktail, viability of CD4⁺ cells and SupT1 cells (not shown) was unaffected.

At physical contacts of CD4⁺ cells migrating within collagen fibers containing quenched FITC, no in situ-focal fluorescence was detected (Fig. 28c, **color plate 6**), compared to highly detectable focal fluorescence in situ at migrating tumor cells (Fig. 12). Hence, MT1-MMP and further potential collagenases in CD4⁺ T cells and SupT1 lymphoma cells did not generate collagenolysis while the cells were moving.

2.5.2.2. Persistent migration in the presence of protease inhibitor cocktail

To further investigate, whether the enzymatic function of proteases contributes to the migration of ConA stimulated CD4⁺ T cells and SupT1 cells, migration experiments were performed in the absence and presence of protease inhibitor cocktail (Fig. 29). Presence of inhibitor cocktail did not change the morphodynamics and movement of CD4⁺ cells (movie 11, initial time frame shown in Fig. 29a,) and SupT1 cells (not shown), as represented by oscillatory structure of cell paths for 120 min (Fig. 29b). The migration velocity was approximately 6 $\mu\text{m}/\text{min}$ for both, non-treated and inhibitor cocktail-exposed CD4⁺ T cells (Fig. 29c, left). Also, the stop-and go-pattern of migrating cells, represented as the percentage of steady-state percentage of locomoting cells, remained unchanged (Fig. 29c, right). Similarly, protease inhibitor treatment did not affect migratory parameters for SupT1 cells (Fig. 29d). Hence, both cell types, stimulated CD4⁺ T cell blasts as well as SupT1 lymphoma cells do not engage functional collagenases for their migration through 3D fibrillar collagen matrix.

Figure 29. Persistent T cell migration in the presence of protease inhibitor cocktail. Migration experiments in the absence or presence of modified inhibitor cocktail (for concentrations see legend of Fig. 28) were performed for CD4⁺ (a-c) and SupT1 cells (d). (a,b) CD4⁺ T blasts migrating in the absence or presence of protease inhibitor cocktail as shown on images obtained from video-recordings (bars, 100 μm) (a) and by digitized cell paths (time frame: 2 hr) (b). (c,d) Velocity (left) and percentage of migrating CD4⁺ T cells (c) and SupT1 cells (right) (d) within the populations (means \pm SD) over time. n=3; 120 cells.



2.5.3. Biophysics of non-proteolytic amoeboid T cell migration

Since T cell migration was not inhibited by protease inhibitor cocktail, the cellular mechanism of how T cells penetrate the 3D fibrillar collagen barrier and whether remodeling of the fiber structure by migrating T cells occurs, was investigated by high resolution confocal microscopy (Fig. 30, **color plate 6**). Cells adapted their morphology to the preformed matrix structure (Fig. 30a). Upon detection of dynamic and flexible cell movement it became clear that cells orientate and align along the preformed matrix network for migratory guidance (Fig. 30b, white arrowheads, cell path originated from moving cell shown in Fig. 25), as already detected for non-collagenolytic tumor cells, though containing 10-20 times bigger volume (see Fig. 22b). Upon migration, both, untreated (Fig. 30c) as well as inhibitor cocktail-treated (Fig. 30d) T cells showed squeezing and formation of constriction rings (Fig. 30c,d; c5,6; d2; white arrowheads) at regions of narrow space, coupled to amoeboid and rapidly adapting morphodynamics along fiber strands for contact guidance (Fig. 30c,d; c2-4; d3,4; black arrowheads, movie 12). In conclusion, the non-proteolytic T cell movement is a constitutive process that shares a highly adaptive and flexible morphodynamics with tumor cells treated with protease inhibitor cocktail as a cellular mechanism to overcome a 3D matrix barrier.

Figure 28c (color plate 6) Lack of in situ collagen degradation by T blasts. CD4⁺ T cells were incorporated in a 3D collagen lattice containing 5% FITC-collagen, and examined by confocal microscopy. The outline of the cell boundary was duplicated from the image monitored simultaneously by transmission mode and placed orthotopically on the image shown here. Subsequently, the cell body was filled with red colour using Adobe Photoshop software. Physical cell contact to collagen fibers did not result in increased cleavage-related fluorescence of quenched collagen-FITC; Bar, 5 μ m. Compare with positive control for in situ proteolysis of HT-MT1 cells in Fig. 12.

Figure 30 (color plate 6). Amoeboid T cell migration within 3D collagen matrix in the absence (a-c) and presence of protease inhibitor cocktail (d): physical cell-fiber interaction and contact guidance. ConA activated T cells migrating within 3D collagen matrices were examined by confocal microscopy. (a) T cell alignment along matrix fibers based on morphology (white arrowheads). The outline of the cell boundary was duplicated from the image monitored simultaneously by transmission mode, placed orthotopically on the image shown here, and filled with red colour, as described for Fig. 28c. Black arrow, direction of migration. (b) From the cell depicted in Fig. 25 (minutes 16 to 23), the red line represents the central path of the migrating cell and the blue line the outline of the cell boundary for each 24 seconds time interval. Polymerized collagen fibers are shown in green. The cellular morphodynamics and physical fiber structure of the 3D collagen matrix was orthotopically reconstructed. Fibers of polymerized collagen matrix are used as guidance cues by the migrating T-cell as indicated by bright blue superimposition of cell edge and guiding fibers (white arrowheads; compare to Fig. 22b). Both, non-treated (c) and protease inhibitor cocktail-treated (d) calcein-stained T cells crawl and squeeze through narrow matrix gaps (white arrowheads: constriction ring) and align to preformed matrix structures for contact guidance (black arrowheads). In both cells, oscillatory morphodynamics and flexible shape change support a highly dynamic migration type. Images represent 8 min (c) and 3 min (d) in real time. Note the absence of detectable difference in morphodynamic features of both cells. Bars, 5 μ m.

Figure 28c

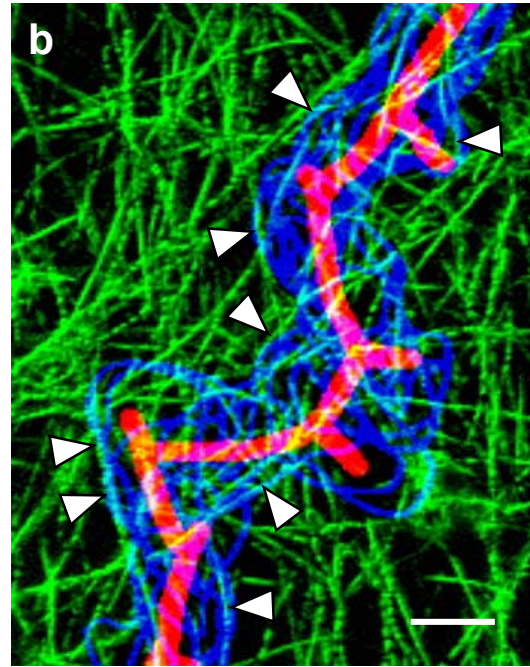
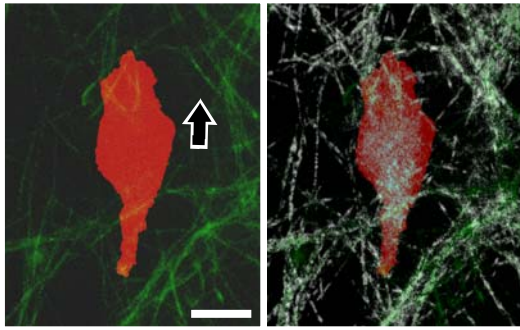
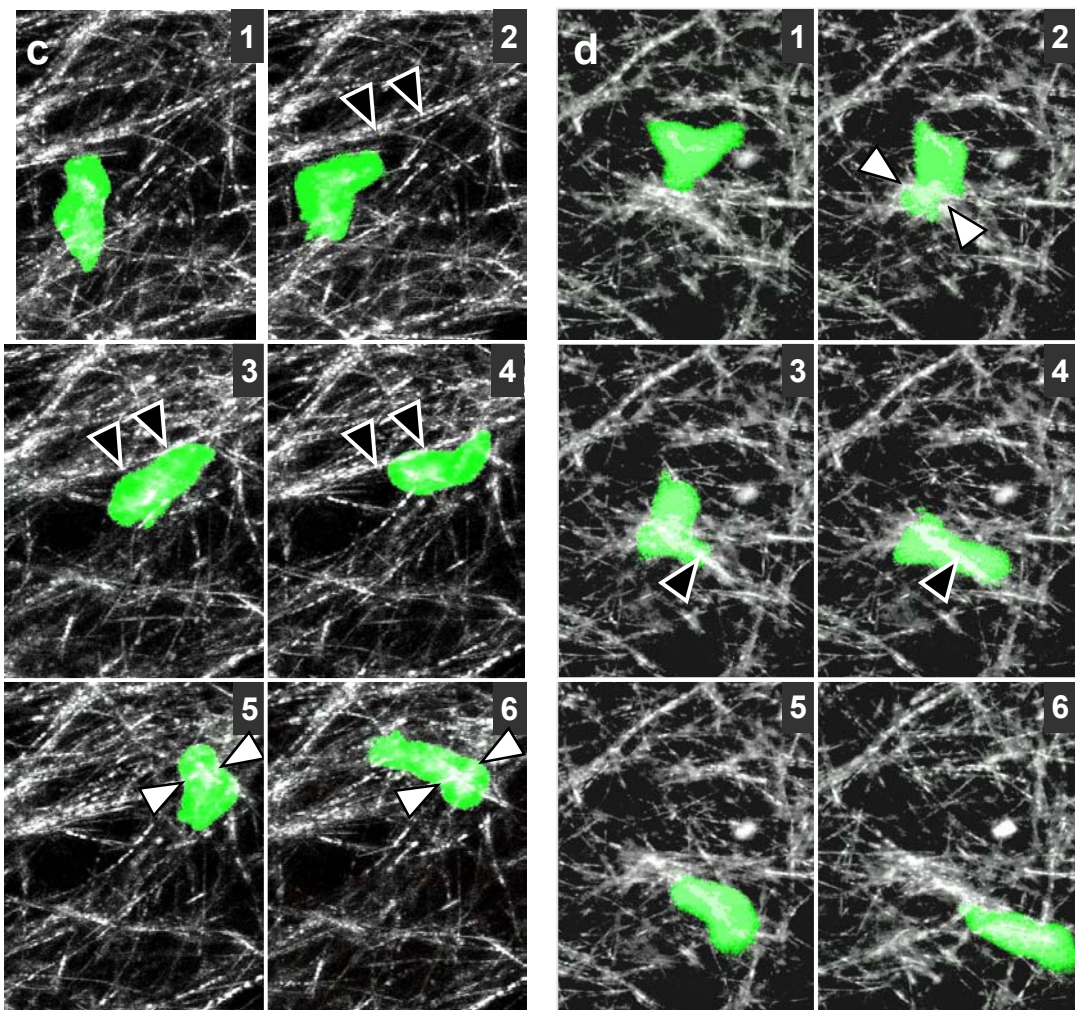
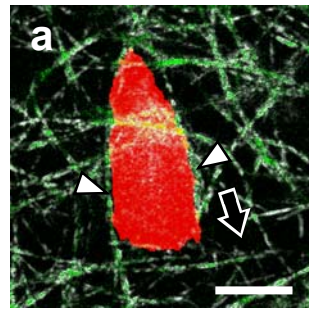


Figure 30



3. DISCUSSION

In this thesis, the contribution of matrix degradation by cell-derived proteases was investigated for different cell types, i.e. tumor cells and T lymphocytes, which reveal different constitutive migration strategies. The data identify significant diversity as well as plasticity in cellular and molecular migration strategies after the inhibition of the cellular capacity to cleave ECM.

3.1. Contribution of proteases to tumor cell migration

The transition from proteolytic and „mesenchymal“ to protease-independent and „amoeboid“ movement reveals a novel cellular and molecular adaptation pathway in sustaining cell migration: the switch from path generating to a path finding migration mode that was termed „mesenchymal-amoeboid transition“ (MAT). Although proteases were used for constitutive migration of proteolytic cells of mesenchymal and epithelial origin, abrogation of pericellular proteolysis was followed by non-proteolytic movement. MAT thus represents a compensatory migration mode in vitro and in vivo to bypass physical matrix resistance by amoeboid shape change.

3.1.1. Constitutive proteolytic mesenchymal migration of tumor cells

Important concepts on cell migration are derived from the movement of fibroblasts and myoblasts (Lauffenburger and Horwitz, 1996). In 3D in vitro and in vivo tissues, fibroblasts develop elongated, spindle-shaped morphology mediated by cortical F-actin and occasional stress fibers (Welch et al., 1990). Fibroblast migration is dependent on $\beta 1$ integrin function (Doane and Birk, 1991; Cukierman et al., 2001) and further coupled to the cleavage and remodeling of ECM components using MMPs and other proteases (Langholz et al., 1995). A similar type of mesenchymal behavior is developed by MV3 melanoma cells, HT-1080 fibrosarcoma cells and MDA-MB-231 mammary carcinoma cells in 3D collagen matrices. These cells move as individual spindle-shaped cells, that utilize $\beta 1$ integrin-mediated binding to collagen fibers for elongation and translocation. Similarly to fibroblasts, a range of ECM-degrading enzymes is expressed and co-clustered with integrins at interactions to substrate. Therefore, both MMP surface

expression and localization, as well as fiber cleavage and degradation strongly support the concept of cell-bound focalized proteolysis for a 3D collagen-based model, which propels migration as shown for MT1-MMP overexpressing cells. In contrast, proteases secreted into the supernatant, such as MMP-2, under both serum-containing and serum-free conditions, did not generate degradation of fibrillar collagen, which is consistent with the neutralization function of TIMPs (Birkedal-Hansen, 1995). Focalized proteolysis might be used for the generation of tube-like matrix defects that correspond to known clearance tracks in other models (d'Ortho et al., 1998; Nakahara et al., 1997; Friedl et al., 1998a). Because the cell diameter of mesenchymal-like cells exceeds the mean pore size within the fiber network (Friedl et al., 1997), contact-dependent focal degradation of collagen barriers may facilitate migration by locally lowering the physical resistance of the ECM barrier (Murphy and Gavrilovic, 1999).

3.1.2. Constitutive non-proteolytic amoeboid migration

In some cell types, migration results from more dynamic, transient and less defined cell-substrate contacts associated with amoeboid shape [(Friedl and Brocker, 2000) and Refs. therein]. The concept of amoeboid movement is most clearly established from the single cell state of the lower eucaryote *Dictyostelium discoideum*. *Dictyostelium* is an ellipsoid cell that translocates by rapidly alternating cycles of morphological expansion and contraction, relatively low-affinity integrin-independent interactions to the substrate, and extraordinary deformability (Killich et al., 1993; Yumura et al., 1984; Devreotes and Zigmond, 1988; Friedl et al., 2001). In higher eucaryotic cells, such as leukocytes and certain types of tumor cells, hallmarks of amoeboid motion are retained, including rapid low affinity gliding coupled by shape change and the ability to squeeze through preformed matrix gaps (Lewis, 1934; Schor et al., 1981; Haston et al., 1982; Friedl et al., 1998b; Friedl et al., 2001). Thus, amoeboid migration appears to comprise morphodynamic mechanisms to bypass tissue barriers.

3.1.3. Mesenchymal-amoeboid transition: induced amoeboid migration

ECM-degrading proteases contribute to tumor cell migration in different invasion and migration models. Under several experimental conditions, however, a varying degree of residual migration is obtained after abrogation of protease function (Deryugina et al.,

1997a; Hiraoka et al., 1998; Kurschat et al., 1999; Ntayi et al., 2001). The finding, that a constitutive proteolytic migration within collagen-rich tissues is sustained by protease-independent mechanisms, i.e. shape change and morphodynamic adaptation, suggests that proteases may be dispensable for the migratory process. In order to provide maximum inhibition efficiency, five pharmacological inhibitors were used to simultaneously target different protease classes known to contribute to ECM degradation and remodeling, including MMPs, serine proteases, and cathepsins expressed by HT-1080 and MDA-MB-231 cells. It was reasoned that more specific approaches, such as genetic ablation of individual proteases, might be hampered by proteolytic redundancy and functional compensation.

Using a combined biochemical and structural approach, the effectiveness of the protease inhibition strategy was shown by: i) near-total inhibition of FITC-release using FITC-labeled fibrillar collagen; ii) abrogation of macroscopic structural degradation of the collagen lattice by HT-1080 cells; and iii) the lack of newly generated tube-like matrix defects in the wake of the cells visualized by 4D confocal backscatter microscopy.

Inhibition of constitutive proteolysis, instead of causing the cells to become „trapped“ by the fibrillar network, induced a program of morphodynamic changes that allowed the maintenance of the migratory action (Fig. 31).

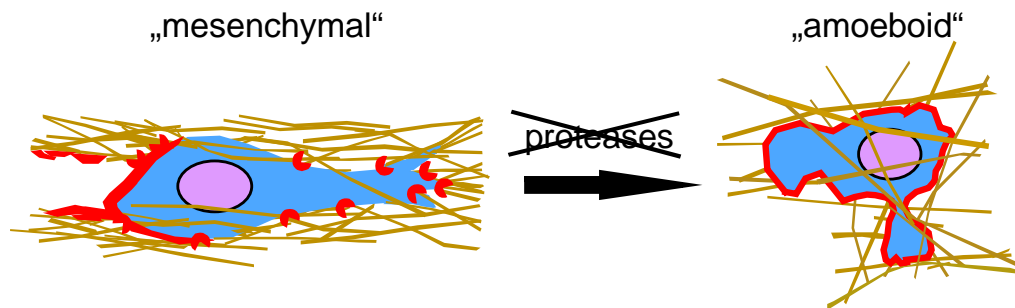


Figure 31. Mesenchymal-amoeboid transition. Adaption from spindle-shaped proteolytic towards amoeba-like non-proteolytic tumor cell migration strategy upon blocking of tumor-cell-derived proteolysis.

These changes included a reduced elongation, yet increased morphodynamic flexibility, the loss of focal integrin and MT1-MMP clustering at interactions to matrix fibers, and a more diffuse cortical actin distribution, mimicking a phenotype similar to amoeboid moving cells (Yumura et al., 1984; Devreotes and Zigmond, 1988; Killich et al., 1993; Friedl et al., 2001). One possible explanation for the loss of MT1-MMP from focal contacts at the cell surface upon MMP inhibition is, that the association of MT1-MMP

with a compartment-specific regulatory protein (gC1qR) involved in intracellular transport is interrupted, which leads to MT1-MMP accumulation within the cell (Rozañov et al., 2002). This induced amoeboid behavior generated significant migratory activity, yet the transmigrated collagen architecture remained intact by means of biochemical and structural analysis. These data therefore show an alternative inhibitor-induced non-proteolytic migration type, here termed mesenchymal-amoeboid transition (MAT) (Fig. 31). Pericellular proteolysis appeared dispensable as long as cells could compensate for constraining matrix barriers by amoeboid shape change. Induced protease-independent movement was observed for two different collagen-based tissue models, 3D collagen lattices in vitro and the mouse dermis in vivo. As reconstructed by intravital microscopy, the loose connective tissue of the mouse dermis exhibits strong structural similarity to 3D collagen matrices. Both models provide 3D fibrillar collagenous strands bordering matrix gaps and pores in the range of 1 - 15 μm , while the cell diameter is in the range of 15 - 25 μm (Friedl et al., 1997) (K. Wolf and P. Friedl, unpublished). Migratory alignment and shape change along preformed fiber strands, constriction, and propulsion hence represent non-proteolytic, physical strategies employed by large tumor cells (10–30 fold larger volume than amoeba or leukocytes) to bypass structural ECM barriers. While the spacing of such loose connective tissue supports protease-independent cell movement, future studies will be necessary to determine under which conditions transmigration of more densely interconnected ECM, such as basement membranes, can occur by non-proteolytic means.

The finding that blocking proteases induces transition from a dedifferentiated mesenchymal phenotype to amoeboid movement sheds light on how disseminating tumor cells may react in response to protease inhibitor-based therapy. In established tumor disease, tumor cells have already reached interstitial tissue compartments (Stetler-Stevenson et al., 1995) that are likely to support shape-driven migration independent of pericellular proteolysis. Therefore, protease-independent tumor cell dissemination may represent a candidate escape mechanism upon protease inhibitor-based treatment of progressive cancer disease (Zucker et al., 2000; Kruger et al., 2001; Coussens et al., 2002).

3.1.4. MAT- molecular implications

From a cytomechanic perspective, the molecular events involved in MAT can be best explained by changes in cell-matrix interaction strength. Although different experimental systems are difficult to directly relate, exaggerated mesenchymal-like phenotypes can be induced by strengthening cell-ECM contacts or reducing their turn-over: by stabilizing interactions towards collagen fibers after arresting $\beta 1$ integrins in a high affinity ligand-bound state (Maaser et al., 1999) or by stabilizing stress fibers leading to spread-out, elongated morphology through activation of the small GTPase Rho (Nobes and Hall, 1995). Conversely, reduced length axis and amoeba-like morphodynamics may emerge from weakening substrate-binding strength by reducing integrin adhesive function (Dufour et al., 1988; Chan et al., 1992) or by inhibiting Rho-kinase (Nobes and Hall, 1999). In addition to integrins, several of the proteases blocked in this study are known to regulate cellular morphodynamics, including a mesenchymal phenotype (Lochter et al., 1997; Sternlicht et al., 1999). MMP-3 overexpression in epithelial cells leads to the cleavage of E-cadherin and induces epithelial-mesenchymal transition, i.e. single cell detachment and mesenchymal invasion (Lochter et al., 1997). Proteases further control cell adhesion, cytoskeletal organization, and the release of soluble factors [(Sternlicht and Werb, 2001) and Refs. therein]. These functions comprise cleavage of adhesion receptors (e.g. L-selectin); cleavage and activation of cytokines (e.g. IL-1 and TNF- α) or growth factors (e.g. EGF and bFGF); and the regulation of focal contact assembly and turn-over by cleavage of talin or integrin cytoplasmic domains through e.g. calpain (Pfaff et al., 1999). The identification of pathways involved in MAT will thus require further studies on different cytoskeletal and signaling checkpoints that control cell shape and cell-matrix interactions.

3.1.5. MAT-comparison to other morphodynamic processes

Plasticity and adaptation in cell behavior are well established in other morphodynamic processes governed by cell-cell- and cell-substrate interactions. In epithelial-mesenchymal transition, a normally non-migrating epithelial collective abandons cell-cell cohesion after cadherin-mediated cell-cell contacts are weakened, allowing detachment of single cells, and conversion towards mesenchymal morphology and migration (Birchmeier and Birchmeier, 1995; Sternlicht et al., 1999). In another example,

differentiating muscle precursor cells quit cell movement and fuse via N- and E-cadherin to form a multicellular contractile syncytium (Redfield et al., 1997). In conclusion, MAT may represent a basic morphodynamic event that converts cell dynamics from stringent, adhesive, and proteolytic cell-ECM contacts towards evolutionary old less intimate, less defined, and less proteolytic interactions with extracellular scaffolds reminiscent of amoeboid single cell movement.

3.2. Contribution of proteases to T cell migration

T cell recirculation for homeostasis but also for inflammation requires the trafficking through peripheral as well as lymphatic tissues rich in extracellular matrix components including fibrillar type I and III collagens as the predominant constituents. Current concepts on the function of proteases in leukocyte movement were adapted from the established findings in tumor cells and fibroblasts, suggesting that successful migration within ECM-rich tissues requires the lowering of physical matrix resistance towards the advancing cell body through limited matrix degradation and remodeling mediated by secreted as well as cell-bound matrix proteases (Murphy and Gaborovic, 1999; Friedl et al., 2000). Likewise, the migration of neutrophils and monocytes on 2D substrata is accompanied by localized proteolytic clearance tracks (Owen and Campbell, 1999), and degradation of ECM components by matrix-degrading enzymes is thought to be fundamental in the creation of a proteolytic path, thereby enabling immune cells to penetrate tissue barriers (Goetzl et al., 1996; Vaday and Lider, 2000). However, direct proof that proteolytic action is a prerequisite for leukocyte migration and trafficking is lacking.

Previous evidence suggested that naïve T cells are largely devoid of proteases, such as MMP-2 and -9, while these and other proteases are upregulated in T blasts and T lymphoma cells (Leppert et al., 1995a and b, Xia et al., 1995; Hauenberger et al., 1999). Therefore, this study was focussed on ConcanavalinA-activated T cells expressing several matrix-degrading proteases and the SupT1-lymphoma line that were previously shown to engage MMPs for the migration through matrigel-coated filters (Xia et al., 1996). This study here shows for T cell movement within 3D collagen matrices, that MMPs and other matrix-degrading proteases, although expressed by activated T cells, neither degrade

fibrillar collagen while the cells are migrating, nor do they contribute to the migration process as such.

3.2.1. Expression of proteases in activated T cells

Expression of proteases from different classes has been previously investigated in leukocytes. Monocytes and neutrophils express a broad spectrum of proteases, including metalloproteinases (MMPs; ADAMs, also termed sheddases), cysteine and aspartatic proteases (cathepsins), and serine proteases (cathepsin G, PA/plasmin-system, tryptase, chymase, HLE, granzymes A and B, proteinase 3) (Owen and Campbell, 1999). In primary activated T cells, a more limited number of proteases is detected, including members of the PA/plasmin-system, MMP-2 and MMP-9, TIMP-2, and HLE (Bristow et al., 1991; Montgomery et al., 1993; Zhou et al., 1993; Leppert et al., 1995a; Gunderson et al., 1997).

In the present study, mRNA expression of additional proteases from different classes as well as MT1-MMP surface expression was detected. In particular, mRNA expression of MT1-MMP, MT4-MMP, cathepsin L, and ADAM 9 and 15 is shown here for primary activated T lymphocytes, which is similar to protease profiles in T cell lines (Lokshina et al., 1993; Esparza et al., 1999; Ivanoff et al., 1999). MT1-MMP at neutral pH and Cathepsin L at acid pH, as well as HLE, act as potent collagenases towards type I collagen (Ohuchi et al., 1997; Kagegawa et al., 1993; Bieth, 1986). In contrast to previous evidence on 7-10 days activated PHA T blasts (Leppert et al., 1995a), or T cell clones (Romanic et al., 1994), MMP-2 was not detected in highly purified T cells activated for 3 days only, which is consistent with other work on exclusive MMP-9 expression in T lymphoma cells (Zhou et al., 1993). The substrates for the detected enzymes comprise a broad spectrum of tissue components including fibrillar collagen.

3.2.2. T cell migration in 3D collagen independent of proteolytic matrix degradation

3.2.2.1. Lack of in situ collagenolysis

Although a spectrum of collagenolytic enzymes including HLE (Bristow et al., 1991), Cathepsin L and MT1-MMP is expressed by T cells, no degradation of the collagen

migration substrate was detected by different experimental approaches. Lack of collagen degradation by migrating T cells over prolonged observation periods was obtained by (i) FITC-collagen release from FITC-labelled collagen, (ii) lack of focal in situ cleavage sites at T cell-interactions to collagen fibers containing quenched FITC molecules, and (iii) lack of structural fiber remodeling as detected by high-resolution confocal backscatter microscopy. At high reproducibility, FITC released by ConA T blasts was at background “noise” range (0.1-0.2% of the total FITC content). This value is by 10-fold lower than collagenolysis exerted by MV3 melanoma cells (compare Fig. 11b) and more than 100-fold lower than by HT-1080 fibrosarcoma cells overexpressing MT1-MMP used as positive control. Upon dynamic confocal backscatter analysis, migrating T cells neither bundled or extensively pulled fibers nor were focal cleavage of quenched FITC-collagen or defects of reorganized matrix generated. Hence, on a descriptive basis and in contrast to HT-1080 fibrosarcoma cells, T cells display a constitutive non-proteolytic migration strategy, which is consistent with the lack of collagenolysis by non-activated T cells from radioactive-labelled collagen matrices (Schor et al., 1983). While minor cleavage of collagen fibers below detection sensitivity of radioactive or FITC-based assays cannot be excluded, the lack of structural changes in collagen fiber integrity upon T cell migration as detected by confocal backscatter microscopy argues against biophysically relevant macroscopic and microscopic changes in matrix architecture. Hence, despite the expression of several proteases by activated T blasts, no evidence on their action towards fibrillar type I collagen was obtained.

3.2.2.2. Lack of inhibitory effects of protease inhibitors on T cell migration

To block any matrix protease activity in activated T cells, the protease inhibitor cocktail previously established for tumor cells (see Table 3) was adapted for a modified yet equally efficient dose (see legend of Fig. 28). In proteolytic HT-MT1 cells, this protease inhibitor cocktail is effective in inhibiting collagenolysis by 95-98% and further blocks fiber remodeling and proteolytic path generation, suggesting that no biophysically relevant matrix remodeling is maintained in the presence of inhibitor cocktail. Continuous-time high-resolution analysis in T blasts showed that the protease inhibitor cocktail did not affect cellular morphodynamics and migration efficiency, including the following parameters: migration velocity; stop-and go pattern; the total distance migrated over time; the structure and extension of individual paths; cell polarization and short-lived

interaction dynamics with collagen fibers. Therefore, the enzymatic function of proteases expressed by T cells is dispensable for interaction with collagen fibers and migration of T cells. Indirectly, the data further exclude a significant contribution of endoproteinases cleaving intracellular or transmembrane proteins, such as calpain involved in the regulation of integrin-cytoskeleton interactions or ADAMs involved in the release of promigratory cytokines and growth factors from transmembrane precursors, such as EGF or TNF- α (Dethlefsen et al., 1998; Cerretti, 1999).

3.2.3. Non-proteolytic, biophysical mechanisms supporting T cell migration through matrix barriers

T cell migration in 3D collagen is independent of $\beta 1$, $\beta 2$, $\beta 3$ and αv integrins (Friedl, 1998b); in addition, no T cell trafficking defects are obtained in mice lacking $\beta 1$ integrins in hematopoietic precursor cells including the T cell lineage (Brakebusch et al., 2002). Similar to *Dictyostelium* amoebae that lack an integrin homologue, T cells appear to utilize amoeboid migration mechanisms of high dynamics and shape change, yet little adhesivity to the surrounding substrate (Friedl et al., 2001). Dynamic reconstructions of fluorescent labelled T cells and the 3D collagen lattice architecture by 4D confocal backscatter microscopy show that T cells develop random paths by aligning along fibers that border random gaps and trails preexisting in the collagen matrix, thereby following preformed random paths of least resistance along fibrillar guidance cues (“contact guidance”) (Wilkinson et al., 1982). Because of a high morphological adaptivity and a parallel to fiber strands orienting cell body, the gliding through even narrow gaps occurs in the absence of structural matrix remodeling, allowing a high migration velocity up to 25 $\mu\text{m}/\text{min}$, similar to in vivo migration of T cells within intact lymph nodes (Miller et al., 2002). Upon contact with matrix barriers of more densely interwoven collagen fibers, two different adaptation responses are able to sustain non-proteolytic movement: i) squeezing through the narrow region by adapting the cell body and the formation of constriction rings (Lewis, 1934) that allow for cytoplasmic streaming through the narrow zone; ii) if matrix gaps are too narrow (approximately 2 - 3 μm) in diameter, personal observation), T cells change their direction for migration and move around the obstacle. In summary, reconstruction of cell body outline and transmigrated matrix architecture suggest that the volume of the cell body precisely reflects volume, space and extension of

preformed trails and gaps in the collagen matrix and includes only minor but fully reversible pulling and widening of matrix fibers.

While this study shows non-proteolytic T cell migration for a 3D collagen matrix model *in vitro*, circumstantial evidence argues against protease function in T cell migration *in vivo*: 1) lack of obvious T cell trafficking defect in patients receiving MMP and other protease inhibitor therapy (Chris M. Overall, personal communication); 2) the capacity of resting T cells to enter lymphatic and periperal tissues and recirculate, although they produce little to no proteases (Schor, 1983; Leppert, 1995a); 3) the high migration velocity of resting as well as activated T cells up to 30 $\mu\text{m}/\text{min}$ *in vivo* (Miller et al., 2002) resulting in contact time towards individual collagen fibers in the range of only 5 to 20 seconds; 4) lack of matrix degradation from *in vivo* imaging in the intact lymph node (Miller et al., 2002); 5) the abundant presence of loose connective tissue regions in virtually all organs supporting oedematous swelling and widening of matrix gaps in response to vasodilatation and inflammation. In the dermis, such loose connective tissue zones are present as perivascular spaces along vessels, along the basement membrane towards the epidermis (“junction zone”), and the dermal papillae (Friedl and Broecker, 2000b). As an example of severe yet non-destructive inflammation in atopic or contact dermatitis, T cell-dominated infiltrates are not accompanied by matrix degradation, suggesting that T cell trafficking and infiltration does not require histologically detectable proteolytic tissue remodeling (Friedl and Broecker, 2000b). The principle of protease-independent T cell migration in a basic system such as a 3D collagen lattice devoid of additional ECM components and resident tissue cells, however, does not exclude the possibility that proteases from bystander cells such as endothelial cells, fibroblasts and other leukocytes facilitate and therefore contribute to T cell navigation through regions of matrix remodeling.

In conclusion, ameoboid T cell migration coupled with biophysical contact guidance along the preformed matrix pattern support an efficient non-proteolytic migration strategy generated by an adaptive actin cytoskeleton. These characteristics set T cells apart from proteolytic migration strategies of other cell types such as fibroblasts and tumor cells.

3.3. Diversity and plasticity of protease functions in the migration of different cell types

3.3.1. Diversity

Protease functions in different cell types have been examined and compared extensively in this study. According to protease expression, cell size, and adhesion mediated by integrins, different cell types considerably vary in proteolytic capacity upon migration within extracellular matrix (Fig. 32).

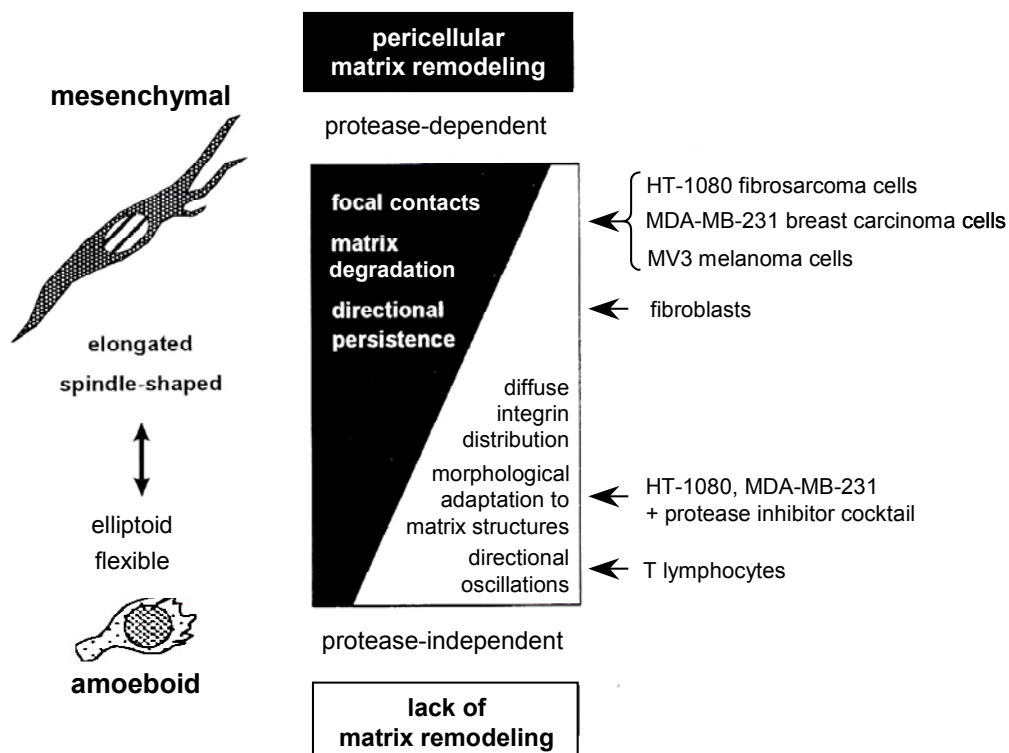


Figure 32. Model for the contribution of matrix proteases to migration strategies of different cell types.

1) Different cell types may constitutively vary from proteolytic, matrix-degrading to non-proteolytic, non-matrix-degrading mechanisms. 2) Migratory phenotypes may undergo transition upon inhibition of proteases from proteolytic, matrix-degrading to non-proteolytic, non-matrix-degrading mechanisms. Overlapping characteristics may exist.

T cells, small in size, do not degrade the matrix while migrating and utilize flexible form changes resulting in morphological adaptations to preformed matrix structures to overcome fibrillar matrix barriers, following the paradigm of amoeboid movement. Tumor cells, on the other hand, such as HT-1080, MV3 or MDA-MB-231 cells, migrate

relatively slowly (10 – 30 fold slower than T cells), and accompanied by matrix degradation and remodeling via cell-derived proteases and the generation of circumscribed tube-like matrix defects. The degree of matrix degradation is further reflected by the amount of $\beta 1$ integrins engaged in clusters at cellular interactions (e.g. focal adhesions or contacts) with the collagen substrate. Cells that form more prominent focal contacts at interactions to collagen fibers appear to reorganize ECM more efficiently, such as mesenchymally migrating cells (Friedl et al., 1998a). In contrast, T cells lacking clustered integrins establish only very transient and non-reorganizing interactions with collagen fibers with low adhesivity not blocked by integrin antagonists.

3.3.2. Plasticity

The model on diversity in migration strategies may further explain transition from a given constitutive towards a newly acquired migration strategy. Upon blockage of proteolytic capacity preventing the degradation of the extracellular matrix substrate, tumor cells lose both integrin clustering and proteolytic capacity and, as a consequence, continue migration by newly acquired amoeboid shape change along preformed matrix structures, here termed mesenchymal-amoeboid transition (see Fig. 31). In summary, the spectrum of proteolytic and non-proteolytic migration as well as transition and adaptation upon protease inhibitor therapy suggest a concept of diversity and adaptation in cell migration strategies (see Fig. 32).

3.4. Implications and outlook

Concepts on diversity and plasticity of cell migration described in this work have several implications for the understanding of cellular trafficking in health and disease, as well as therapeutic targeting of cell motility.

1) Unpublished results from our laboratory on the function of $\beta 1$ integrins in fibroblast-like, mesenchymal tumor cell migration within 3D collagen lattices show that partial integrin inhibition or reduced expression result in fast amoeboid movement, while complete inhibition yields slow, yet still significant amoeboid movement of tumor cells (N. Daryab, in preparation). These findings suggest that plasticity in migration may be

determined at the integrin level, according to the model depicted in Fig. 2 and further implicate cross-function of proteases with integrins by mechanisms that remain to be identified.

2) Upon treatment of cancer patients with protease inhibitors, such as the MMP inhibitors marimastat or others (Heath et al., 2000; Zucker et al., 2000; Giavazzi et al., 2001; Hidalgo et al., 2002), adaptation of migrating tumor cell to preformed matrix structures may represent an escape strategy of tumor cells to overcome and bypass matrix barriers, although matrix degrading enzymes are inhibited. Such non-proteolytic migration might contribute to persistent cancer cell spread and undiminished metastasis, as reported by recently failed MMP inhibitor clinical trials in patients suffering from advanced cancer (Zucker et al., 2000; Matrisian et al., 2002; Overall et al., 2002).

3) It is unlikely that a therapeutic inhibition of the complex, yet robust process of cell migration may be achieved by blocking of a single adhesion receptor or a limited group of proteases. Furthermore, even total inhibition of integrins and proteases may not be sufficient to arrest the motility of tumor cells or, for treatment of autoimmune disease, leukocytes. In particular, in cancer diseases where cell motility can cause death, targeting invasion and migration will further require a deeper knowledge on cellular and molecular “escape strategies” allowing compensation and, putatively, the outgrowth of cell subsets and clones resistant to a given treatment with biological response modifiers, such as protease or integrin antagonists. Additional knowledge and research on basic mechanisms of adhesion and proteolysis involved in cell migration in 3D tissues both in vitro and in vivo will be important in designing effective combination protocols for specific therapeutic targeting of different types of migratory processes.

4. MATERIALS AND METHODS

4.1. Antibodies

The following antibodies were used for flow cytometry analysis and confocal microscopy studies of human cells: mouse IgG₁-anti-β1 integrin monoclonal antibody (mAb) (clone 4B4) and mouse IgG_{2a}-anti-β1 integrin mAb (clone K20) (Coulter-Immunotech, Krefeld, Germany), rabbit IgG-polyclonal anti-MT1-MMP and anti-MMP-2 Ab (Chemicon, Hofheim, Germany), mouse IgG₁-anti-TIMP-2 (clone T2-101) and anti-MMP-9 mAbs (clone 7-11C) (Oncogene, Schwalbach, Germany), and unfractionated rabbit cathepsin D antiserum (Dako, Carpinteria, CA). Goat polyclonal anti-uPA, anti-PAI-1, anti-PAI-2 Abs and mouse anti-uPA-R mAb (clone 15.4.1) were kindly provided by M. Kramer, Heidelberg, Germany. Mouse anti-human IgG₁ (Dianova, Hamburg, Germany) was used as isotype control for mouse mAbs and rabbit or goat anti-human IgG (Sigma, Taufkirchen, Germany) as isotype control for polyclonal Abs. Phalloidin-fluoresceine was obtained from Molecular Probes, Leiden, The Netherlands. As secondary Abs were used: polyclonal FITC-and Rhodamin-Red-X- conjugated goat anti-rabbit and -mouse F(ab')₂ fragments (Dianova). For Western blotting, primary polyclonal rabbit IgG-anti-MT1-MMP Ab (Chemicon) or mouse IgG₁-anti-MMP-2 mAb (clone 42-5D11) (Oncogene) and secondary horseradish peroxidase-conjugated donkey anti-rabbit IgG (Dianova) or goat anti-mouse IgG Abs (Biorad, Hercules, CA) were used.

4.2. Human cell lines and culture

The following invasive and metastatic tumor cell lines were used as model cells that developed spontaneous migration in collagen matrices: MV3 melanoma cells (Van Muijen et al., 1991) were kindly provided by G. Van Muijen (University of Nijmegen, Nijmegen, The Netherlands). MV3 cells express high levels of α2β1 and α3β1 integrins for interaction to collagen type I, and show intermediate or no expression of other integrins (Danen et al., 1993). MV3 culture was performed in RPMI medium (PAN, Heidenheim, Germany). HT-1080 fibrosarcoma cells transfected with MT1-MMP (clone HT-MT23, in this study named: HT-MT1) or neo vector (HT-neo) (Deryugina et al., 1997a, 1998) were kindly provided by A. Strongin (The Burnham Institute, La Jolla, California). HT-1080 cells were cultured in DMEM (PAN) additionally containing 0,2

mg/ml G418 (Oncogene). MDA-MB-231 epithelial breast carcinoma cells (Chen et al., 1994; Ishibashi et al., 1999; Bachmeier et al., 2001; Saad et al, 2002) were obtained from the "European collection of Cell Cultures" (ECACC, Salisbury, UK) and cultured in Leibovitz-15 medium containing 15% heat-inactivated fetal calf serum (FCS) (Biowhittaker, Verviers, Belgium). The human lymphoma CD4+ T cell line SupT1 was obtained from the "Deutsche Sammlung für Mikroorganismen und Zellkulturen" (DSMZ, Braunschweig, Germany). SupT1 cells were cultured as suspension in RPMI medium (PAN). If not indicated otherwise, primary cells and cell lines were cultured in medium containing 50 U/ml penicillin and 50 µg/ml streptomycin (PAN), and 10% heat-inactivated FCS (Biowhittaker). All cell cultures were maintained at 37°C in humidified 5% CO₂ atmosphere.

4.3. Isolation and culture of human T lymphocytes

Human PBMCs were separated from other peripheral blood cells by density centrifugation on a ficoll gradient („Lymphoprep“; Axis-Shield, Oslo, Norway), (density 1,077 g/ml), washed and stimulated for 3 days with 1,25 µg/ml Concavalin A (Oncogene) and 100 U/ml IL-2 (Strathman Biotech, Hamburg, Germany) in RPMI. CD4+ T cells from stimulated PBMC cultures were obtained by positive immunomagnetic selection and a secondary detachment step. CD4+ T cells were incubated with mouse IgM-anti-CD4 mAb (clone 66.1) coupled to superparamagnetic beads (Dynal, Hamburg, Germany) for 7 min (4°C). Detachment was achieved by polyclonal anti-mouse-Fab fragments (Detach-a-Bead, Dynal) (45 min, 20°C). Purity of isolated cell populations was determined by flow cytometry using FITC-conjugated mouse IgG₁-anti-human CD4 mAb and phycoerythrine (PE)-conjugated mouse IgG₁-anti-CD8 mAb (Dianova, Hamburg, Germany). FITC- or PE-conjugated mouse anti-human IgG₁ were used as isotypic controls (Dianova). Flow cytometric analysis (FACScan; Becton-Dickinson, Heidelberg, Germany) yielded in a purity of 95-99% CD4+ T cells. The percentage of blast formation (as detected by morphology dot blot in FACS) was 30 to 60%. T cell experiments were performed at the same day of purification, and in the absence of ConA and IL-2.

4.4. Protease inhibitors

For MMP inhibition studies, broad-spectrum inhibitor BB-2516 (marimastat) was used. BB-2516 blocks most MMPs in nM or low µM ranges (British Biotech, Oxford, UK) and, to some extent, ADAMs (Roghani et al., 1999). For confirmation studies, additional

MMP inhibitors phenanthroline (Molecular Probes), GM-6001 (ilomastat) (Oncogene), BB-94 (batimastat) and BB-3103 (British Biotech), Ro-206-0222 and Ro-28-2653 (Roche-Diagnostics, Penzberg, Germany) were used. Further protease inhibitors were aprotinin, trans-Epoxy succinyl-L-leucylamide-(4-guanidino)butane (E-64), pepstatin A (all from Sigma), and leupeptin (Molecular Probes). Inhibitor specificity, inhibitory concentration range and used concentrations are indicated in Table 3 (chapter 2.2.2.1.).

4.5. Construction of migration chambers

For monitoring of cell migration, migration chambers were self-constructed. A glass slide and a coverslip (22x22 mm) were connected on 3 sides in a distance of ~ 500 µm by a 1:1 mixture of paraffine and vaseline, leaving one side open for placing a cell-collagen mixture and medium. The approximate chamber size was ~ 20x20x0,5 mm, resulting in a volume of ~ 200 µl. After addition of collagen solution and medium (details see below), the chamber was sealed by paraffine/ vaseline.

4.6. Preparation of 3D collagen lattices

3D collagen matrix cultures were prepared as described (Friedl et al., 1993). Adherent subconfluent cells were detached by EDTA (2 mM) at 37°C for 10 min, washed with Ca²⁺- and Mg²⁺- free PBS (Life Technology, Karlsruhe, Germany), suspended in medium, counted, and adjusted to defined cell density (1x10⁶ cells/ml). Non-adherent T-cells were washed and suspended in medium (3x10⁶ cells/ml). One part of cell suspension was then incorporated into two parts of a bicarbonate-buffered 3D-lattice from dermal bovine type I collagen (Vitrogen; Cohesion, Palo Alto, CA) complemented with Minimal Essential Eagle's Medium (MEM; ICN, Meckenheim, Germany). The collagen was resistant to trypsin and sensitive to degradation by MT1-MMP, confirming its native state (C. Overall and E. Tam, unpublished). For collagen-degradation measurement, 2% ^{DQ} FITC-collagen type I monomers from bovine skin (Molecular Probes) was added to the collagen solution prior to polymerization. The final collagen concentration was 1,67 mg/ml. Cell-collagen mixtures were then either placed on a coverslip, into a well-plate, or the migration chamber. After polymerization of the collagen lattice, medium was added. For inhibition studies, adhesion-pertubing anti-β1 integrin mAb 4B4 (10 µg/ml) or protease inhibitors (Table 3, chapter 2.2.2.1.) were added to the collagen lattice as well as to the supernatant.

4.7. Time-lapse videomicroscopy

Cells in collagen matrices were monitored by light microscopy using inverse microscopes (DM-IL; Leica, Heidelberg, Germany) coupled to CCD cameras (VPC-175; Sony, Berlin, Germany) at a 320 fold (tumor cells) or 80 fold (T cells) acceleration by time-lapse videomicroscopy (BR-S920E and SR-970E video recorders; JVC, Friedberg, Germany). The microscope stage was maintained at 37°C by an infrared heating system.

4.8. Analysis of cell viability

Cell viability in the presence of pharmacological compounds (i.e. protease inhibitors) was assessed in dose-and time-dependent studies for both, liquid as well as collagen culture. For the latter, cells were released from the collagen lattice by collagenase I digestion (*Clostridium histolyticum*; Sigma) for 30 min at 37°C. Cells were then stained by propidium iodide (Sigma) and analyzed by flow cytometry (FACS). To exclude toxicity-induced migratory alterations after 20 hr of time-lapse videomicroscopy, cells from collagen lattices were routinely examined for viability by propidium iodide staining.

4.9. Computer-assisted cell tracking

Locomotor parameters were obtained by computer-assisted cell tracking and reconstruction of the xy coordinates of cell paths, as described (Friedl et al., 1993). The average speed and percentage of locomoting cells in a population were calculated from each 15 min tracking interval for all cells divided by the number of cells (in general 40 cells). Single cell “speed” represents the total length of a cell path divided by time. “Velocity” of cells represents the total length of a cell path divided by time, excluding time periods of no cell movement. The number of locomoting cells represents the percentage of moving cells in a population at defined time points or, for single cells, the percentage of step intervals the cell was moving.

4.10. Statistical analysis

For statistical analysis, the Students two-tailed *t*-test and the non-parametric Mann-Whitney *U*-test was used.

4.11. Flow cytometry

Cells were cultured for 20-24 hr in liquid culture or within 3D collagen lattices. To release cells from the collagen lattice, collagen digestion was performed by highly purified collagenase type VII from *Clostridium histolyticum* (Sigma), as described (Friedl et al., 1995). Cells from liquid culture were detached using 2 mM EDTA. 100.000 cells/vial were stained on ice by primary monoclonal mouse or polyclonal rabbit Ab (10 µg/ml, 1 hr), washed twice, and incubated with secondary FITC-conjugated goat or rabbit F(ab')₂ fragments-anti-mouse IgG (H+L) (1 µg/ml, 30 min). For detection of β1 integrin expression, cells were stained by FITC-conjugated anti-β1 integrin mAb (10 µg/ml, 30 min). Cell surface expression was detected by flow cytometry (FACScan, Becton-Dickinson). In control experiments using collagenase-treated cells of different origin from liquid and collagen cultures, neither integrin (Maaser et al., 1999), nor other adhesion receptors (Friedl et al., 1995), or MMP expression (own observations) were affected by the highly purified collagenase.

4.12. Gel electrophoresis and Western blotting

For the detection of MMPs by Western blot, subconfluent adherent cells were cultured in collagen lattice (see 4.6.) in the absence of FCS for 24 hr. The conditioned medium was removed and concentrated by Ultrafree filters (cut-off: >10 kD) (Millipore, Schwalbach, Germany). Cells from the collagen lattice were released by collagenase VII treatment, counted, and lysed on ice in NP-40 buffer (1% NP-40; 1% SDS; 0,5% Triton-X100; 150 mM NaCl; 50 mM Tris-HCl; 1 mM CaCl₂; 1mM MgCl₂), containing 2 µg/ml aprotinin, 1 mM PMSF (Molecular Probes) and 1 µM pepstatin A. Control experiments were performed using supernatants and cells from liquid culture, confirming band locations and expression levels (not shown). Cell lysates were adjusted to 2,5x10⁵ cells/lane, and concentrated conditioned medium from supernatants to equivalents of 0,5x10⁵ cells/lane. Samples were then mixed with sample buffer (with a final concentration of 62,5 mM Tris-HCl, pH 6,8; 2% SDS; 10% glycerol; 0,1% bromphenolblue) including 5% mercaptoethanol for reduction of disulfide bonds. Samples and Kaleidoskop prestained molecular weight marker (Biorad) were separated on 8% SDS-polyacrylamide gels at 125 V for approximately 100 min. Proteins were transferred onto a nylon membrane (Amersham, Freiburg, Germany) at 0,5 mA/ cm² for 1 hr. Membranes were incubated in 3%BSA/ TBS-T (50 mM Tris-HCl, pH 7,5; 200 mM NaCl; 0,2% Tween 20) for 1 hr to

reduce unspecific Ab-binding, and incubated with polyclonal anti-MT1-MMP Ab (1 µg/ml) (Chemicon) in 3% bovine serum albumin (BSA)/ TBS-T or monoclonal anti-MMP-2 Ab (Oncogene) in 0,5% BSA/ TBS-T overnight at 4°C. Blots were washed in TBS-T and incubated with horseradish peroxidase-conjugated anti-rabbit (1:15.000, 50 ng/ml; Dianova) or -mouse IgG Ab (1:6.000 following the manufacturers instructions; Biorad) in TBS-T containing 3% or 0,5% BSA at 20°C for 1 hr. Protein bands were visualized by an enhanced chemiluminescence (ECL) detection kit (Amersham), photographed and digitally scanned for documentation.

4.13. Zymography

Tumor cells were cultured in conventional plastic culture or collagen lattice (see 4.6.) in the absence of FCS for 24 hr. Collagen lattices were centrifuged (15.000 g, 15 min, 4°C) and the supernatant was removed. The pellet containing both, cells and collagen was incubated in sample buffer (for details see 4.12.) at non-reducing conditions until the mixture was solubilized. Samples were then adjusted to $2,5 \times 10^5$ cells/lane. Supernatant was concentrated, and a volume corresponding to conditioned medium from $0,5 \times 10^5$ cells was mixed with non-reducing sample buffer as well. For zymography, samples were separated by 8% SDS-free polyacrylamide gels containing 1 mg/ml native collagen. After electrophoresis, the gel was incubated at 37°C overnight in enzyme buffer (50 mM Tris-HCl, pH 7,5; 200 mM NaCl; 5 mM CaCl₂; 5 mM MgCl₂; 0,02% Brij-35). In some cases, to confirm the inhibition efficiency, BB-2516 was added at different concentrations to the enzyme buffer. Gels were stained with Coomassie Blue (0,5 mg/ml) in 30% methanol/ 10% acidic acid, and collagenolytic bands were obtained from reduced staining. Excess color was removed by 30% methanol/ 10% acidic acid and gels were digitally scanned for documentation.

4.14. RT-PCR

Total RNA from cells grown in fluid culture was isolated using the RNeasy kit (Qiagen, Hilden, Germany). 1 µg of total RNA was reverse transcribed (1st Strand cDNA Synthesis Kit; Roche Diagnostics, Mannheim, Germany) to cDNA in a 20 µl reaction containing AMV Reverse Transcriptase (1000 U/ml), dNTPs (1mM each), MgCl₂ (5mM), random primer p(dN)₆ (80 µg/ml), gelatine (10 µg/ml), RNase inhibitor (2500 U/ml) and reaction buffer (10 mM Tris; 50 mM KCl; pH 8,3). Each 0,25 µg cDNA was amplified by PCR in a reaction using bacterial recombinant Taq DNA polymerase (12,5 U/ml), dNTPs (0,2

mM), MgCl₂ (1,5 mM), sense and antisense primer (0,2 μM each) (listed in Table 4, page 73) and reaction buffer (10 mM Tris-HCl, pH 8,8; 50 mM KCl; 0,08% NP40), (Life Technologies, Karlsruhe, Germany). PCRs were performed at 94°C for 2-3 min (denaturation), individual annealing temperature and time (see Table 4, page 73), 72°C for 1-2 min (elongation) (each 30 cycles) and a final elongation step (5-10 min). Absence of cDNA contamination was confirmed by subjecting total cell lysates (0,25 μg total RNA) to PCR in the absence of Reverse Transcriptase. The resulting PCR products were analyzed by electrophoresis at 120 V in a 2% agarose gel, stained with ethidium bromide (1 μg/ml), destained, photographed and scanned. The length of each PCR product determined the specificity, and uniqueness of region was confirmed using the NCBI blastn program.

4.15. Collagenolysis assays

4.15.1. Qualitative collagenolysis assay using a native non-labelled collagen matrix

Native fibrillar 3D collagen lattices (1,67 mg/ml) were prepared without (control) or with protease inhibitor cocktail (Table 3, chapter 2.2.2.1.) and filled at 1 ml volume into 6-well plates before polymerization, resulting in 100 μm thickness of the fiber network. Human recombinant soluble MT1-MMP lacking the transmembrane domain and MMP-2 (InVitek, Berlin, Germany) (1 μg each in 5 μl PBS), or tumor cells from subconfluent cultures (0,5x10⁶ cells in 50 μl FCS-free medium, with or without protease inhibitor cocktail) were placed as a drop on top of each lattice, and incubated (40 hr, 37°C, 5% CO₂, humidified atmosphere). Zones of collagenolysis and collagen degradation in the remaining lattice were detected as regions of reduced staining by Commassie Blue. The lattice was destained by 30% methanol/ 5% acidic acid, digitally scanned for documentation and further examined by confocal reflexion microscopy.

4.15.2. Quantitative Collagen-FITC-release-assay

A quantitative collagenolysis assay was established by co-polymerizing 2% ^{DQ} FITC-collagen type I monomers from bovine skin (Molecular Probes) with rat-tail collagen (final concentration 1,65 mg/ml) (Becton Dickinson). Cells were suspended in medium without phenol red (1x10⁵ cells/ 0,1 ml medium/ well). After migration of cells in FITC-containing lattices for 40 hr in the absence or presence of protease inhibitors, solid-phase collagen containing embedded cells was pelleted (15.000 g, 10 min, 4°C). The

supernatant (500 μ l yield) containing released FITC was analyzed by spectrofluorometry. 100% values were obtained by complete collagenase digestion of cell-free collagen lattices. Background fluorescence was calculated by measuring the supernatant of pelleted non-digested cell-free lattices. No auto-fluorescence was detected for either cells or inhibitors. FITC-collagen was sensitive to degradation by recombinant MT1-MMP, MMP-2, and trypsin (C. Overall and E. Tam, unpublished). While FITC-release detected both, classical collagenases as well as trypsin-like activity, FITC-release induced by HT-MT1 cells was highly sensitive to MMP-inhibitor BB-2516 (reduction by 80%; Fig. 16), indicating MMPs as primary collagenases in these cells.

4.16. Confocal laser-scanning microscopy

3D confocal laser-microscopy of fixed samples was carried out on a Leica-TCS 4D system, (Leica, Bensheim, Germany). After 6-15 hr of incubation, cell-containing collagen lattices were fixed with either 4% paraformaldehyde at 37°C for 30 min or methanol at -20°C for 20 min and rinsed with PBS. Lattices were stained with unconjugated primary mouse or rabbit anti-human Ab (10 μ g/ml; 4°C, overnight), rinsed, and stained with secondary Rhodamin-Red-X-conjugated goat anti-mouse or -rabbit Fab fragments (20 or 40 μ g/ml; 4°C, 45 min). For double fluorescence staining, cells were subsequently stained with FITC-conjugated primary antibody (10 μ g/ml; 4°C, 45 min) or Fluoresceine-Phalloidin (66 nM; 4°C, 45 min). Stained lattices were then embedded in a self-constructed scanning chamber and monitored by individual or simultaneous 4-channel scanning microscopy including two fluorescence channels, reflection and transmission signal. Obtained images were three-dimensionally reconstructed, as described (Maaser et al., 1999). For viable samples, dynamic sequences were obtained by 3D time-lapse confocal laser microscopy at a Leica-SP2 system (Leica). Cells migrating within the collagen lattice for 4-6 hr were labeled by calcein-AM or Orange Cell Tracker (each 1 μ M) (Molecular Probes) and scanned at 2,5 min time intervals as 3D stacks from 3 to 4 z-sections. For dynamic reconstruction, fluorescence, reflection and transmission signal were collected simultaneously. Movies were obtained from three-dimensionally reconstructed stacks or a selected slice level over time.

4.17. Quantitative visual analysis of cellular polarity and morphodynamics

Cellular polarity was calculated as elongation index for each cell (length axis divided by width) and displayed as box-blot ranging from 25th to 75th percentile including the median and whiskers from 5th to 95th percentile. For quantification of cellular morphodynamics, the

proportion of elongated (“mesenchymal”) versus more round-shaped (“amoeboid”) migration type was assessed 9 hr (HT-1080) or 18 hr (MDA-MB-231) after addition of protease inhibitor cocktail by visual blinded analysis of a 60 min time frame. Cells were categorized into mesenchymal fraction upon highly elongated, polarized cell form, and relative straight-forward or -backward movement. Amoeboid fraction represented cells with a more roundish morphology and highly flexible pseudopod protrusions in all directions resulting in partially increased movement. In a substantial subset of cells (20-40%), morphology could not be clearly categorized, representing morphological transition states, dividing or non-migrating cells.

4.18. Intravital multi-photon microscopy

Reconstruction of HT-MT1 cell positioning and extracellular matrix structure were monitored by multi-photon microscopy (Maiti et al., 1997) of the mouse dermis in adult C57BL/6 mice, using a novel modification of a bone-marrow intravital videomicroscopy model (Mazo et al., 1998). The epidermis and upper dermis including hair follicles of the frontoparietal scalp were removed by careful separation from the underlying connective tissue using microscissors. A fixation ring was inserted into the incision to spread the skin, and HEPES-buffered medium containing 10% fetal bovine serum was applied. Subconfluent HT-MT1 cells were preincubated for 3-4 hr in protease inhibitor cocktail (each 20 μ M BB-2516, pepstatin A, E-64; 0,7 μ M aprotinin; 2 μ M leupeptin) or medium alone. Control cells and inhibitor cocktail-treated cells were labeled with calcein-AM (green) or TRITC (red) (Molecular Probes), respectively, washed twice, suspended together in medium (1×10^4 cells/ 3 μ l each), and carefully injected into the mid dermis over the immobilized mouse skull. After injection, a temperature of 37°C was maintained by a water circulation system through the fixation ring and the use of a tempered water-immersion objective. Intravital multi-photon microscopy was performed on an Olympus BX 50 WI microscope coupled to a Ti:Sapphire laser (Spectraphysics) and a Radiance 2000MP confocal-multi-photon imaging system controlled by the Lasersharp software (all from BioRad, Hercules, CA). Multi-photon excitation light of 800 nm was introduced into the sample. Connective tissue structures were visualized via autofluorescence and second harmonic generation imaging at 400/40 nm. Labeled tumor cells were detected at 525/30 nm (calcein) and 600/100 nm (TRITC). Image reconstruction from z-series scans up to a penetration depth of 800 μ m was performed using the freeware Confocal Assistant (copyright 1994-96, T.C. Brelije).

Table 4. Primer sequences of all used primers for RT-PCR, annealing temperatures and times, length of resulting PCR products in base pairs (bp) and source.

mRNA	sense (5'-3' direction) antisense (5'-3' direction)	annealing temp. (°C)	annealing time (min)	bp	source (only first author)
MMP-1	GACTCTAGAAACACAAGAGCAAGA AAGGTTAGCTTACTGTCACAGCTT	59	1	786	Hofmann, 1999
MMP-2	GTGCTGAAGGACACACTAAAGAAGA TTGCCATCCTTCTCAAAGTTGTAGG	59	1	580	Hofmann, 1999
MMP-3	AGATGCTGTTGATTCTGCTGTTGAG' ACAGCATCAAAGGACAAAGCAGGAT	59	1	515	Hofmann, 1999
MMP-7	GTGGTCACCTACAGGATCGT ACCATCCGTCACAGCGTTCAT	62	1	282	Kontinen, 1999
MMP-8	ATGGACCAACACCTCCGCAA GTCAATTGCTTGGACGCTGC	64	1	532	Kontinen, 1999
MMP-9	CACTGTCCACCCCTCAGAGC GCCACTTGTCGGCGATAAAGG	59	1	243	Hofmann, 1999
MMP-13	CTATGGTCCAGGAGATGAAG AGAGTCTTGCCTGTATCCTC	62	1	390	Kontinen, 1999
MT1-MMP	CCCTATGCCTACATCCGTGA TCCATCCATCACTTGGTTAT	59	1	550	Hofmann, 1999
MT2-MMP	GCATCCAGAACTACACGGAG TACCGTAGAGCTGCTGGATG	62	1	474	Kontinen, 1999
MT3-MMP	TGTACTTGACCAAGACAAGAG AGTGTCCATGGCTCATCTGA	58	1	384	Kontinen, 1999
MT4-MMP	GACCTGTTTGCAGTGGCTGT ACGATCTTGTGGTCGCTGGT	64	1	473	Kontinen, 1999
TIMP-1	ATCCTGTTGTGCTGTGGCTGATAG TGCTGGGTGGTAACTCTTTATTTCA	59	1	667	Hofmann, 1999
TIMP-2	AAACGACATTTATGGCAACCCTATC ACAGGAGCCGTCACCTTCTCTGATG	59	1	405	Hofmann, 1999
ADAM-9	AGTGCAGAGGACTTTGAGAA TGCCGTTGTAGCAATAGGCT	55	1	391	McCulloch, 2000
ADAM-10	TGGATTGTGGCTTCATTGGTG TGCAGTTAGCGTCTCATGTGTC	55	1	236	McCulloch, 2000
ADAM-11	CAGGTGCTGAAGTTGAAGGC CAGTGCCAGGTTCTTTGGG	50	1	384	McCulloch, 2000
ADAM-12S	CAGGATCCAGAGAGACCCTCAAG CAACTCGAGCGGCAGGTTAAACAG	55	0,5	392	Iba, 1999
ADAM-15	GGCTGGCAGTGTCTCCTACCAGAGGG GGTGCACCCAGCTGCAGTTCAGCTCAGTCC	50	1	421	McCulloch, 2000
ADAM-17	CAGCACAGCTGCCAAGTCATT CCAGCATCTGCTAAGTCACTTCC	55	1	234	McCulloch, 2000
Cathepsin B	GCCTGCAAGCTTCGATGCAC CTATTGGAGACGCTGTAGGA	60	0.5	464	Bühling, 1999
Cathepsin D	CCAGCCCCAATCCCAACCCACCTCCAG CACTGAAGCTGGGAGGCAAAGGCTACAAGC	45	2	842	Liu, 1997
Cathepsin K	TCCATCCATAACCTTGAGGCTT CCACAGCCATCATTCTCAGACACA	60	0.5	361	Bühling, 1999
Cathepsin L	CAGGCAGGTGATGAATGGCT CAGGCCTCCATTATCCTGAA	60	0.5	324	Bühling, 1999
u-PA	AAAATGCTGTGTGCTGCTGACC CCCTGCCCTGAAGTCGTTAGTG	59	1	790	Fibbi, 2001
u-PAR	GGTCACCCGCCGCTG CCACTGCGGTACTGGACA	59	1	910	Fibbi, 2001
PAI-1	GAACAAGGATGAGATCAGCACC ACTATGACAGCTGTGGATGAGG	59	1	770	Fibbi, 2001
PAI-2	GTTTCATGCAGCAGATCCAGAAG GTAGATGAGCTGTGTGCCTC	60	1		Herouy, 2000
tPA	GCTCAGAAGCAACCGGGTG GGCAGGCTGCCATCTTTGC	60	1		Herouy, 2000
GAPDH	TGAAGGTCGGTGTGAACGGATTGG ACGACATACTCAGCACCAGCATCAC	60	1	269	Darmstrup, 1998
β-Actin	GTGGGGCGCCCCAGGCACCA CTCCTTAATGTCACGCAGGATTC	60	1	540	gift from the laborat. of PD Dr. J. Becker, Derm. Dept., Würzburg.

5. SUMMARY

The extracellular matrix within connective tissues represents a structural scaffold as well as a barrier for motile cells, such as invading tumor cells or passenger leukocytes. It remains unclear how different cell types utilize matrix-degrading enzymes for proteolytic migration strategies and, on the other hand, non-proteolytic strategies to overcome 3D fibrillar matrix networks. To monitor cell migration, a 3D collagen model in vitro or the mouse dermis in vivo were used, in combination with time-lapse video-, confocal- or intravital multiphoton-microscopy, and computer-assisted cell tracking. Expression of proteases, including several MMPs, ADAMs, serine proteases and cathepsins, was shown by flow cytometry, Western blot, zymography, and RT-PCR. Protease activity by migrating HT-1080 fibrosarcoma cells resulting in collagenolysis in situ and generation of tube-like matrix defects was detected by three newly developed techniques: (i) quantitative FITC-release from FITC-labelled collagen, (ii) structural alteration of the physical matrix structure (macroscopically and microscopically), and (iii) the visualization of focal in situ cleavage of individual collagen fibers. The results show that highly invasive collagenolytic cells utilized a spindle-shaped “mesenchymal” migration strategy, which involved $\beta 1$ integrin-dependent interaction with fibers, coclustering of $\beta 1$ integrins and matrix metalloproteinases (MMPs) at fiber bundling sites, and the proteolytic generation of a tube-like matrix-defect by MMPs and additional proteases. In contrast to tumor cells, activated T cells migrated through the collagen fiber network by flexible “amoeboid” crawling including a roundish, ellipsoid shape and morphological adaptation along collagen fibers, which was independent of collagenase function and fiber degradation. Abrogation of collagenolysis in tumor cells was achieved by a cocktail of broad-spectrum protease inhibitors at non-toxic conditions blocking collagenolysis by up to 95%. While in T cells protease inhibition induced neither morphodynamic changes nor reduced migration rates, in tumor cells a time-dependent conversion was obtained from proteolytic mesenchymal to non-proteolytic amoeboid migration in collagen lattices in vitro as well as the mouse dermis in vivo monitored by intravital microscopy. Tumor cells vigorously squeezed through matrix gaps and formed constriction rings in regions of narrow space, while the matrix structure remained intact. MMPs were excluded from fiber binding sites and $\beta 1$ integrin distribution was non-clustered linear. Besides for fibrosarcoma cells, this mesenchymal-to-amoeboid transition (MAT) was confirmed for epithelial MDA-MB-231 breast carcinoma cells. In conclusion, cells of different origin exhibit significant diversity as well as plasticity of protease function in migration. In tumor cells, MAT could represent a functionally important cellular and molecular escape pathway in tumor invasion and migration.

6. ZUSAMMENFASSUNG

Die extrazelluläre Matrix (EZM) des Bindegewebes stellt sowohl ein strukturelles Gerüst als auch eine Barriere für migrierende Zellen dar, wie z.B. invadierende Tumorzellen oder zirkulierende Leukozyten. Es ist bisher unklar, wie diese verschiedenen Zelltypen matrix-degradierende Enzyme für eine proteolytische Migrationsstrategie benutzen bzw. ob und wie sie ohne deren Hilfe durch das Gewebe gelangen. Um Zellmigration in EZM zu untersuchen, wurde ein dreidimensionales Kollagenmodell *in vitro* wie auch Maus-Dermis *in vivo* eingesetzt und Zellmigration mittels Zeitraffer-Video-, Konfokal- und Multiphoton-Mikroskopie sowie computer-gestützter Zelltracking-Analyse dargestellt. Expression von Proteasen verschiedener Klassen, wie der MMPs, ADAMs, Serinproteasen und Cathepsine, wurde mittels Durchfluss-Zytometrie, Western blot, Zymographie oder RT-PCR detektiert. Gegen Kollagen gerichtete zelluläre Protease-Aktivität wurde mit Hilfe drei neu entwickelter Techniken dargestellt: (i) quantitative Messung von löslichem FITC aus FITC-markiertem fibrillärem Kollagen, (ii) mikro- und makroskopische Reorganisation der physikalischen Matrix-Struktur, und (iii) Visualisierung der Topologie fokaler Degradation von Matrixfasern. Die Ergebnisse zeigen, dass hochinvasive spindelförmige HT-1080 Fibrosarkomzellen eine sogenannte "mesenchymale" Migrationsstrategie mit folgenden Charakteristika entwickelten: (i) $\beta 1$ Integrin-abhängige Interaktion mit Kollagenfasern, (ii) das „Co-clustering“ von $\beta 1$ Integrinen und Matrix-Metalloproteinasen an Faserzugstellen und (iii) eine röhrenförmige, durch Proteasen verursachte Matrixdefektbildung. Im Gegensatz zu proteolytischen Tumorzellen migrierten T-Zellen rundlich-ellipsoid mittels flexibler Morphodynamik, ähnlich wie Amöben, durch das Kollagennetzwerk und orientierten sich entlang Kollagenfasern, wobei sie keine biochemisch und strukturell detektierbare Faserdegradation zeigten. Um Tumorzell-vermittelte Kollagenolyse zu hemmen, wurde ein Cocktail, bestehend aus Breitspektrum-Protease-Inhibitoren, etabliert, der die Kollagenolyse unter nicht-toxischen Bedingungen um bis zu 98% blockierte. Während in T-Zellen keine morphodynamischen Veränderungen detektiert wurden, entwickelten Tumorzellen eine Verschiebung von proteolytisch mesenchymaler zu unverminderter nicht-proteolytisch amöboider Migration ("mesenchymale-amöboide Transition - MAT) aus, sowohl in Kollagenmatrices *in vitro* als auch in Maus-Dermis *in vivo*, dargestellt mittels Intravital-Multiphoton-Mikroskopie. Die Tumorzellen „quetschten“ sich dabei durch Lücken in der Matrix und bildeten sogenannte Konstriktionsringe aus, während die Matrixstruktur intakt blieb. MMPs lokalisierten nicht mehr an Faser-Kontaktstellen auf der Zelloberfläche, und $\beta 1$ Integrine lagen nicht mehr geclustert vor. Neben HT-1080 Fibrosarkomzellen wurde MAT auch für MDA-MB-231 Brustkrebszellen epithelialer Herkunft nach Protease-Blockade detektiert. Somit entwickeln migrierende Zellen verschiedener Herkunft eine signifikante Diversität wie auch Plastizität bei der Migration durch EZM aus, resultierend aus der Funktionalität von Matrix-Proteasen. In Tumorzellen könnte MAT einen funktionell wichtigen zellulären und molekularen Anpassungsmechanismus für die Tumordinvasion und -migration darstellen.

7. REFERENCES

- Aimes, R.T. and Quigley, J.P., **1995**, Matrix metalloproteinase-2 is an interstitial collagenase. Inhibitor-free enzyme catalyzes the cleavage of collagen fibrils and soluble native type I collagen generating the specific 3/4- and 1/4-length fragments: *J.Biol.Chem.*, 270, 5872-5876.
- Allan, J.A., Docherty, A.J., Barker, P.J., Huskisson, N.S., Reynolds, J.J., and Murphy, G., **1995**, Binding of gelatinases A and B to type-I collagen and other matrix components: *Biochem.J.*, 309, 299-306.
- Amano, M., Chihara, K., Kimura, K., Fukata, Y., Nakamura, N., Matsuura, Y., and Kaibuchi, K., **1997**, Formation of actin stress fibers and focal adhesions enhanced by Rho-kinase: *Science*, 275, 1308-1311.
- Amour, A., Slocombe, P.M., Webster, A., Butler, M., Knight, C.G., Smith, B.J., Stephens, P.E., Shelley, C., Hutton, M., Knauper, V., Docherty, A.J., and Murphy, G., **1998**, TNF-alpha converting enzyme (TACE) is inhibited by TIMP-3: *FEBS Lett.*, 435, 39-44.
- Andreasen, P.A., Egelund, R., and Petersen, H.H., **2000**, The plasminogen activation system in tumor growth, invasion, and metastasis: *Cell Mol.Life Sci.*, 57, 25-40.
- Andreasen, P.A., Kjoller, L., Christensen, L., and Duffy, M.J., **1997**, The urokinase-type plasminogen activator system in cancer metastasis: a review: *Int.J.Cancer*, 72, 1-22.
- Aota, S. and Yamada, K.M., **1997**, Integrin functions and signal transduction: *Adv.Exp.Med.Biol.*, 400B:669-82.
- Aznavoorian, S., Stracke, M.L., Parsons, J., McClanahan, J., and Liotta, L.A., **1996**, Integrin alphavbeta3 mediates chemotactic and haptotactic motility in human melanoma cells through different signaling pathways: *J.Biol.Chem.*, 271, 3247-3254.
- Bachmeier, B.E., Nerlich, A.G., Lichtinghagen, R., and Sommerhoff, C.P., **2001**, Matrix metalloproteinases (MMPs) in breast cancer cell lines of different tumorigenicity: *Anticancer Res.*, 21, 3821-3828.
- Baramova, E.N., Bajou, K., Remacle, A., L'Hoir, C., Krell, H.W., Weidle, U.H., Noel, A., and Foidart, J.M., **1997**, Involvement of PA/plasmin system in the processing of pro-MMP-9 and in the second step of pro-MMP-2 activation: *FEBS Lett.*, 405, 157-162.
- Basbaum, C.B. and Werb, Z., **1996**, Focalized proteolysis: spatial and temporal regulation of extracellular matrix degradation at the cell surface: *Curr.Opin.Cell Biol.*, 8, 731-738.
- Bauvois, B., **2001**, Transmembrane proteases in focus: diversity and redundancy?: *J.Leukoc.Biol.*, 70, 11-17.
- Bedi, G.S. and Williams, T., **1994**, Purification and characterization of a collagen-degrading protease from *Porphyromonas gingivalis*: *J.Biol.Chem.*, 269, 599-606.

Belkin, A.M., Akimov, S.S., Zaritskaya, L.S., Ratnikov, B.I., Deryugina, E.I., and Strongin, A.Y., **2001**, Matrix-dependent proteolysis of surface transglutaminase by membrane-type metalloproteinase regulates cancer cell adhesion and locomotion: *J.Biol.Chem.*, 276, 18415-18422.

Bieth, J.G., **1986**, Elastases: catalytic and biological properties. In: *Biology of the extracellular matrix: Regulation of matrix accumulation*, 217-320, R.P. Mechan (ed), Academic Press, New York.

Birchmeier, W. and Birchmeier, C., **1995**, Epithelial-mesenchymal transitions in development and tumor progression: *EXS.*, 74:1-15, 1-15.

Birkedal-Hansen, H., **1995**, Proteolytic remodeling of extracellular matrix: *Curr.Opin.Cell Biol.*, 7, 728-735.

Black, R.A. and White, J.M., **1998**, ADAMs: focus on the protease domain: *Curr.Opin.Cell Biol.*, 10, 654-659.

Bond, M., Murphy, G., Bennett, M.R., Amour, A., Knauper, V., Newby, A.C., and Baker, A.H., **2000**, Localization of the death domain of tissue inhibitor of metalloproteinase-3 to the N terminus. Metalloproteinase inhibition is associated with proapoptotic activity: *J.Biol.Chem.*, 275, 41358-41363.

Bossard, M.J., Tomaszek, T.A., Thompson, S.K., Amegadzie, B.Y., Hanning, C.R., Jones, C., Kurdyla, J.T., McNulty, D.E., Drake, F.H., Gowen, M., and Levy, M.A., **1996**, Proteolytic activity of human osteoclast cathepsin K. Expression, purification, activation, and substrate identification: *J.Biol.Chem.*, 271, 12517-12524.

Brakebusch, C., Fillatreau, S., Potocnik, A.J., Bungartz, G., Wilhelm, P., Svensson, M., Kearney, P., Korner, H., Gray, D., and Fassler, R., **2002**, Beta1 integrin is not essential for hematopoiesis but is necessary for the T cell-dependent IgM antibody response: *Immunity*, 16, 465-477.

Bristow, C.L., Lyford, L.K., Stevens, D.P., and Flood, P.M., **1991**, Elastase is a constituent product of T cells: *Biochem.Biophys.Res.Commun.*, 181, 232-239.

British Biotech Inc., **1998**, Guidelines for the clinical use of marimastat, Oxford, UK.

Brooks, P.C., Stromblad, S., Sanders, L.C., von Schalscha, T.L., Aimes, R.T., Stetler-Stevenson, W.G., Quigley, J.P., and Cheresch, D.A., **1996**, Localization of matrix metalloproteinase MMP-2 to the surface of invasive cells by interaction with integrin alpha v beta 3: *Cell*, 85, 683-693.

Buehling, F., Gerber, A., Hackel, C., Kruger, S., Kohnlein, T., Bromme, D., Reinhold, D., Ansorge, S., and Welte, T., **1999**, Expression of cathepsin K in lung epithelial cells: *Am.J.Respir.Cell Mol.Biol.*, 20, 612-619.

Burleigh, M.C., Barrett, A.J., and Lazarus, G.S., **1974**, Cathepsin B1. A lysosomal enzyme that degrades native collagen: *Biochem.J.*, 137, 387-398.

Cajot, J.F., Bamat, J., Bergonzelli, G.E., Kruithof, E.K., Medcalf, R.L., Testuz, J., and Sordat, B., **1990**, Plasminogen-activator inhibitor type 1 is a potent natural inhibitor of

extracellular matrix degradation by fibrosarcoma and colon carcinoma cells: *Proc.Natl.Acad.Sci.U.S.A.*, 87, 6939-6943.

Cao, J., Hymowitz, M., Conner, C., Bahou, W.F., and Zucker, S., **2000**, The propeptide domain of membrane type 1-matrix metalloproteinase acts as an intramolecular chaperone when expressed in trans with the mature sequence in COS-1 cells: *J.Biol.Chem.*, 275, 29648-29653.

Callas, D., Bacher, P., Iqbal, O., Hoppensteadt, D., and Fareed, J., **1994**, Fibrinolytic compromise by simultaneous administration of site-directed inhibitors of thrombin: *Thromb.Res.*, 74, 193-205.

Cavaillès, V., Garcia, M., and Rochefort, H., **1989**, Regulation of cathepsin-D and pS2 gene expression by growth factors in MCF7 human breast cancer cells: *Mol.Endocrinol.*, 3, 552-558.

Cerretti, D.P., **1999**, Characterization of the tumour necrosis factor alpha-converting enzyme, TACE/ADAM17: *Biochem.Soc.Trans.*, 27, 219-223.

Chan, B.M., Kassner, P.D., Schiro, J.A., Byers, H.R., Kupper, T.S., and Hemler, M.E., **1992**, Distinct cellular functions mediated by different VLA integrin alpha subunit cytoplasmic domains: *Cell*, 68, 1051-1060.

Chapman, H.A., **1997**, Plasminogen activators, integrins, and the coordinated regulation of cell adhesion and migration: *Curr.Opin.Cell Biol.*, 9, 714-724.

Chen, W.T., Lee, C.C., Goldstein, L., Bernier, S., Liu, C.H., Lin, C.Y., Yeh, Y., Monsky, W.L., Kelly, T., and Dai, M., **1994**, Membrane proteases as potential diagnostic and therapeutic targets for breast malignancy: *Breast Cancer Res.Treat.*, 31, 217-226.

Clark, I.M. and Cawston, T.E., **1989**, Fragments of human fibroblast collagenase. Purification and characterization: *Biochem.J.*, 263, 201-206.

Coussens, L.M., Fingleton, B., and Matrisian, L.M., **2002**, Matrix metalloproteinase inhibitors and cancer: trials and tribulations: *Science*, 295, 2387-2392.

Coussens, L.M., Shapiro, S.D., Soloway, P.D., and Werb, Z., **2001**, Models for gain-of-function and loss-of-function of MMPs. Transgenic and gene targeted mice: *Methods Mol.Biol*, 151, 149-79.

Coussens, L.M. and Werb, Z., **1996**, Matrix metalloproteinases and the development of cancer: *Chem.Biol.*, 3, 895-904.

Cukierman, E., Pankov, R., Stevens, D.R., and Yamada, K.M., **2001**, Taking cell-matrix adhesions to the third dimension: *Science*, 294, 1708-1712.

d'Ortho, M.P., Stanton, H., Butler, M., Atkinson, S.J., Murphy, G., and Hembry, R.M., **1998**, MT1-MMP on the cell surface causes focal degradation of gelatin films: *FEBS Lett.*, 421, 159-164.

Damstrup, L., Rude, V.B., Spang-Thomsen, M., Brunner, N., and Skovgaard, P.H., **1998**, In vitro invasion of small-cell lung cancer cell lines correlates with expression of epidermal growth factor receptor: *Br.J.Cancer*, 78, 631-640.

Dandachi, N., Hauser-Kronberger, C., More, E., Wiesener, B., Hacker, G.W., Dietze, O., and Wirl, G., **2001**, Co-expression of tenascin-C and vimentin in human breast cancer cells indicates phenotypic transdifferentiation during tumour progression: correlation with histopathological parameters, hormone receptors, and oncoproteins: *J.Pathol*, 193, 181-189.

Danen, E.H., van Muijen, G.N., ten Berge, P.J., and Ruiter, D.J., **1993**, Integrins and melanoma progression: Recent Results. *Cancer Res.*, 128:119-32.

Davis, G.E., **1992**, Affinity of integrins for damaged extracellular matrix: alpha v beta 3 binds to denatured collagen type I through RGD sites: *Biochem.Biophys.Res.Comm.*, 182, 1025-1031.

DeClerck, Y.A. and Imren, S., **1994**, Protease inhibitors: role and potential therapeutic use in human cancer: *Eur.J.Cancer*, 30A, 2170-2180.

Delany, A.M., Jeffrey, J.J., Rydziel, S., and Canalis, E., **1995**, Cortisol increases interstitial collagenase expression in osteoblasts by post-transcriptional mechanisms: *J.Biol.Chem.*, 270, 26607-26612.

Della, P.P., Soeltl, R., Krell, H.W., Collins, K., O'Donoghue, M., Schmitt, M., and Kruger, A., **1999**, Combined treatment with serine protease inhibitor aprotinin and matrix metalloproteinase inhibitor Batimastat (BB-94) does not prevent invasion of human esophageal and ovarian carcinoma cells in vivo.: *Anticancer Res.*, 19, 3809-3816.

Deryugina, E.I., Ratnikov, B., Monosov, E., Postnova, T.I., DiScipio, R., Smith, J.W., and Strongin, A.Y., **2001**, MT1-MMP initiates activation of pro-MMP-2 and integrin alphavbeta3 promotes maturation of MMP-2 in breast carcinoma cells: *Exp.Cell Res.*, 15, 209-223.

Deryugina, E.I., Bourdon, M.A., Jungwirth, K., Smith, J.W., and Strongin, A.Y., **2000**, Functional activation of integrin alpha V beta 3 in tumor cells expressing membrane-type 1 matrix metalloproteinase: *Int.J.Cancer*, 86, 15-23.

Deryugina, E.I., Bourdon, M.A., Reisfeld, R.A., and Strongin, A., **1998**, Remodeling of collagen matrix by human tumor cells requires activation and cell surface association of matrix metalloproteinase-2: *Cancer Res.*, 58, 3743-3750.

Deryugina, E.I., Luo, G.X., Reisfeld, R.A., Bourdon, M.A., and Strongin, A., **1997a**, Tumor cell invasion through matrigel is regulated by activated matrix metalloproteinase-2: *Anticancer Res.*, 17, 3201-3210.

Deryugina, E.I., Bourdon, M.A., Luo, G.X., Reisfeld, R.A., and Strongin, A., **1997b**, Matrix metalloproteinase-2 activation modulates glioma cell migration: *J.Cell Sci.*, 110, 2473-2482.

Desban, N. and Duband, J.L., **1997**, Avian neural crest cell migration on laminin: interaction of the alpha1beta1 integrin with distinct laminin-1 domains mediates different adhesive responses: *J.Cell Sci.*, 110, 2729-2744.

Dethlefsen, S.M., Raab, G., Moses, M.A., Adam, R.M., Klagsbrun, M., and Freeman, M.R., **1998**, Extracellular calcium influx stimulates metalloproteinase cleavage and

secretion of heparin-binding EGF-like growth factor independently of protein kinase C: *J.Cell Biochem.*, 69, 143-153.

Devreotes, P.N. and Zigmond, S.H., **1988**, Chemotaxis in eukaryotic cells: a focus on leukocytes and Dictyostelium: *Annu.Rev.Cell Biol.*, 4, 649-686.

Doane, K.J. and Birk, D.E., **1991**, Fibroblasts retain their tissue phenotype when grown in three- dimensional collagen gels: *Exp.Cell Res.*, 195, 432-442.

Drake, F.H., Dodds, R.A., James, I.E., Connor, J.R., Debouck, C., Richardson, S., Lee-Rykaczewski, E., Coleman, L., Rieman, D., Barthlow, R., Hastings, G., and Gowen, M., **1996**, Cathepsin K, but not cathepsins B, L, or S, is abundantly expressed in human osteoclasts: *J.Biol.Chem.*, 271, 12511-12516.

Dufour, S., Duband, J.L., Humphries, M.J., Obara, M., Yamada, K.M., and Thiery, J.P., **1988**, Attachment, spreading and locomotion of avian neural crest cells are mediated by multiple adhesion sites on fibronectin molecules: *EMBO J.*, 7, 2661-2671.

Dunsmore, S.E., Saarialho-Kere, U.K., Roby, J.D., Wilson, C.L., Matrisian, L.M., Welgus, H.G., and Parks, W.C., **1998**, Matrilysin expression and function in airway epithelium: *J.Clin.Invest.*, 102, 1321-1331.

Eccles, S.A., Box, G.M., Court, W.J., Bone, E.A., Thomas, W., and Brown, P.D., **1996**, Control of lymphatic and hematogenous metastasis of a rat mammary carcinoma by the matrix metalloproteinase inhibitor batimastat (BB-94): *Cancer Res.*, 56, 2815-2822.

Ellerbroek, S.M., Wu, Y.I., Overall, C.M., and Stack, M.S., **2001**, Functional interplay between type I collagen and cell surface matrix metalloproteinase activity: *J.Biol.Chem.*, 276, 24833-24842.

Esparza, J., Vilardell, C., Calvo, J., Juan, M., Vives, J., Urbano-Marquez, A., Yague, J., and Cid, M.C., **1999**, Fibronectin upregulates gelatinase B (MMP-9) and induces coordinated expression of gelatinase A (MMP-2) and its activator MT1-MMP (MMP-14) by human T lymphocyte cell lines. A process repressed through RAS/MAP kinase signaling pathways: *Blood*, 94, 2754-2766.

Etoh, T., Byers, H.R., and Mihm, M.C.J., **1992**, Integrin expression in malignant melanoma and their role in cell attachment and migration on extracellular matrix proteins: *J.Dermatol.*, 19, 841-846.

Fibbi, G., Barletta, E., Dini, G., Del Rosso, A., Pucci, M., Cerletti, M., and Del Rosso, M., **2001**, Cell invasion is affected by differential expression of the urokinase plasminogen activator/urokinase plasminogen activator receptor system in muscle satellite cells from normal and dystrophic patients: *Lab.Invest.*, 81, 27-39.

Folkman, J., Watson, K., Ingber, D., and Hanahan, D., **1989**, Induction of angiogenesis during the transition from hyperplasia to neoplasia: *Nature*, 339, 58-61.

Friedl, P., Borgmann, S., and Bocker, E. B., **2001**, Leukocyte crawling through extracellular matrix and the Dictyostelium paradigm of movement - lessons from a social ameba: *J.Leukoc.Biol.*, 70, 491-509.

- Friedl, P. and Bröcker, E.-B., **2000**, The biology of cell locomotion within three-dimensional extracellular matrix: *Cell.Mol.Life Sci.*, 57, 41-64.
- Friedl, P. and Brocker, E.B., **2000b**, T cell migration in three-dimensional extracellular matrix: guidance by polarity and sensations: *Dev.Immunol.*, 7, 249-266.
- Friedl, P., Zanker, K.S., and Bröcker, E.-B., **1998a**, Cell migration strategies in 3-D extracellular matrix: differences in morphology, cell matrix interactions, and integrin function: *Microsc.Res.Tech.*, 43, 369-378.
- Friedl, P., Entschladen, F., Conrad, C., Niggemann, B., and Zanker, K.S., **1998b**, CD4+ T lymphocytes migrating in three-dimensional collagen lattices lack focal adhesions and utilize beta1 integrin-independent strategies for polarization, interaction with collagen fibers and locomotion: *Eur.J.Immunol.*, 28, 2331-2343.
- Friedl, P., Maaser, K., Klein, C.E., Niggemann, B., Krohne, G., and Zanker, K.S., **1997**, Migration of highly aggressive MV3 melanoma cells in 3-dimensional collagen lattices results in local matrix reorganization and shedding of alpha2 and beta1 integrins and CD44: *Cancer Res.*, 57, 2061-2070.
- Friedl, P., Noble, P.B., and Zänker, K.S., **1995**, T Lymphocyte locomotion in a three-dimensional collagen matrix. Expression and function of cell adhesion molecules: *J.Immunol.*, 154, 4973-4985.
- Friedl, P., Noble, P.B., and Zanker, K.S., **1993**, Lymphocyte locomotion in three-dimensional collagen gels. Comparison of three quantitative methods for analysing cell trajectories: *J.Immunol.Methods*, 165, 157-165.
- Friedlander, M., Theesfeld, C.L., Sugita, M., Fruttiger, M., Thomas, M.A., Chang, S., and Cheresch, D.A., **1996**, Involvement of integrins alpha v beta 3 and alpha v beta 5 in ocular neovascular diseases: *Proc.Natl.Acad.Sci.U.S.A.*, 93, 9764-9769.
- Geiger, B., **2001**, Encounters in space: *Science*. 294, 1661-1663.
- Giavazzi, R. and Taraboletti, G., **2001**, Preclinical development of metalloproteinase inhibitors in cancer therapy: *Crit.Rev.Oncol.Hematol.*, 37, 53-60.
- Goetzl, E.J., Banda, M.J., and Leppert, D., **1996**, Matrix metalloproteinases in immunity: *J.Immunol.*, 156, 1-4.
- Gomez, D.E., Alonso, D.F., Yoshiji, H., and Thorgeirsson, U.P., **1997**, Tissue inhibitors of metalloproteinases: structure, regulation and biological functions: *Eur.J.Cell Biol.*, 74, 111-122.
- Gullberg, D.E. and Lundgren-Akerlund, E., **2002**, Collagen-binding I domain integrins--what do they do?: *Prog.Histochem.Cytochem.*, 37, 3-54.
- Gum, R., Wang, H., Lengyel, E., Juarez, J., and Boyd, D., **1997**, Regulation of 92 kDa type IV collagenase expression by the jun aminoterminal kinase- and the extracellular signal-regulated kinase-dependent signaling cascades: *Oncogene*, 14, 1481-1493.
- Gundersen, D., Tran-Thang, C., Sordat, B., Mourali, F., and Ruegg, C., **1997**, Plasmin-induced proteolysis of tenascin-C: modulation by T lymphocyte-derived urokinase-type

plasminogen activator and effect on T lymphocyte adhesion, activation, and cell clustering: *J.Immunol.*, 158, 1051-1060.

Gunzer, M., Schäfer, A., Borgmann, S., Grabbe, S., Zänker, K. S., Bröcker, E.-B., Kämpgen, E., and Friedl, P., **2000**, Antigen presentation in three-dimensional extracellular matrix: interactions of T cells with dendritic cells are dynamic, short lived, and sequential: *Immunity* 13, 323-332.

Gunzer, M., Kämpgen, E., Bröcker, E.-B., Zänker, K.S., and Friedl, P., **1997**, Migration of dendritic cells in 3D-collagen lattices: visualisation of dynamic interactions with the substratum and the distribution of surface structures via a novel confocal reflection imaging technique: *Adv.Exp.Med.Biol.*, 417, 97-103.

Hanahan, D. and Weinberg, R.A., **2000**, The hallmarks of cancer: *Cell*, 100, 57-70.

Hangan, D., Morris, V.L., Boeters, L., von Ballestrem, C., Uniyal, S., and Chan, B.M., **1997**, An epitope on VLA-6 (alpha6beta1) integrin involved in migration but not adhesion is required for extravasation of murine melanoma B16F1 cells in liver: *Cancer Res.*, 57, 3812-3817.

Haston, W.S., Shields, J.M., and Wilkinson, P.C., **1982**, Lymphocyte locomotion and attachment on two-dimensional surfaces and in three-dimensional matrices: *J.Cell Biol.*, 92, p. 747-752.

Hauzenberger, D., Bergstrom, S.E., Klominek, J., and Sundqvist, K.G., **1999**, Spectrum of extracellular matrix degrading enzymes in normal and malignant T lymphocytes: *Anticancer Res.*, 19, 1945-1952.

Heath, E.I. and Grochow, L.B., **2000**, Clinical potential of matrix metalloprotease inhibitors in cancer therapy: *Drugs.*, 59, 1043-1055.

Heath, J. P. and Peachey, L. D., **1989**, Morphology of fibroblasts in collagen gels: a study using 400 keV electron microscopy and computer graphics. *Cell Motil.Cytoskel.*, 14, 382-392.

Hebert, C.A. and Baker, J.B., **1988**, Linkage of extracellular plasminogen activator to the fibroblast cytoskeleton: colocalization of cell surface urokinase with vinculin: *J.Cell Biol.*, 106, 1241-1247.

Herouy, Y., Trefzer, D., Hellstern, M.O., Stark, G.B., Vanscheidt, W., Schopf, E., and Norgauer, J., **2000**, Plasminogen activation in venous leg ulcers: *Br.J.Dermatol.*, 143, 930-936.

Hidalgo, M. and Eckhardt, S.G., **2001**, Development of matrix metalloproteinase inhibitors in cancer therapy: *J.Natl.Cancer Inst.*, 7, 178-193.

Hiraoka, N., Allen, E., Apel, I.J., Gyetko, M.R., and Weiss, S.J., **1998**, Matrix metalloproteinases regulate neovascularization by acting as pericellular fibrinolysins: *Cell*, 95, 365-377.

- Hofmann, U.B., Westphal, J.R., Waas, E.T., Zendman, A.J., Cornelissen, I.M., Rüter, D.J., and van Muijen, G.N., **1999**, Matrix metalloproteinases in human melanoma cell lines and xenografts: increased expression of activated matrix metalloproteinase-2 (MMP-2) correlates with melanoma progression.: *Br.J.Cancer*, 81, 774-782.
- Holmbeck, K., Bianco, P., Caterina, J., Yamada, S., Kromer, M., Kuznetsov, S.A., Mankani, M., Robey, P.G., Poole, A.R., Pidoux, I., Ward, J.M., and Birkedal-Hansen, H., **1999**, MT1-MMP-deficient mice develop dwarfism, osteopenia, arthritis, and connective tissue disease due to inadequate collagen turnover: *Cell*, 99, 81-92.
- Hotary, K., Allen, E., Punturieri, A., Yana, I., and Weiss, S.J., **2000**, Regulation of cell invasion and morphogenesis in a three-dimensional type I collagen matrix by membrane-type matrix metalloproteinases 1, 2, and 3: *J.Cell Biol.*, 149, 1309-1323.
- Huttenlocher, A., Sandborg, R.R., and Horwitz, A.F., **1995**, Adhesion in cell migration: *Curr.Opin.Cell Biol.*, 7, 697-706.
- Hynes, R.O., **1992**, Integrins: versatility, modulation, and signaling in cell adhesion: *Cell*, 69, 11-25.
- Iba, K., Albrechtsen, R., Gilpin, B.J., Loechel, F., and Wewer, U.M., **1999**, Cysteine-rich domain of human ADAM 12 (meltrin alpha) supports tumor cell adhesion: *Am.J.Pathol.*, 154, 1489-1501.
- Imai, K., Ohta, S., Matsumoto, T., Fujimoto, N., Sato, H., Seiki, M., and Okada, Y., **1997**, Expression of membrane-type 1 matrix metalloproteinase and activation of progelatinase A in human osteoarthritic cartilage: *Am.J.Pathol.*, 151, 245-256.
- Ishibashi, O., Mori, Y., Kurokawa, T., and Kumegawa, M., **1999**, Breast cancer cells express cathepsins B and L but not cathepsins K or H: *Cancer Biochem.Biophys.*, 17, 69-78.
- Itoh, Y. and Nagase, H., **1995**, Preferential inactivation of tissue inhibitor of metalloproteinases-1 that is bound to the precursor of matrix metalloproteinase 9 (progelatinase B) by human neutrophil elastase: *J.Biol.Chem.*, 270, 16518-16521.
- Ivanoff, A., Ivanoff, J., Hultenby, K., and Sundqvist, K.G., **1999**, Infiltrative capacity of T leukemia cell lines: a distinct functional property coupled to expression of matrix metalloproteinase-9 (MMP-9) and tissue inhibitor of metalloproteinases-1 (TIMP-1): *Clin.Exp.Metastasis*, 17, 695-711.
- Kagami, S., Urushihara, M., Kondo, S., Loster, K., Reutter, W., Tamaki, T., Yoshizumi, M., and Kuroda, Y., **2001**, Requirement for tyrosine kinase-ERK1/2 signaling in alpha 1 beta 1 integrin-mediated collagen matrix remodeling by rat mesangial cells: *Exp.Cell Res.*, 268, 274-283.
- Kakegawa, H., Nikawa, T., Tagami, K., Kamioka, H., Sumitani, K., Kawata, T., Drobnic-Kosorok, M., Lenarcic, B., Turk, V., and Katunuma, N., **1993**, Participation of cathepsin L on bone resorption: *FEBS Lett.*, 321, 247-250.
- Kamohara, H., Yamashiro, S., Galligan, C., and Yoshimura, T., **2001**, Discoidin domain receptor 1 isoform-a (DDR1alpha) promotes migration of leukocytes in three-dimensional collagen lattices: *FASEB J.*, 15, 2724-2726.

- Keely, P.J., Westwick, J.K., Whitehead, I.P., Der, C.J., and Parise, L.V., **1997**, Cdc42 and Rac1 induce integrin-mediated cell motility and invasiveness through PI(3)K: *Nature*, 390, 632-636.
- Kheradmand, F., Werner, E., Tremble, P., Symons, M., and Werb, Z., **1998**, Role of Rac1 and oxygen radicals in collagenase-1 expression induced by cell shape change: *Science*, 280, 898-902.
- Killich, T., Plath, P.J., Wei, X., Bultmann, H., Rensing, L., and Vicker, M.G., **1993**, The locomotion, shape and pseudopodial dynamics of unstimulated *Dictyostelium* cells are not random: *J.Cell Sci.*, 106, 1005-1013.
- Kim, J.P., Zhang, K., Kramer, R.H., Schall, T.J., and Woodley, D.T., **1992**, Integrin receptors and RGD sequences in human keratinocyte migration: unique anti-migratory function of alpha 3 beta 1 epiligrin receptor: *J.Invest.Dermatol.*, 98, 764-770.
- Kirchhofer, D., Languino, L.R., Ruoslahti, E., and Pierschbacher, M.D., **1990**, Alpha 2 beta 1 integrins from different cell types show different binding specificities: *J.Biol.Chem.*, 265, 615-618.
- Kirschke, H., Kembhavi, A.A., Bohley, P., and Barrett, A.J., **1982**, Action of rat liver cathepsin L on collagen and other substrates: *Biochem.J.*, 201, 367-372.
- Klein, C. E., Dressel, D., Steinmacher, T., Mauch, C., Eckes, B., Krieg, T., Bankert, R., and Weber, L. **1991**, Integrin alpha2beta1 is upregulated in fibroblasts and highly aggressive melanoma cells in three-dimensional collagen lattices and mediates the reorganization of collagen I fibrils. *J.Cell Biol.* 115, 1427-1436.
- Kleiner, D.E. and Stetler-Stevenson, W.G., **1994**, Quantitative zymography: detection of picogram quantities of gelatinases: *Anal.Biochem.*, 218, p. 325-329.
- Klominek, J., Sumitran, K.S., and Hauzenberger, D., **1997**, Differential motile response of human malignant mesothelioma cells to fibronectin, laminin and collagen type IV: the role of beta1 integrins: *Int.J.Cancer*, 72, 1034-1044.
- Knauper, V., Docherty, A.J., Smith, B., Tschesche, H., and Murphy, G., **1997**, Analysis of the contribution of the hinge region of human neutrophil collagenase (HNC, MMP-8) to stability and collagenolytic activity by alanine scanning mutagenesis: *FEBS Lett.*, 405, 60-64.
- Knauper, V., Will, H., Lopez-Otin, C., Smith, B., Atkinson, S.J., Stanton, H., Hembry, R.M., and Murphy, G., **1996**, Cellular mechanisms for human procollagenase-3 (MMP-13) activation. Evidence that MT1-MMP (MMP-14) and gelatinase a (MMP-2) are able to generate active enzyme: *J.Biol.Chem.*, 271, 17124-17131.
- Koblinski, J.E., Ahram, M., and Sloane, B.F., **2000**, Unraveling the role of proteases in cancer: *Clin.Chim.Acta*, 291, 113-135.
- Kolkenbrock, H., Orgel, D., Hecker-Kia, A., Zimmermann, J., and Ulbrich, N., **1995**, Generation and activity of the ternary gelatinase B/TIMP-1/LMW-stromelysin-1 complex: *Biol.Chem.Hoppe Seyler*, 376, 495-500.

- Konttinen, Y.T., Ainola, M., Valleala, H., Ma, J., Ida, H., Mandelin, J., Kinne, R.W., Santavirta, S., Sorsa, T., Lopez-Otin, C., and Takagi, M., **1999**, Analysis of 16 different matrix metalloproteinases (MMP-1 to MMP-20) in the synovial membrane: different profiles in trauma and rheumatoid arthritis: *Ann.Rheum.Dis.*, 58, 691-697.
- Kruger, A., Soeltl, R., Sopov, I., Kopitz, C., Arlt, M., Magdolen, V., Harbeck, N., Gansbacher, B., and Schmitt, M., **2001**, Hydroxamate-type matrix metalloproteinase inhibitor batimastat promotes liver metastasis: *Cancer Res.*, 61, 1272-1275.
- Kurschat, P., Zigrino, P., Nischt, R., Breitkopf, K., Steurer, P., Klein, C.E., Krieg, T., and Mauch, C., **1999**, Tissue inhibitor of matrix metalloproteinase-2 regulates matrix metalloproteinase-2 activation by modulation of membrane-type 1 matrix metalloproteinase activity in high and low invasive melanoma cell lines: *J.Biol.Chem.*, 274, 21056-21062.
- Langholz, O., Rockel, D., Mauch, C., Kozłowska, E., Bank, I., Krieg, T., and Eckes, B., **1995**, Collagen and collagenase gene expression in three-dimensional collagen lattices are differentially regulated by alpha 1 beta 1 and alpha 2 beta 1 integrins: *J.Cell Biol.*, 131, 1903-1915.
- Lauffenburger, D.A. and Horwitz, A.F., **1996**, Cell migration: a physically integrated molecular process: *Cell*, 84, 359-369.
- Laug, W.E., Cao, X.R., Yu, Y.B., Shimada, H., and Kruithof, E.K., **1993**, Inhibition of invasion of HT1080 sarcoma cells expressing recombinant plasminogen activator inhibitor 2: *Cancer Res.*, 53, 6051-6057.
- Laurent, V. and Salzet, M., **1995**, Isolation of a renin-like enzyme from the leech *Theromyzon tessulatum*: *Peptides*, 16, 1351-1358.
- Lehti, K., Valtanen, H., Wickstrom, S., Lohi, J., and Keski-Oja, J., **2000**, Regulation of membrane-type-1 matrix metalloproteinase activity by its cytoplasmic domain: *J.Biol.Chem.*, 275, 15006-15013.
- Leppert, D., Waubant, E., Galardy, R., Bunnett, N.W., and Hauser, S.L., **1995a**, T cell gelatinases mediate basement membrane transmigration in vitro: *J.Immunol.*, 154, 4379-4389.
- Leppert, D., Hauser, S. L., Kishiyama, J. L., An, S., Zeng, L., and Goetzl, E. J. **1995b**, Stimulation of matrix-metalloproteinase-dependent migration of T cells by eicosanoids. *FASEB J.* 1473-1481.
- Lewis, W. H. **1934**, On the locomotion of the polymorphonuclear neutrophils of the rat in autoplasm cultures. *Bull.Johns Hopkins.Hosp.* 4, 273-279.
- Liotta, L.A., Stracke, M.L., Aznavoorian, S.A., Beckner, M.E., and Schiffmann, E., **1991**, Tumor cell motility: *Semin.Cancer Biol.*, 2, 111-114.
- Liotta, L.A., Rao, C.N., and Wewer, U.M., **1986**, Biochemical interactions of tumor cells with the basement membrane: *Annu.Rev.Biochem.*, 55, 1037-1057.

- Liu, Z., Brattain, M.G., and Appert, H., **1997**, Differential display of reticulocalbin in the highly invasive cell line, MDA-MB-435, versus the poorly invasive cell line, MCF-7: *Biochem.Biophys.Res.Commun.*, 231, 283-289.
- Lo, S.H., Janmey, P.A., Hartwig, J.H., and Chen, L.B., **1994**, Interactions of tensin with actin and identification of its three distinct actin-binding domains: *J.Cell Biol.*, 125, 1067-1075.
- Lochter, A., Galosy, S., Muschler, J., Freedman, N., Werb, Z., and Bissell, M.J., **1997**, Matrix metalloproteinase stromelysin-1 triggers a cascade of molecular alterations that leads to stable epithelial-to-mesenchymal conversion and a premalignant phenotype in mammary epithelial cells: *J.Cell Biol.*, 139, 1861-1872.
- Lokshina, L.A., Bylinkina, V.S., Samoilova, R.S., Gureeva, T.A., Golubeva, N.V., and Polianskaia, A.M., **1993**, Proteolytic enzymes in human lymphocytic leukemia cells. I. Activity of dipeptidylaminopeptidase IV, plasminogen activator and cathepsins B and L in cells with different immunologic phenotype: *Biokhimiia.*, 58, 1104-1115.
- Maaser, K., Wolf, K., Klein, C.E., Niggemann, B., Zanker, K.S., Brocker, E.B., and Friedl, P., **1999**, Functional hierarchy of simultaneously expressed adhesion receptors: integrin alpha2beta1 but not CD44 mediates MV3 melanoma cell migration and matrix reorganization within three-dimensional hyaluronan-containing collagen matrices: *Mol.Biol.Cell*, 10, 3067-3079.
- Maiti, S., Shear, J.B., Williams, R.M., Zipfel, W.R., and Webb, W.W., **1997**, Measuring serotonin distribution in live cells with three-photon excitation: *Science*, 275, 530-532.
- Mauviel, A., **1993**, Cytokine regulation of metalloproteinase gene expression: *J.Cell Biochem.*, 53, 288-295.
- Mazo, I.B., Gutierrez-Ramos, J.C., Frenette, P.S., Hynes, R.O., Wagner, D.D., and von Andrian, U.H., **1998**, Hematopoietic progenitor cell rolling in bone marrow microvessels: parallel contributions by endothelial selectins and vascular cell adhesion molecule 1 [published erratum appears in *J Exp Med* 1998 Sep 7;188(5):1001]: *J.Exp.Med.*, 188, 465-474.
- McCawley, L.J. and Matrisian, L.M., **2000**, Matrix metalloproteinases: multifunctional contributors to tumor progression: *Mol.Med.Today*, 6, 149-156.
- McCulloch, D.R., Harvey, M., and Herington, A.C., **2000**, The expression of the ADAMs proteases in prostate cancer cell lines and their regulation by dihydrotestosterone: *Mol.Cell Endocrinol.*, 167, 11-21.
- McQuibban, G.A., Gong, J.H., Tam, E.M., McCulloch, C.A., Clark-Lewis, I., and Overall, C.M., **2000**, Inflammation dampened by gelatinase A cleavage of monocyte chemoattractant protein-3: *Science*. 289, 1202-1206.
- Mignatti, P., Robbins, E., and Rifkin, D.B., **1986**, Tumor invasion through the human amniotic membrane: requirement for a proteinase cascade: *Cell*, 47, 487-498.
- Miller, M.J., Wei, S.H., Parker, I., and Cahalan, M.D., **2002**, Two-photon imaging of lymphocyte motility and antigen response in intact lymph node: *Science*, 296, 1869-1873.

Millichip, M.I., Dallas, D.J., Wu, E., Dale, S., and McKie, N., **1998**, The metallo-disintegrin ADAM10 (MADM) from bovine kidney has type IV collagenase activity in vitro: *Biochem.Biophys.Res.Commun.*, 245, 594-598.

Mitsiades, N., Poulaki, V., Mitsiades, C.S., and Anderson, K.C., **2001**, Induction of tumour cell apoptosis by matrix metalloproteinase inhibitors: new tricks from a (not so) old drug: *Expert.Opin.Investig.Drugs.*, 10, 1075-1084.

Miyamoto, S., Teramoto, H., Gutkind, J.S., and Yamada, K.M., **1996**, Integrins can collaborate with growth factors for phosphorylation of receptor tyrosine kinases and MAP kinase activation: roles of integrin aggregation and occupancy of receptors: *J.Cell Biol.*, 135, 1633-1642.

Miyamoto, S., Teramoto, H., Coso, O.A., Gutkind, J.S., Burbelo, P.D., Akiyama, S.K., and Yamada, K.M., **1995**, Integrin function: molecular hierarchies of cytoskeletal and signaling molecules: *J.Cell Biol.*, 131, 791-805.

Montgomery, A.M., Sabzevari, H., and Reisfeld, R.A., **1993**, Production and regulation of gelatinase B by human T-cells: *Biochim.Biophys.Acta*, 1176, 265-268.

Montcourrier, P., Mangeat, P.H., Salazar, G., Morisset, M., Sahuquet, A., and Rochefort, H., **1990**, Cathepsin D in breast cancer cells can digest extracellular matrix in large acidic vesicles: *Cancer Res.*, 50, 6045-6054.

Muellberg, J., Durie, F.H., Otten-Evans, C., Alderson, M.R., Rose-John, S., Cosman, D., Black, R.A., and Mohler, K.M., **1995**, A metalloprotease inhibitor blocks shedding of the IL-6 receptor and the p60 TNF receptor: *J.Immunol.*, 155, 5198-5205.

Mueller, S.C., Ghersi, G., Akiyama, S.K., Sang, Q.X., Howard, L., Pineiro-Sanchez, M., Nakahara, H., Yeh, Y., and Chen, W.T., **1999**, A novel protease-docking function of integrin at invadopodia: *J.Biol.Chem.*, 274, 24947-24952.

Murphy, G. and Gavrilovic, J., **1999**, Proteolysis and cell migration: creating a path?: *Curr.Opin.Cell Biol.*, 11, 614-621.

Murphy, G., Nguyen, Q., Cockett, M.I., Atkinson, S.J., Allan, J.A., Knight, C.G., Willenbrock, F., and Docherty, A.J., **1994**, Assessment of the role of the fibronectin-like domain of gelatinase A by analysis of a deletion mutant: *J.Biol.Chem.*, 269, 6632-6636.

Nagase, H., **1997**, Activation mechanisms of matrix metalloproteinases: *Biol.Chem.*, 378, 151-160.

Nakahara, H., Howard, L., Thompson, E.W., Sato, H., Seiki, M., Yeh, Y., and Chen, W.T., **1997**, Transmembrane/cytoplasmic domain-mediated membrane type 1-matrix metalloprotease docking to invadopodia is required for cell invasion: *Proc.Natl.Acad.Sci.U.S.A.*, 94, 7959-7964.

Netzer, K.O., Suzuki, K., Itoh, Y., Hudson, B.G., and Khalifah, R.G., **1998**, Comparative analysis of the noncollagenous NC1 domain of type IV collagen: identification of structural features important for assembly, function, and pathogenesis: *Protein Sci.*, 7, 1340-1351.

- Nisbet, A.J. and Billingsley, P.F., **1999**, Hydrolytic enzymes of *Psoroptes cuniculi* (Delafond): *Insect Biochem.Mol.Biol.*, 29, 25-32.
- Nobes, C.D. and Hall, A., **1999**, Rho GTPases control polarity, protrusion, and adhesion during cell movement: *J.Cell Biol.*, 144, 1235-1244.
- Nobes, C.D. and Hall, A., **1995**, Rho, rac, and cdc42 GTPases regulate the assembly of multimolecular focal complexes associated with actin stress fibers, lamellipodia, and filopodia: *Cell*, 81, 53-62.
- Noe, V., Fingleton, B., Jacobs, K., Crawford, H.C., Vermeulen, S., Steelant, W., Bruyneel, E., Matrisian, L.M., and Mareel, M., **2001**, Release of an invasion promoter E-cadherin fragment by matrilysin and stromelysin-1: *J.Cell Sci.*, 114, 111-118.
- Ntayi, C., Lorimier, S., Berthier-Vergnes, O., Hornebeck, W., and Bernard, P., **2001**, Cumulative influence of matrix metalloproteinase-1 and -2 in the migration of melanoma cells within three-dimensional type I collagen lattices: *Exp.Cell Res.*, 270, 110-118.
- Ohuchi, E., Imai, K., Fujii, Y., Sato, H., Seiki, M., and Okada, Y., **1997**, Membrane type 1 matrix metalloproteinase digests interstitial collagens and other extracellular matrix macromolecules: *J.Biol.Chem.*, 272, 2446-2451.
- Okumura, Y., Sato, H., Seiki, M., and Kido, H., **1997**, Proteolytic activation of the precursor of membrane type 1 matrix metalloproteinase by human plasmin. A possible cell surface activator: *FEBS Lett.*, 402, 181-184.
- Overall, C.M. and Lopez-Otin, C., **2002**, Strategies for MMP inhibition in cancer: innovations for the post-trial era: *Nat.Rev Cancer*, 2, 657-672
- Overall, C.M., **2001**, Matrix metalloproteinase substrate binding domains, modules and exosites. Overview and experimental strategies: *Methods Mol.Biol.*, 151, 79-120.
- Overall, C.M. and Sodek, J., **1987**, Initial characterization of a neutral metalloproteinase, active on native 3/4-collagen fragments, synthesized by ROS 17/2.8 osteoblastic cells, periodontal fibroblasts, and identified in gingival crevicular fluid: *J.Dent.Res.*, 66, 1271-1282.
- Owen, C.A. and Campbell, E.J., **1999**, The cell biology of leukocyte-mediated proteolysis: *J.Leukoc.Biol.*, 65, 137-150.
- Palecek, S.P., Loftus, J.C., Ginsberg, M.H., Lauffenburger, D.A., and Horwitz, A.F., **1997**, Integrin-ligand binding properties govern cell migration speed through cell-substratum adhesiveness: *Nature*, 385, 537-540.
- Patterson, M.L., Atkinson, S.J., Knauper, V., and Murphy, G., **2001**, Specific collagenolysis by gelatinase A, MMP-2, is determined by the hemopexin domain and not the fibronectin-like domain: *FEBS Lett.*, 503, 158-162.
- Pendas, A.M., Balbin, M., Llano, E., Jimenez, M.G., and Lopez-Otin, C., **1997**, Structural analysis and promoter characterization of the human collagenase-3 gene (MMP13): *Genomics*, 40, 222-233.
- Pfaff, M., Du, X., and Ginsberg, M.H., **1999**, Calpain cleavage of integrin beta cytoplasmic domains: *FEBS Lett.*, 460, 17-22.

Pilcher, B.K., Dumin, J., Schwartz, M.J., Mast, B.A., Schultz, G.S., Parks, W.C., and Welgus, H.G., **1999**, Keratinocyte collagenase-1 expression requires an epidermal growth factor receptor autocrine mechanism: *J.Biol.Chem.*, 274, 10372-10381.

Powell, W.C., Fingleton, B., Wilson, C.L., Boothby, M., and Matrisian, L.M., **1999**, The metalloproteinase matrilysin proteolytically generates active soluble Fas ligand and potentiates epithelial cell apoptosis: *Curr.Biol.*, 9, 1441-1447.

Primakoff, P. and Myles, D.G., **2000**, The ADAM gene family: surface proteins with adhesion and protease activity: *Trends.Genet.*, 16, 83-87.

Redfield, A., Nieman, M.T., and Knudsen, K.A., **1997**, Cadherins promote skeletal muscle differentiation in three-dimensional cultures: *J.Cell Biol.*, 138, 1323-1331.

Regen, C.M. and Horwitz, A.F., **1992**, Dynamics of beta 1 integrin-mediated adhesive contacts in motile fibroblasts: *J.Cell Biol.*, 119, 1347-1359.

Roghani, M., Becherer, J.D., Moss, M.L., Atherton, R.E., Erdjument-Bromage, H., Arribas, J., Blackburn, R.K., Weskamp, G., Tempst, P., and Blobel, C.P., **1999**, Metalloprotease-disintegrin MDC9: intracellular maturation and catalytic activity: *J.Biol.Chem.*, 274, 3531-3540.

Romanic, A.M. and Madri, J.A., **1994**, The induction of 72-kD gelatinase in T cells upon adhesion to endothelial cells is VCAM-1 dependent: *J.Cell Biol.*, 125, 1165-1178.

Rozañov, D., Ghebrehiwet, B., Ratnikov, B., Monosov, E., Deryugina, E., and Strongin, A., **2002**, The cytoplasmic tail peptide sequence of membrane type-1 matrix metalloproteinase (MT1-MMP) directly binds to gC1qR, a compartment-specific chaperone-like regulatory protein: *FEBS Lett.*, 527, 51-57.

Saad, S., Gottlieb, D.J., Bradstock, K.F., Overall, C.M., and Bendall, L.J., **2002**, Cancer cell-associated fibronectin induces release of matrix metalloproteinase-2 from normal fibroblasts: *Cancer Res.*, 62, 283-289.

Sassi, M.L., Eriksen, H., Risteli, L., Niemi, S., Mansell, J., Gowen, M., and Risteli, J., **2000**, Immunochemical characterization of assay for carboxyterminal telopeptide of human type I collagen: loss of antigenicity by treatment with cathepsin K: *Bone*, 26, 367-373.

Schon, M., Schon, M.P., Kuhrober, A., Schirmbeck, R., Kaufmann, R., and Klein, C.E., **1996**, Expression of the human alpha2 integrin subunit in mouse melanoma cells confers the ability to undergo collagen-directed adhesion, migration and matrix reorganization: *J.Invest.Dermatol.*, 106, 1175-1181.

Schor, S.L., Allen, T.D., and Winn, B., **1983**, Lymphocyte migration into three-dimensional collagen matrices: a quantitative study: *J.Cell Biol.*, 96, 1089-1096.

Schor, S.L., Schor, A.M., and Bazill, G.W., **1981**, The effects of fibronectin on the migration of human foreskin fibroblasts and Syrian hamster melanoma cells into three-dimensional gels of native collagen fibres: *J.Cell Sci.*, 48, 301-314.

Sheetz, M.P., Felsenfeld, D.P., and Galbraith, C.G., **1998**, Cell migration: regulation of force on extracellular-matrix-integrin complexes: *Trends.Cell Biol.*, 8, 51-54.

- Shimada, T., Nakamura, H., Ohuchi, E., Fujii, Y., Murakami, Y., Sato, H., Seiki, M., and Okada, Y., **1999**, Characterization of a truncated recombinant form of human membrane type 3 matrix metalloproteinase: *Eur.J.Biochem.*, 262, 907-914.
- Shipley, J.M., Doyle, G.A., Fliszar, C.J., Ye, Q.Z., Johnson, L.L., Shapiro, S.D., Welgus, H.G., and Senior, R.M., **1996**, The structural basis for the elastolytic activity of the 92-kDa and 72-kDa gelatinases. Role of the fibronectin type II-like repeats: *J.Biol.Chem.*, 271, 4335-4341.
- Shrivastava, A., Radziejewski, C., Campbell, E., Kovac, L., McGlynn, M., Ryan, T.E., Davis, S., Goldfarb, M.P., Glass, D.J., Lemke, G., and Yancopoulos, G.D., **1997**, An orphan receptor tyrosine kinase family whose members serve as nonintegrin collagen receptors: *Mol.Cell*, 1, 25-34.
- Sloane, B.F., Moin, K., Sameni, M., Tait, L.R., Rozhin, J., and Ziegler, G., **1994**, Membrane association of cathepsin B can be induced by transfection of human breast epithelial cells with c-Ha-ras oncogene: *J.Cell Sci.*, 107, 373-384.
- Sottrup-Jensen, L. and Birkedal-Hansen, H., **1989**, Human fibroblast collagenase-alpha-macroglobulin interactions. Localization of cleavage sites in the bait regions of five mammalian alpha-macroglobulins: *J.Biol.Chem.*, 264, 393-401.
- Stahle-Backdahl, M. and Parks, W.C., **1993**, 92-kd gelatinase is actively expressed by eosinophils and stored by neutrophils in squamous cell carcinoma: *Am.J.Pathol.*, 142, 995-1000.
- Stamenkovic, I., **2000**, Matrix metalloproteinases in tumor invasion and metastasis: *Semin.Cancer Biol.*, 10, 415-433.
- Sternlicht, M.D. and Werb, Z., **2001**, How matrix metalloproteinases regulate cell behavior: *Annu.Rev.Cell Dev.Biol.*, 17, 463-516.
- Sternlicht, M.D., Lochter, A., Sympon, C.J., Huey, B., Rougier, J.P., Gray, J.W., Pinkel, D., Bissell, M.J., and Werb, Z., **1999**, The stromal proteinase MMP3/stromelysin-1 promotes mammary carcinogenesis: *Cell*, 98, 137-146.
- Stetler-Stevenson, W.G., Aznavoorian, S., and Liotta, L.A., **1993**, Tumor cell interactions with the extracellular matrix during invasion and metastasis: *Annu.Rev.Cell Biol.*, 9, 541-573.
- Stoecker, W. and Bode, W., **1995**, Structural features of a superfamily of zinc-endopeptidases: the metzincins: *Curr.Opin.Struct.Biol.*, 5, 383-390.
- Strongin, A. D., Collier, I., Bannikov, G., Marmer, B. L., Grant, G. A., and Goldberg, G. I. **1995**, Mechanism of cell surface activation of 72-kDa type IV collagenase. Isolation of the activated form of the metalloprotease. *J.Biol.Chem.*, 270, 5331-5338.
- Tulla, M., Pentikainen, O.T., Viitasalo, T., Kapyla, J., Impola, U., Nykvist, P., Nissinen, L., Johnson, M.S., and Heino, J., **2001**, Selective binding of collagen subtypes by integrin alpha 1I, alpha 2I, and alpha 10I domains: *J.Biol.Chem.*, 276, 48206-48212.
- Turk, B., Turk, D., and Turk, V., **2000**, Lysosomal cysteine proteases: more than scavengers: *Biochim.Biophys.Acta.* 1477, 98-111.

Ueda, T. and Kobatake, Y., **1984**, Oscillation in cell shape and size during locomotion of amoeboid cells. In: *Cell Motility: Mechanisms and regulation*, 299-307, Ishikawa H., Hatano S. and Sato H. (eds), Alan R. Liss, New York.

Vaday, G.G. and Lider, O., **2000**, Extracellular matrix moieties, cytokines, and enzymes: dynamic effects on immune cell behavior and inflammation: *J.Leukoc.Biol.*, 67, 149-159.

van Muijen, G.N., Jansen, K.F., Cornelissen, I.M., Smeets, D.F., Beck, J.L., and Ruitter, D.J., **1991**, Establishment and characterization of a human melanoma cell line (MV3) which is highly metastatic in nude mice: *Int.J.Cancer*, 48, 85-91.

Velling, T., Kusche-Gullberg, M., Sejersen, T., and Gullberg, D., **1999**, cDNA cloning and chromosomal localization of human alpha(11) integrin. A collagen-binding, I domain-containing, beta(1)-associated integrin alpha-chain present in muscle tissues: *J.Biol.Chem.*, 274, 25735-25742.

Vogel, W.F., **2001**, Collagen-receptor signaling in health and disease: *Eur.J.Dermatol.*, 11, 506-514.

Ward, C.J., Crocker, J., Chan, S.J., Stockley, R.A., and Burnett, D., **1990**, Changes in the expression of elastase and cathepsin B with differentiation of U937 promonocytes by GM-CSF: *Biochem.Biophys.Res.Comm.*, 167, 659-664.

Weaver, V.M., Petersen, O.W., Wang, F., Larabell, C.A., Briand, P., Damsky, C., and Bissell, M.J., **1997**, Reversion of the malignant phenotype of human breast cells in three-dimensional culture and in vivo by integrin blocking antibodies: *J.Cell Biol.*, 137, 231-245.

Wei, Y., Lukashev, M., Simon, D.I., Bodary, S.C., Rosenberg, S., Doyle, M.V., and Chapman, H.A., **1996**, Regulation of integrin function by the urokinase receptor: *Science*, 273, 1551-1555.

Welch, A.R., Holman, C.M., Huber, M., Brenner, M.C., Browner, M.F., and Van Wart, H.E., **1996**, Understanding the P1' specificity of the matrix metalloproteinases: effect of S1' pocket mutations in matrilysin and stromelysin-1: *Biochemistry*, 35, 10103-10109.

Welch, M.P., Odland, G.F., and Clark, R.A., **1990**, Temporal relationships of F-actin bundle formation, collagen and fibronectin matrix assembly, and fibronectin receptor expression to wound contraction: *J.Cell Biol.*, 110, 133-145.

Werb, Z., **1997**, ECM and cell surface proteolysis: regulating cellular ecology: *Cell*, 91, 439-442.

Westermarck, J. and Kahari, V.M., **1999**, Regulation of matrix metalloproteinase expression in tumor invasion: *FASEB J.*, 13, 781-792.

Wilkinson, P.C., Shields, J.M., and Haston, W.S., **1982**, Contact guidance of human neutrophil leukocytes: *Exp.Cell Res.*, 140, 55-62.

Will, H., Atkinson, S.J., Butler, G.S., Smith, B., and Murphy, G., **1996**, The soluble catalytic domain of membrane type 1 matrix metalloproteinase cleaves the propeptide of progelatinase A and initiates autoproteolytic activation. Regulation by TIMP-2 and TIMP-3: *J.Biol.Chem.*, 271, 17119-17123.

- Windsor, L.J., Birkedal-Hansen, H., Birkedal-Hansen, B., and Engler, J.A., **1991**, An internal cysteine plays a role in the maintenance of the latency of human fibroblast collagenase: *Biochemistry*, 30, 641-647.
- Woessner, J.F.J., **1991**, Matrix metalloproteinases and their inhibitors in connective tissue remodeling: *FASEB J.*, 5, 2145-2154.
- Wu, C., Fields, A.J., Kapteijn, B.A., and McDonald, J.A., **1995**, The role of alpha 4 beta 1 integrin in cell motility and fibronectin matrix assembly: *J.Cell Sci.*, 108, 821-829.
- Xia, M., Leppert, D., Hauser, S.L., Sreedharan, S.P., Nelson, P.J., Krensky, A.M., and Goetzl, E.J., **1996**, Stimulus specificity of matrix metalloproteinase dependence of human T cell migration through a model basement membrane: *J.Immunol.*, 156, 160-167.
- Xu, J., Zutter, M.M., Santoro, S.A., and Clark, R.A., **1998**, A three-dimensional collagen lattice activates NF-kappaB in human fibroblasts: role in integrin alpha2 gene expression and tissue remodeling: *J.Cell Biol.*, 140, 709-719.
- Yamada, K.M. and Geiger, B., **1997**, Molecular interactions in cell adhesion complexes: *Curr.Opin.Cell Biol.*, 9, 76-85.
- Yamada, K.M., Kennedy, D.W., Yamada, S.S., Gralnick, H., Chen, W.T., and Akiyama, S.K., **1990**, Monoclonal antibody and synthetic peptide inhibitors of human tumor cell migration: *Cancer Res.*, 50, 4485-4496.
- Yamamoto, S., Higuchi, Y., Yoshiyama, K., Shimizu, E., Kataoka, M., Hijiya, N., and Matsuura, K., **1999**, ADAM family proteins in the immune system: *Immunol.Today*, 20, 278-284.
- Yavari, R., Adida, C., Bray-Ward, P., Brines, M., and Xu, T., **1998**, Human metalloprotease-disintegrin Kuzbanian regulates sympathoadrenal cell fate in development and neoplasia: *Hum.Mol.Genet.*, 7, 1161-1167.
- Yoshiyama, K., Higuchi, Y., Kataoka, M., Matsuura, K., and Yamamoto, S., **1997**, CD156 (human ADAM8): expression, primary amino acid sequence, and gene location: *Genomics*, 41, 56-62.
- Yumura, S., Mori, H., and Fukui, Y., **1984**, Localization of actin and myosin for the study of ameboid movement in Dictyostelium using improved immunofluorescence: *J.Cell Biol.*, 99, 894-899.
- Zhou, H., Bernhard, E.J., Fox, F.E., and Billings, P.C., **1993**, Induction of metalloproteinase activity in human T-lymphocytes: *Biochim.Biophys.Acta*, 1177, 174-178.
- Zucker, S., Cao, J., and Chen, W.T., **2000**, Critical appraisal of the use of matrix metalloproteinase inhibitors in cancer treatment: *Oncogene*, 19, 6642-6650.
- Zutter, M.M., Santoro, S.A., Staatz, W.D., and Tsung, Y.L., **1995**, Re-expression of the alpha 2 beta 1 integrin abrogates the malignant phenotype of breast carcinoma cells: *Proc.Natl.Acad.Sci.U.S.A.*, 92, 7411-7415

8. LIST OF FIGURES

- Fig. 1. Schematic domain structure of vertebrate MMPs.
- Fig. 2. Model for different migration strategies on adhesive function in 3D collagen lattices.
- Fig. 3. Cell surface expression of $\beta 1$ integrins, proteases and protease inhibitors from tumor cells migrating in liquid culture versus 3D collagen.
- Fig. 4. Protein expression of MMP-2 and MT1-MMP from tumor cells migrating in 3D collagen by Western blot.
- Fig. 5. MMP function and activation from cells migrating in liquid culture versus 3D collagen in zymography.
- Fig. 6. mRNA expression of selected tumor-associated proteases and endogenous protease inhibitors by MV3 and HT-1080 cells from liquid culture.
- Fig. 7. Spontaneous, $\beta 1$ integrin-dependent migration of HT-1080 cells in 3D collagen lattice.
- Fig. 8. Subcellular distribution and shedding of $\beta 1$ integrins, MMPs and organization of the actin cytoskeleton.
- Fig. 9. Biophysical organization of type I collagen: comparison of 3D fibrillar matrix to collagen in polyacrylamide gel.
- Fig. 10. MMP- and cell-associated degradation of 3D collagen matrices.
- Fig. 11. In situ collagenolysis by migrating cells within FITC-labeled collagen matrix.
- Fig. 12. Detection of in situ collagenolysis by HT-MT1 cells.
- Fig. 13. Spontaneous migration of HT-1080 cells transfected with neo- or MT1-MMP-vector: increase in migration speed.
- Fig. 14. Collagen zymography for MMP-2, -9, and MT1-MMP: inhibition by BB-2516.
- Fig. 15. Lack of BB-2516 absorption by fibrillar collagen.
- Fig. 16. Reduced collagenolysis from cell-derived MMPs by BB-2516.
- Fig. 17. Persistent migration of MV3 and HT-1080 cells in the presence of BB-2516.
- Fig. 18. Subtotal inhibition of collagenolytic activity by protease inhibitor cocktail.
- Fig. 19. Persistent migration in the presence of protease inhibitor cocktail.
- Fig. 20. Conversion of mesenchymal amoeboid morphodynamics and migration in HT-MT1 cells.

- Fig. 21. Conversion of mesenchymal to amoeboid morpho-dynamics and migration in MDA-MB-231 cells.
- Fig. 22. Squeezing through the fiber network: Induced amoeboid migration lacks fiber degradation and matrix remodeling.
- Fig. 23. Changes in $\beta 1$ integrin and MT1-MMP distribution and cytoskeletal structure in induced amoeboid migration.
- Fig. 24. In vivo translocation and morphology of HT-MT1 cells in the mouse dermis.
- Fig. 25. Spontaneous locomotion of a CD4+ T cell through 3D collagen lattice: Changes in morphology and oscillatory path development.
- Fig. 26. mRNA expression of proteases and endogenous protease inhibitors in CD4+ T cells and SupT1 cells.
- Fig. 27. Upregulation of cell surface-located MMP-9 and MT1-MMP on CD4+ T cells upon activation.
- Fig. 28. Lack of in situ collagen degradation by T blasts and SupT1 cells.
- Fig. 29. Persistent T cell migration in the presence of protease inhibitor cocktail.
- Fig. 30. Amoeboid T cell migration within 3D collagen matrix in the absence and presence of protease inhibitor cocktail.
- Fig. 31. Mesenchymal-amoeboid transition.
- Fig. 32. Model for the contribution of matrix proteases to migration strategies of different cell types.

9. LIST OF TABLES

Table 1. Cell surface receptor binding to ECM ligands associated with migration.	2
Table 2. The MMP family.	4
Table 3. Cocktail of broad spectrum protease inhibitors.	37
Table 4. RT-PCR: Primer sequences of all used primers, annealing temperatures and times, length of resulting PCR products and source.	73

ACKNOWLEDGEMENTS

I very much thank Professor Dr. Eva-B. Bröcker and Professor Dr. Georg Krohne to support and referee this work.

I am particularly grateful to Peter Friedl for providing the topic and supervising this thesis, continuous and enthusiastic scientific support of this work as well as all personal encouragement including new and often unconventional ideas and many constructive discussions. Due to his help I learned the tools and fair rules of research, and scientific networking including joint experiments with international laboratories.

I want to thank the foundation “Evangelisches Studienwerk Haus Villigst” for not only financial support, but giving me the opportunity to meet and interact constructively with talented and motivated Ph.D. students from all different fields in our society.

Many thanks to Margit Ott for excellent technical assistance and uncomplicated cooperation. She contributed very positively to this project. I am grateful to all my colleagues for their collegiality, a lively atmosphere in the lab, helpful discussions and practical help in optimizing methods, which made working convenient. I also thank Regina Müller who joined the lab for 5 months and collaborated on the data related to T cell migration, in partial fulfillment of her M.D. thesis.

I further acknowledge Jörg Geiger, Institute for Clinical Biochemistry and Pathobiochemistry, Würzburg, for helpful assistance with spectrofluorometry. Many thanks to our collaborators Elena Deryugina and Alex Strongin for providing transfected cell lines and constructive discussions regarding this project. Last, but not least I want to thank Uli von Andrian and his coworkers Harry Leung, Irina Mazo and Katharina Engelke for giving me the possibility to work on intravital multiphoton microscopy, great technical assistance and many helpful and stimulating discussions during my stay at Harvard Medical School in Boston.

Finally, and most beautifully, however, I am thankful to my partner Charles Jama who supported me in the final and essential phase of this work, both personally as well as by expert proof-reading.

During the period of the PhD thesis this work was published or presented at scientific meetings or seminars:

Publications

- 3 **K. Wolf, R. Müller, S. Borgmann, E.-B. Bröcker, and P. Friedl. Amoeboid morphodynamics and contact guidance: T cell crawling through fibrillar collagen is independent of matrix remodeling by MMPs and other proteases.** (submitted)
- 2 **Katarina Wolf, Irina Mazo, Harry Leung, Katharina Engelke, Ulrich H. von Andrian, Elena I. Deryugina, Alex Y. Strongin, Eva-B. Bröcker, and Peter Friedl. Compensation mechanism in tumor cell migration: Mesenchymal-amoeboid transition after blocking of pericellular proteolysis.** (submitted)
- 1 Maaser, K., **K. Wolf**, E. Klein, B. Niggemann, K.S. Zänker, E.-B. Bröcker, and P. Friedl. 1999. **Functional hierarchy of simultaneously expressed adhesion receptors: α 2B1 but not CD44 mediates MV3 melanoma cell migration and matrix reorganization within three-dimensional hyaluronan-containing collagen matrices.** *Mol. Biol. Cell* 19: 3067-3079.

Abstracts (Congresses, Workshops)

- 1 **Wolf, K., E. Deryugina, A. Strongin, E.-B. Bröcker and P. Friedl. Focalized proteolysis provided by matrix-metalloproteinases facilitates cell motility, pericellular matrix reorganization and migration.** Annual Meeting of the German Society for Cell Biology, Karlsruhe, Germany, March 26-30, 2000 (poster and video presentation).
- 2 **Wolf, K., E. Deryugina, A. Strongin, E.-B. Bröcker and P. Friedl. Focalized proteolysis and non-proteolytic migration strategies in tumor cells.** Annual Meeting of the American Association of Cell Biology, San Francisco, USA, December 8-12, 2000 (poster and video presentation). **Reported in: BioMedNet Conference reporter highlights on ASCB 2000.**
- 3 Mayer, C., **K. Wolf**, E.-B. Bröcker and P. Friedl. **Pfadbildung durch invasive Melanomzellen: Matrixdefekte, Zellfragmente und erleichterte Migration.** 10. Jahrestagung der Arbeitsgemeinschaft Dermatologische Onkologie, Mannheim, Germany, Oktober 5-7, 2000 (poster).
- 4 Friedl, P., **K. Wolf**, C. Mayer, and E.-B. Bröcker. **Tumor cell migration through three-dimensional extracellular matrix: diversity of migration and path generation strategies.** Keystone Conference on "Cell Migration and invasion", Granlibakken Resort, Tahoe City, CA, USA, March 11-16, 2001 (poster and video presentation).
- 5 Friedl, P. and **K. Wolf. Plasticity in migration strategies: Conversion of proteolytic mesenchymal migration to non-proteolytic amoeboid crawling in tumor cells.** DFG-Schwerpunkt-meeting on "Cell migration", Berlin, Germany, September 13-15, 2001.
- 6 **Wolf, K., E. Deryugina, A. Strongin, E.-B. Bröcker and P. Friedl. Plasticity in migration strategies: conversion of proteolytic mesenchymal migration to non-proteolytic amoeboid crawling in tumor cells.** 3rd Amsterdam "Zoo" Meeting on "Cell adhesion and migration in inflammation and cancer", Amsterdam, Netherlands, Oktober 17-20, 2001 (poster and video presentation).
- 7 **Wolf, K., E. Deryugina, A. Strongin, E.-B. Bröcker and P. Friedl. Plasticity in migration strategies: conversion of proteolytic mesenchymal migration to non-proteolytic amoeboid crawling in tumor cells.** International conference of the DFG and MDC (Max-

Delbrück-Center for Molecular Medicine) on “Cell migration in Development and Disease”, Berlin, Germany, November 28 - December 1, 2001 (oral presentation and poster).

- 8 **Wolf, K.,** E. Deryugina, A. Strongin, E.-B. Bröcker and P. Friedl. **Plasticity in migration strategies: conversion of proteolytic mesenchymal migration to non-proteolytic amoeboid crawling in tumor cells.** Annual meeting of the ADF (Arbeitskreis Dermatologischer Forschung), Berlin, Germany, February 28 - March 2, 2002 (poster and video presentation).
- 9 Müller, R., **K. Wolf,** E.-B. Bröcker and P. Friedl. **Amoeboid morphodynamics and contact guidance: T cell crawling through fibrillar collagen is independent of proteolytic matrix remodeling.** Annual meeting of the ADF (Arbeitskreis Dermatologischer Forschung), Berlin, Germany, February 28 - March 2, 2002 (poster).
- 10 **K. Wolf,** Müller, R., E.-B. Bröcker and P. Friedl. **Amoeboid morphodynamics and contact guidance: T cell crawling through fibrillar collagen is independent of proteolytic matrix remodeling.** 2nd Joint UK/German Adhesion meeting on “Cellular Interactions in the Immune System”, Berlin, Germany, July 5-6, 2002 (poster and video presentation).
- 11 **Wolf, K.,** E. Deryugina, A. Strongin, E.-B. Bröcker and P. Friedl. **Plasticity in migration strategies: conversion of proteolytic mesenchymal migration to non-proteolytic amoeboid crawling in tumor cells.** 18. Federation of European Connective Tissue Societies Meeting (FECTS), Brighton, UK, July 27-31, 2002 (oral presentation and poster).
- 12 **Wolf, K.,** E. Deryugina, A. Strongin, E.-B. Bröcker and P. Friedl. **Visualization of focalized proteolytic tumor cell migration within three-dimensional extracellular matrices.** 44. Symposium of the Society for Histochemistry on “Proteomics in situ: Imaging proteins at work”, Vlissingen, The Netherlands, September, 25-28, 2002 (oral presentation and poster).

Invited oral presentation

- 13 **Wolf, K.,** E. Deryugina, A. Strongin, E.-B. Bröcker and P. Friedl. **Focalized proteolysis and non-proteolytic migration strategies in tumor cells.** DFG-Workshop “Matrix-Metalloproteinasen – Struktur, Funktion und physiologische Bedeutung”, Bielefeld, Germany, March 7-9, 2001 (oral presentation).

Other oral presentations (without abstracts)

- 1 **”Focalized proteolysis and non-proteolytic migration strategies in tumor cells.”** Roche Diagnostica GmbH, Pharma Research Penzberg, Penzberg, Germany, March 23, 2001.
- 2 **”Focalized proteolysis and non-proteolytic migration strategies in tumor cells.”**
Dept. of Biochemistry, RWTH (Rheinisch-Westfälische Technische Hochschule), Aachen, Germany, May 22, 2001.
- 3 **“Unterschiedliche Migrationsstrategien von Tumorzellen in extrazellulärer Matrix: Bedeutung von Proteasen.”** Dept. of Physiology and Pathophysiology, Mainz, Germany, June 11, 2002.

Curriculum Vitae

Name: Katarina Wolf
Adress: Scheffelstr. 1, 97072 Würzburg
Born: February 16th, 1965 in Dahme, Germany
Degrees: Medical Technical Laboratory Assistant (7/84)
Diploma in Biochemistry, „Free University of Berlin“ (9/98)

School education:

09/71 - 07/81 Polytechnische Oberschule (corresponds to Realschule)
09/81 - 07/84 Medical High School, Potsdam,
Degree: Medical Technical Lab-Assistant (7/84)
08/92 - 06/93 Lise-Meitner-Schule Berlin, Allgemeine Fachhochschulreife
(main emphasis on natural sciences)
Degree: Fachabitur (6/93)

University education:

10/93 - 09/95 Freie Universität Berlin, Faculty of Chemistry;
German equivalent of a Bachelor degree in Biochemistry: 9/95
10/95 - 09/98 Freie Universität Berlin, Studies in Biochemistry
11/97 - 09/98 Diploma Thesis, Dept. of Immunology, Weizmann-Institute, Rehovot,
Israel (Ofar Lider, Ph.D.):
*Phenotype analysis of T cells interacting with cytokine-associated
extracellular matrix.*
09/98 Diploma in Biochemistry (equivalent to Masters Degree)

Ph.D. thesis:

10/98 - 09/02 Ph.D. Thesis, Dept. of Dermatology, University of Würzburg, Cell
Migration Laboratory (Peter Friedl, M.D., Ph.D):
*Migration of tumor cells and leukocytes in extracellular matrix:
proteolytic and nonproteolytic strategies for overcoming tissue barriers.*

Fellowships

07/96 - 09/98 and
07/99 - 06/02 fellow of the foundation "Evangelisches Studienwerk e.V., Haus Villigst"

Appointments:

09/84 - 05/89 St. Josefs-Hospital, Potsdam, occupation as medical-lab-technician
06/89 - 08/91 Medical High School, Potsdam, teaching position for the practical
training in Microbiology and Histology

Würzburg, September 30th, 2002

Lebenslauf

Name: Katarina Wolf
Adresse: Scheffelstr. 1, 97072 Würzburg
Geboren: am 16. Februar 1965 in Dahme, Deutschland
Berufs-Abschlüsse: Medizinisch-Technische Laborassistentin (7/84)
Diplom in Biochemie (9/98)

Schulausbildung:

09/71 - 07/81 Polytechnische Oberschule
(ehemalige DDR, vergleichbar mit Realschule)

09/81 - 07/84 Medizinische Fachschule, Potsdam;
Abschluss: Medizinisch-Technische Laborassistentin (MTLA) (7/84)

08/92 - 06/93 Lise-Meitner-Schule Berlin, Allgemeine Fachhochschulreife mit
naturwissenschaftlichem Schwerpunkt
Abschluss: Fachabitur (6/93)

Studium:

10/93 - 09/98 Freie Universität Berlin, Fakultät für Chemie;
Biochemie-Studium

09/95 Vordiplom (Biochemie)

10/95 - 10/97 Hauptstudium (Biochemie)

11/97 - 09/98 Anfertigung der Diplomarbeit bei Ofer Lider (Ph.D.) am Dept. of
Immunology, Weizmann-Institut, Rehovot, Israel:
*Phenotype analysis of T cells interacting with cytokine-associated
extracellular matrix.*

09/98 Diplom als Biochemikerin

Doktorarbeit:

10/98 - 09/02 Anfertigung der Doktorarbeit bei Peter Friedl (M.D., Ph.D.) an der
Klinik für Haut- und Geschlechtskrankheiten der Universität Würzburg:
*Migration of tumor cells and leukocytes in extracellular matrix:
proteolytic and nonproteolytic strategies for overcoming tissue barriers.*

Stipendien

07/96 - 09/98 und
07/99 - 06/02 Stipendiatin der Stiftung "Evangelisches Studienwerk e.V., Haus Villigst"

Beschäftigungen:

09/84 - 05/89 St. Josefs-Hospital, Potsdam, Anstellung als MTLA

06/89 - 08/91 Medizinische Fachschule, Potsdam, Lehrerin in der praktischen MTLA-
Ausbildung in den Fächern Mikrobiologie und Histologie

Würzburg, den 30. September 2002

DECLARATION

Herewith I declare:

1. This thesis was performed only by myself and not by other persons. I did not use other sources and helping tools than those that are explicitly noted.
2. This dissertation was never exposed to an examination or similar procedure at this or another faculty.
3. I have never before obtained or tried to obtain a Ph.D. degree in natural sciences or other science areas.

Movie legends

01	Fibroblast-like, mesenchymal migration of HT1080/MT1-MMP cell through 3D collagen matrix (high magnification time lapse videorecording). Pseudopods at the leading edge generate transient attachment to and localized pulling and distortion of collagen fibers for migratory force generation. Image size: 94 x 70 μm . Time frame: bottom left corner (h:m:s).
02	Blocking of $\beta 1$ integrins (mAb 4B4) results in spherical morphology as a consequence of impaired collagen fiber binding, indicating $\beta 1$ integrins as sole receptors to fibrillar type I collagen in HT1080 cells. Non-productive ruffling is insufficient to generate traction-dependent polarization. 70 x 70 μm ; 2 hours 50 min
03	Proteolytic migration of HT-1080/M1 cells (time-lapse confocal microscopy): a) Fiber traction and bundling, and shedding of cellular determinants (3D reconstruction of calcein-labeled cell). b) Detachment-associated generation of a tube-like matrix defect bordered by thickened multi-fibrillar bundles (central slice). 90 x 90 μm ; 82 min
04	Constitutive spindle-shaped, fibroblast-like morphodynamics and migration convert to ameoboid migration in the presence of protease inhibitor cocktail in HT-1080/MT1 cells (simultaneous time-lapse videomicroscopy). Image size: 470 x 350 μm . Time frame: bottom left corner (h:m:s).
05	Induced ameoboid migration HT-1080/MT1 cells in the presence of protease inhibitor cocktail (a) low and b) high magnification). The cell develops small leading filopodia and ameoboid morphology while squeezing through matrix gaps and protruding. a) 78 x 86 μm , 1 hour 57 min; b) 43 x 43 μm , 60 min.
06	<i>Dictiostelium discooidum</i> amoeba, downloaded from the dicty webpage: http://www.dicty.cmb.nwu.edu/dicty/dicty.html
07	MDA-MB-231 cells: conversion of constitutive mesenchymal migration towards non-proteolytic amoeboid movement in the presence of protease inhibitor cocktail (simultaneous time-lapse videomicroscopy). Image size: 470 x 350 μm . Time frame: top left corner (h:m:s).
08	Protease-independent crawling lacks structural matrix remodeling. Fiber bundling at leading and trailing edges is reduced. After detachment, intact fibers rebound to their original position. The cell tends to align in parallel to preformed fibers (contact guidance). 90 x 90 μm ; 65 min
09	Constriction rings: non-proteolytic bypassing of matrix constraints by shape change. a) Calcein-labeled cell (blue false color) squeezing through a 3.5 μm matrix pore by forming a constriction ring (57 x 57 μm , 25 min). b) 3D reconstruction of fixed cell developing two simultaneous constriction rings. Non-clustered $\beta 1$ integrins at fiber contacts (green).
10	Intravital multiphoton microscopy (z-scan): Mesenchymal and induced amoeboid morphology in HT-1080/MT1 cells after injection into the mouse dermis. Position and morphology of calcein-labeled control cells (green) and protease inhibitor cocktail pretreated cells were monitored by z-scanning 3 hr after injection. Ortotopic reconstruction of the matrix fibers (blue) was obtained from multi-photon microscopy and second harmonic generation imaging, showing alternating patterns of loose connective fibrillar tissue and densely packed matrix. (250 x 250 μm , 40 μm in depth).

11	<p>Activated CD4+ T cells: constitutive amoeboid migration in the absence and presence of protease inhibitor cocktail through 3D collagen matrix (overview, time lapse videomicroscopy was simultaneously performed using independent microscopes). Migrating cells in both, non-treated and treated samples display amoeboid morphodynamics resulting in random paths. No change in migration characteristics was induced after inhibition of proteases.</p> <p>Both movies: image size: 470 x 350 μm; time frame: 8 min (top left corner; h:m:s).</p>
12	<p>High resolution confocal reconstruction of flexible amoeboid migration, alignment along fibers in the absence and presence of protease inhibitor cocktail. Migration of calcein-labelled cells in 3D collagen matrices was monitored by high resolution 3D confocal reconstruction over time. In both, control cells and cells treated with protease inhibitor cocktail, contact guidance by matrix fibers and constriction rings were detected (see Fig. 6). No change in physical matrix structure (backscatter signal in grey) was detected.</p> <p>Time rate: 1 image per 20 seconds.</p> <p>Untreated control cell: Image size: 80 x 80 μm, time frame: 9 min, 20 seconds.</p> <p>protease inhibitor cocktail: Image size: 70 x 70 μm, time frame: 10 min.</p>

All copyrights reserved. No unauthorized reproduction or public performance without written consent of the author.